

Automated Variable Selection of Gamma-Ray Spectra by Utilization of LASSO and Elastic Net Techniques for Use in Nuclear Security Applications

Vincent DiNova
NC State University

Defense Presentation
July 12, 2019
Raleigh, NC

Agenda

- Mission of RDRS
- KSU Experimental setup and operation
- Prompt Gamma Neutron Activation Analysis (PGNAA)
- Neutron, gamma, and detector physics
- Monte Carlo Library Least Squares (MCLLS) fitting
- Basics of supervised machine learning
- Regularization methods (LASSO and Elastic Net)
- Library generation and data processing
- KSU results
- RIID simulations and results
- Discussion/Conclusions
- References
- Questions

Replacement of Dangerous Radiological Sources

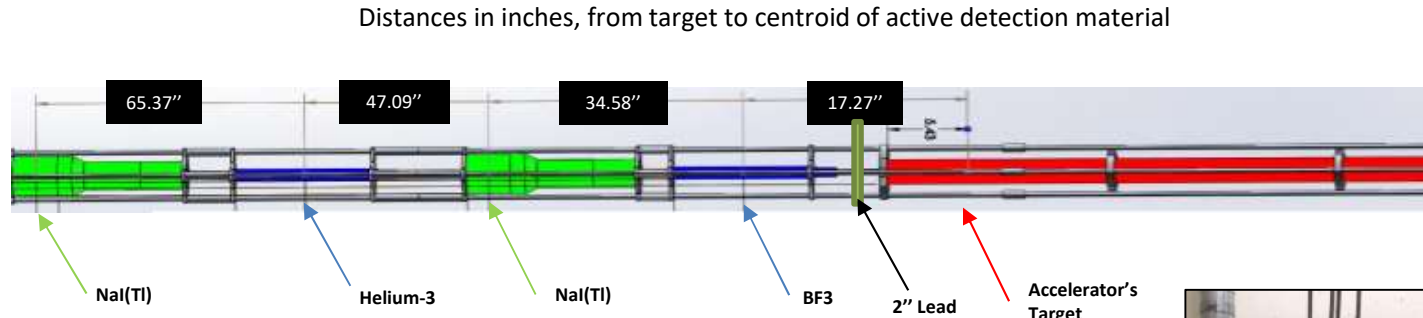
- One of the thrust areas under the Consortium for Nonproliferation Enabling Capabilities (CNEC) tasked with finding suitable alternatives for commonly used radioisotopes
- NC State's contribution to RDRS is to:
 - Develop a practical inverse approach to determine elemental composition, density, and neutron porosity with a 14-MeV neutron well logging tool using adapted Monte Carlo Library Least-Squares methods.
 - Benchmark these methods with data obtained from KSU's test facility and test tool. This tool replaces the two present radioisotope sources in traditional well-logging tools with a single 14-MeV neutron generator.

Motivation

- The National Academy of Sciences (NAS) commissioned a study soon after 9/11/2001 to consider the dangers of long-lived radiological sources:

Radionuclide	Half-life (yr)	Particles-Energies (MeV)	Principal Applications	US Inventory (Ci)
Cs-137	30.17	β -0.518 max; β -1.18 max; γ -0.662	Industrial gauging, Irradiators, Well logging	2,800,000
Co-60	5.27	γ -1.173; γ -1.333	Sterilization, Irradiators, Teletherapy	198,000,000
Am-241	432.2	α -5.64; γ -0.060	Well logging, Gauging	6,482
Pu-238	87.7	α -5.59; γ -0.043	RTGs	937
Sr-90	28.9	β -0.546 max	RTGs	1,730,000
Se-75	119.8 d	γ -0.28 (ave), 0.8 max	Radiography	261
Ir-192	74 d	β -1.46 max] γ -0.38 ave, 1.378 max	Radiography	146,922
Cf-252	2.645	α -6.22; n -2 ave; γ -various; fission products	Well logging Research	7

Benchmarking Tool Design



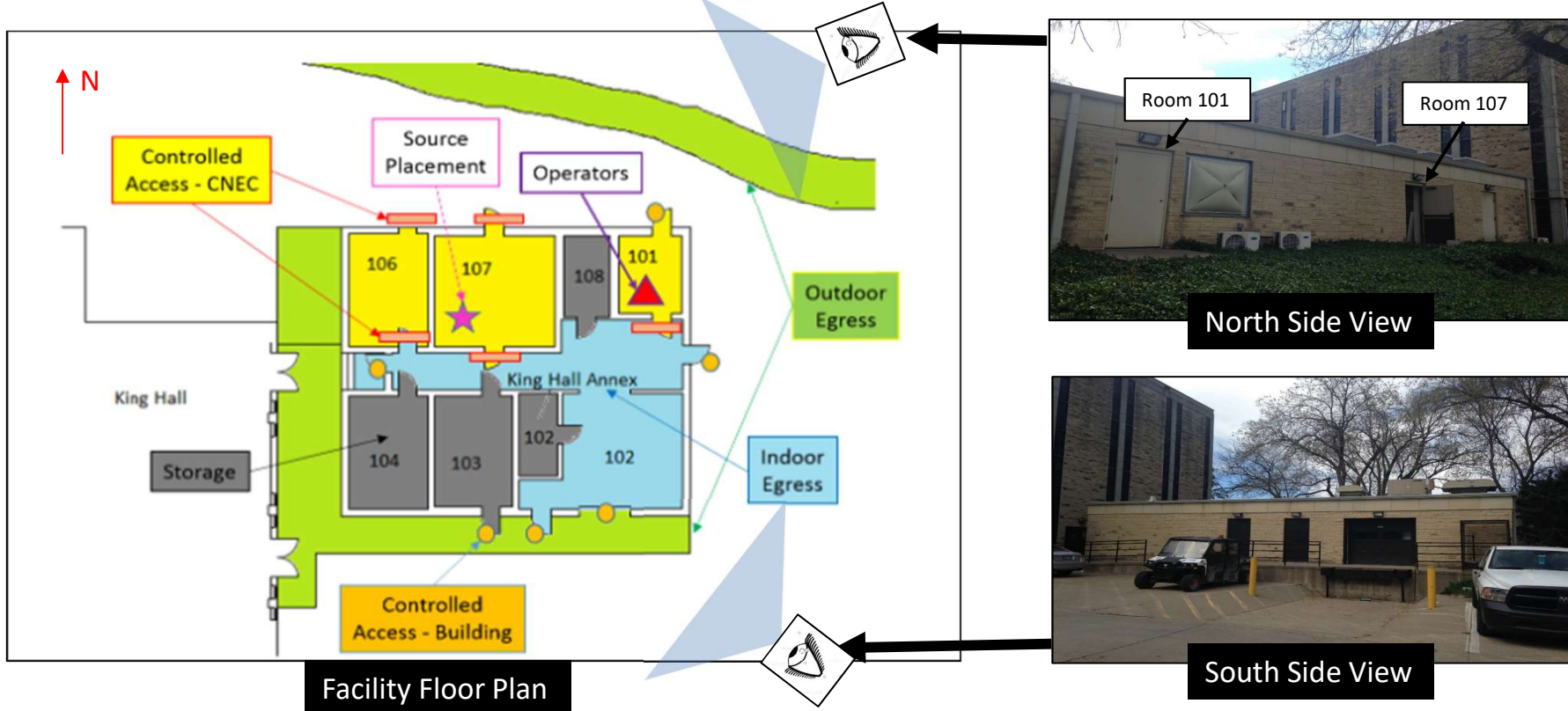
- The benchmarking tool:
 - Skeleton
 - Sources
 - Shielding
 - Sensors
- For the well-logging application:
 - Thermo Fisher D-T generator
 - BF_3 and ^3He neutron sensors
 - NaI(Tl) gamma sensors



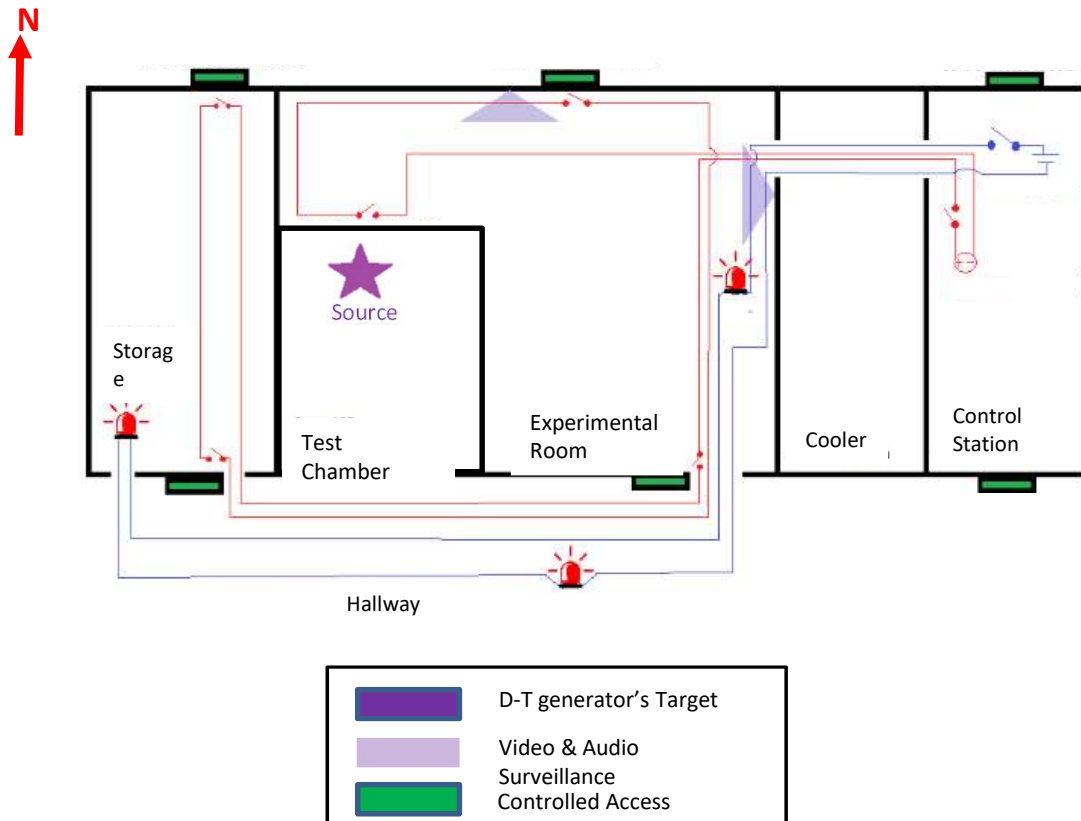
Tool is used to benchmark Monte Carlo simulation results

Test Facility: Location

The KSUMI Test Facility is at King Hall Annex at KSU



Test Facility: Accelerator Enabling and Safeguard Systems



Accelerator Enabling System prevents inadvertent neutron production and entries

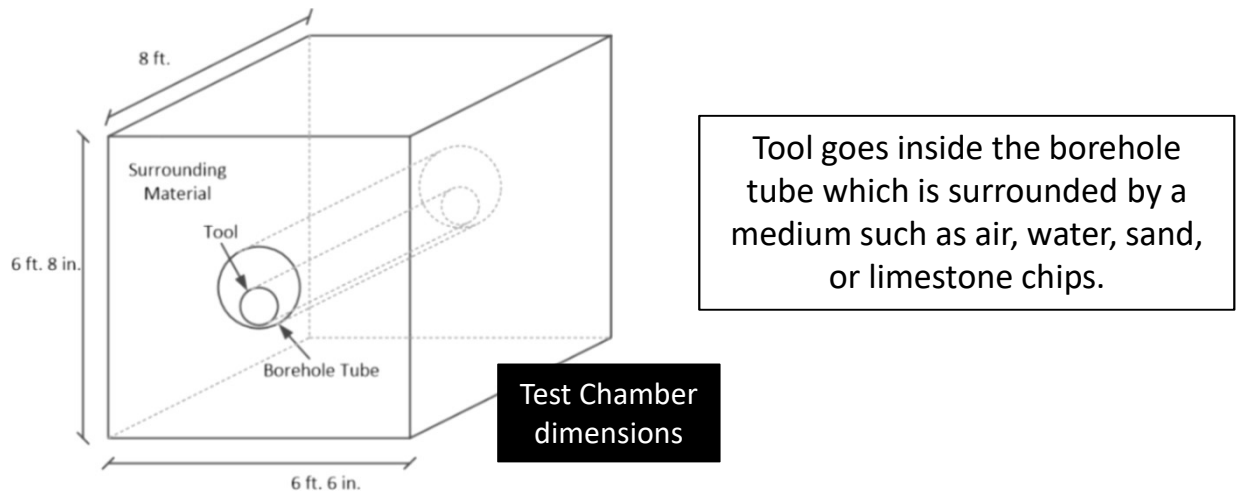
Other Safeguards include:

- Surveillance
- Intercommunication
- Warning lights
- Procedures

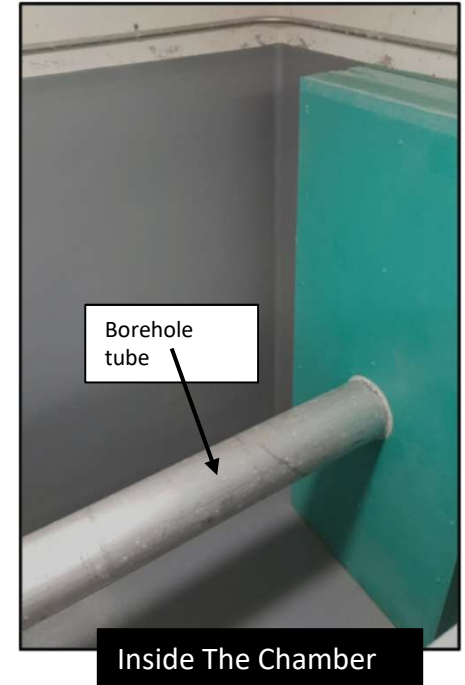
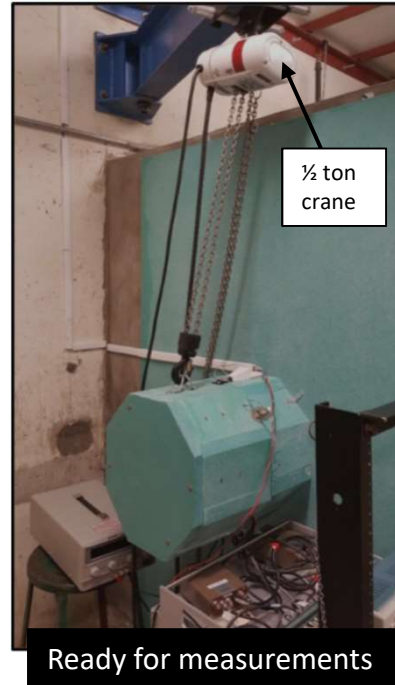
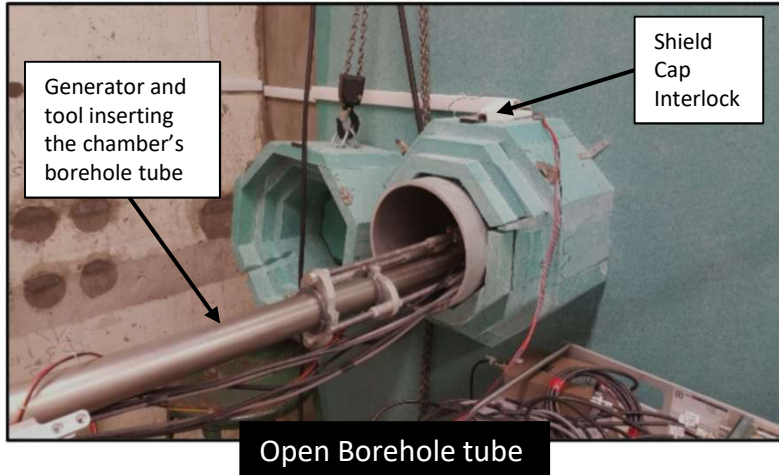
Low dosage for bystanders and workers.
Only workers who enters experiment room requires dosimeters.

Test Facility: Test Chamber Design

- The test chamber is 6'-8" high by 6'-6" wide by 8' deep
- Volume inside the chamber is ~2,500 gal
- When filled with water, the chamber presents an effectively infinite medium to the D-T neutrons



Test Facility: Test Chamber with Benchmark Tool



- Green objects are borated polyethylene
- Test chamber is currently outfitted to benchmark the logging tool

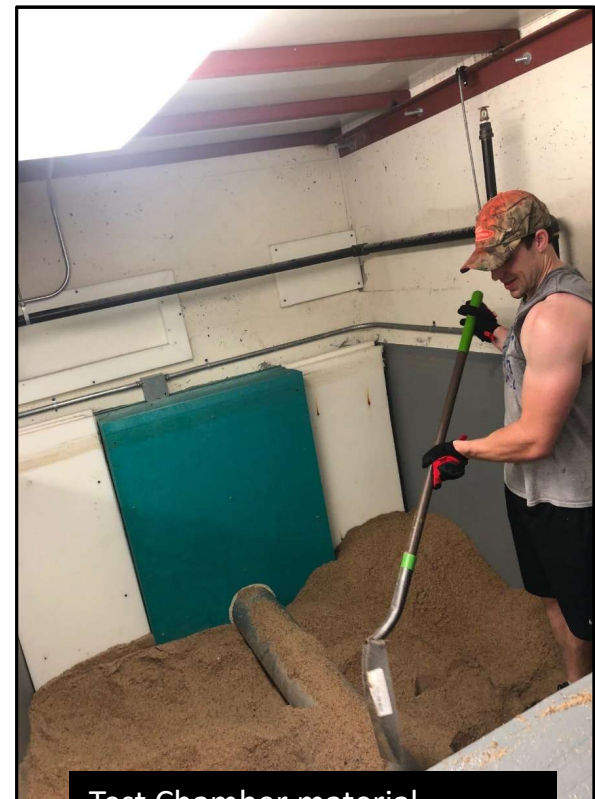
Test Facility: Material Loading



Safety
Evaluation

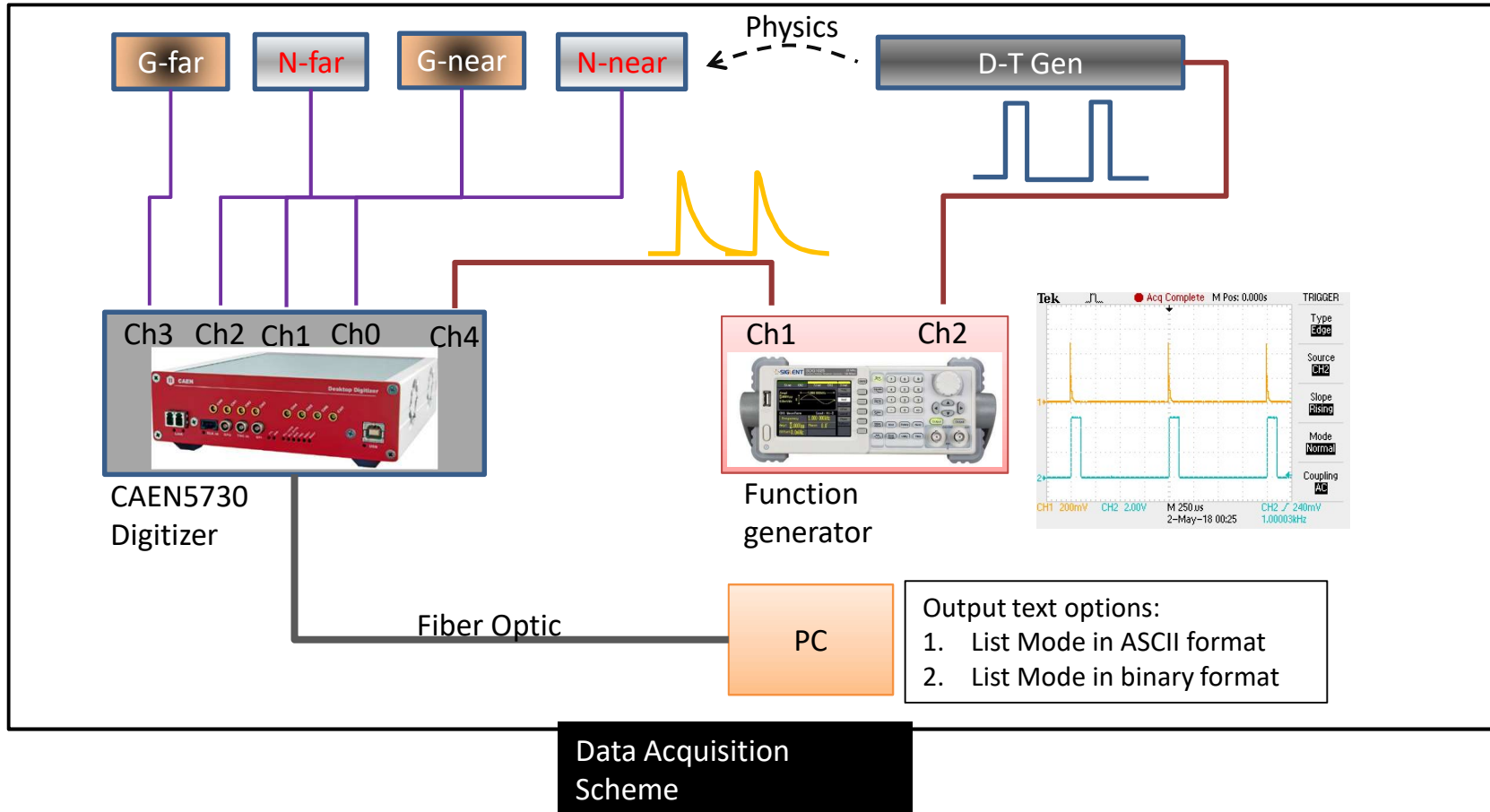


Conveyor Belt system
for material movement



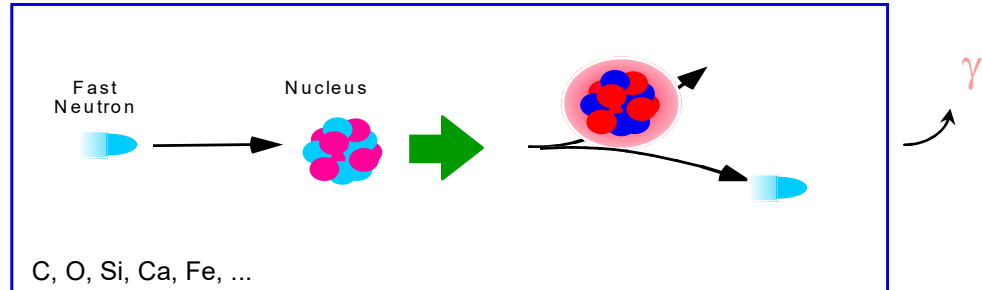
Test Chamber material
leveling

Test Facility: Data Acquisition Scheme

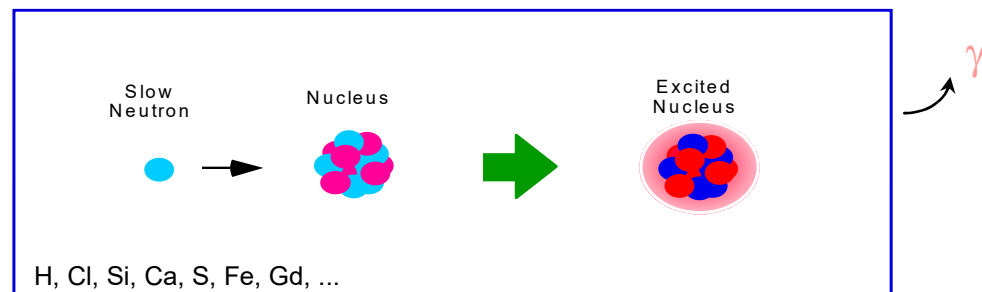


Neutron Interactions

INELASTIC SCATTERING



THERMAL CAPTURE



NEUTRON ACTIVATION

Inelastic or capture reaction that leads to a radioactive element and decay.
Examples:

O-activation	$T_{1/2} = 7.1 \text{ s}$	$(n + {}_8\text{O}^{16} \rightarrow {}_7\text{N}^{16} + \dots \rightarrow {}_8\text{O}^{16} + \gamma + \dots)$
Al-activation	$T_{1/2} = 2.3 \text{ m}$	$(n + {}_{13}\text{Al}^{27} \rightarrow {}_{13}\text{Al}^{28} \rightarrow {}_{14}\text{Si}^{28} + \gamma + \dots)$
Si-activation	$T_{1/2} = 2.3 \text{ m}$	$(n + {}_{14}\text{Si}^{28} \rightarrow {}_{13}\text{Al}^{28} + \dots \rightarrow {}_{14}\text{Si}^{28} + \gamma + \dots)$

(Na, Cu, Fe..... and many more).

Neutron Inelastic Scatter ($n, n'\gamma$)

- Incoming neutron collides with target nucleus and exits with less energy and at a different angle
- Deposited energy excites target nucleus and releases a γ -ray to return to normal energy state:



- For inelastic scattering to take place, the incoming neutron energy must exceed the threshold energy derived from Q value formula:

$$T_n \geq E_{L1} \frac{A+1}{A}$$

Where,

- T_n is the kinetic energy of the incident neutron
- E_{L1} is the energy of the target nucleus' first excited level
- A is the atomic number of the target nucleus

Common Non-elastic Scattering Reactions

Reaction	Gamma Ray Energy, keV	Threshold, MeV	Peak Cross Section, mb	Energy of Peak, MeV
$^{12}\text{C}(\text{n},\text{n}\gamma)^{12}\text{C}$	4438.0	4.8	450.	8.1
$^{16}\text{O}(\text{n},\text{n}\gamma)^{16}\text{O}$	6128.6	6.6	265.	7.5–9.0
$^{16}\text{O}(\text{n},\text{p})^{15}\text{N}$	6128.6	10.6	50.	11.5
$^{16}\text{O}(\text{n},\text{np}\gamma)^{15}\text{N}$	5269.2	16.5	40.	27.5
$^{16}\text{O}(\text{n},\text{n}\alpha\gamma)^{12}\text{C}$	4438.0	12.3	130.	19.
$^{24}\text{Mg}(\text{n},\text{n}\gamma)^{24}\text{Mg}$	1368.6	1.4	600.	2.5–6.0
$^{27}\text{Al}(\text{n},\text{n}\gamma)^{27}\text{Al}$	1014.4	1.1	220.	2.5–6.7
$^{27}\text{Al}(\text{n},\text{n}\gamma)^{27}\text{Al}$	2211.	2.25	210.	7.0–9.5
$^{28}\text{Si}(\text{n},\text{n}\gamma)^{28}\text{Si}$	1779.0	1.8	770.	4.5–6.0
$^{32}\text{S}(\text{n},\text{n}\gamma)^{32}\text{S}$	2230.1	2.3	440.	6.7–10.0
$^{40}\text{Ar}(\text{n},\text{n}\gamma)^{40}\text{Ar}$	1460.8	1.5	800.	3.–10.
$^{40}\text{Ar}(\text{n},\text{p})^{40}\text{Cl}$	1460.8	8.0	20.	14.5
$^{40}\text{Ca}(\text{n},\text{n}\gamma)^{40}\text{Ca}$	3736.5	3.8	130.	7.0
$^{56}\text{Fe}(\text{n},\text{n}\gamma)^{56}\text{Fe}$	846.8	0.9	1150.	6.
$^{56}\text{Fe}(\text{n},\text{n}\gamma)^{56}\text{Fe}$	1238.3	2.1	475.	16.5

Note: Hydrogen does not give off inelastic scatter photons

Neutron Capture (n,γ)

- Highest probability at thermal energies
 - Can occur at high energies, but with reduced cross sections
- Neutron interacts with a target nucleus and is absorbed
- Newly formed nucleus is placed in an excited state, releasing at least 1 photon to form a new ground state:
$${}_0^1n + {}_Z^AX \rightarrow {}_{Z+1}^{A+1}X^* \rightarrow {}_{Z+1}^{A+1}X + \gamma$$
- Each nucleus gives off a distinct signature of intensities and energies allowing for the identification of the sample from the energy signatures

Note: Helium-4 does not undergo neutron capture

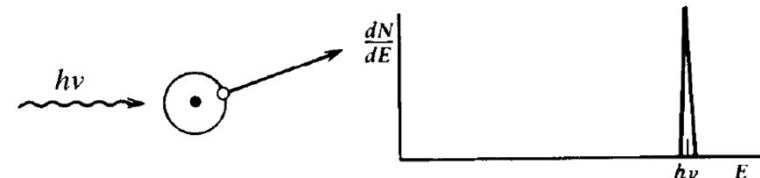
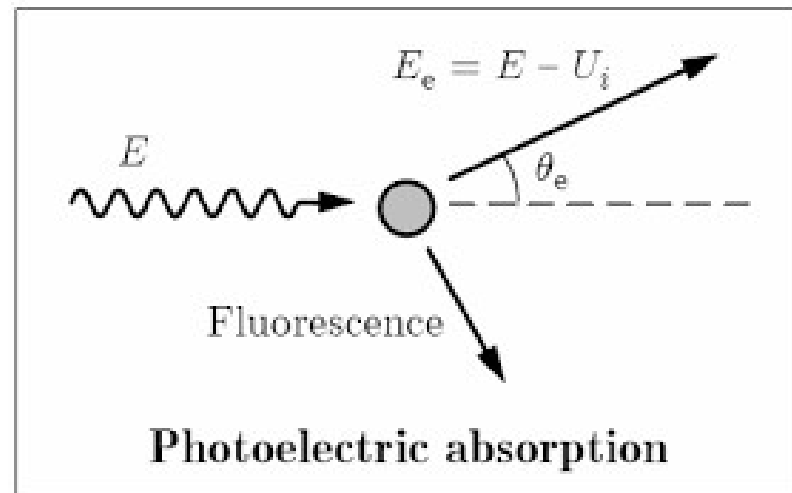
Photon Physics – Photoelectric Absorption

- An incoming photon interacts with a target atoms' electron
- Deposits all energy
- Ejects the electron from its bound shell
- Photoelectron carries an energy given by:

$$E_{e-} = h\nu - E_b$$

Where,

- E_b is the binding energy of the photoelectron in its original shell
- E_{e-} is the energy of the exited photoelectron
- $h\nu$ is the energy of the incoming photon



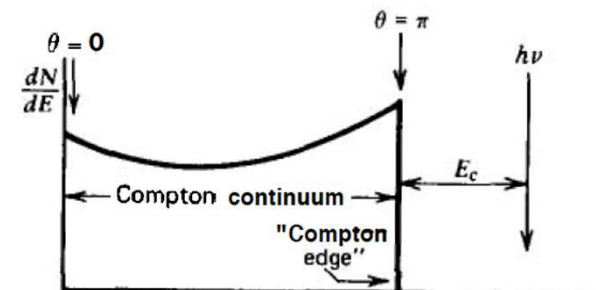
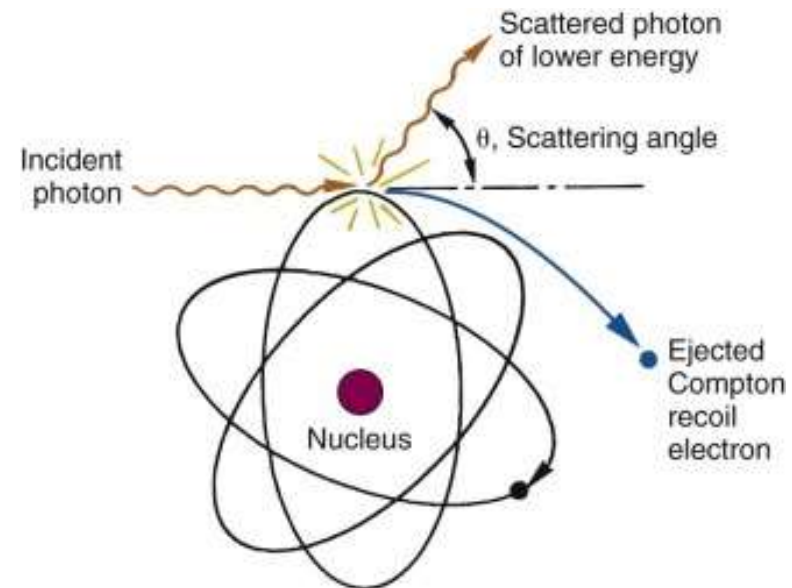
Photon Physics – Compton Scattering

- Photon interacts with an electron in an atom
- Imparts some energy, ejecting an electron, and continuing on a deflected angle
- The energy transferred to the electron can range based on the incoming energy and scattering angle by:

$$E'_\gamma = \frac{E_\gamma}{1 + (1 - \cos\theta)E_\gamma/m_e c^2}$$

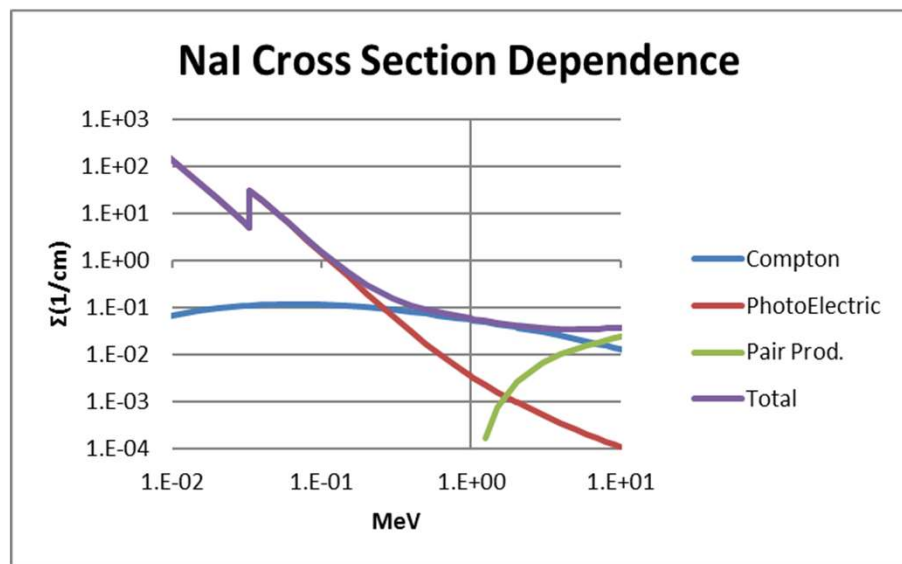
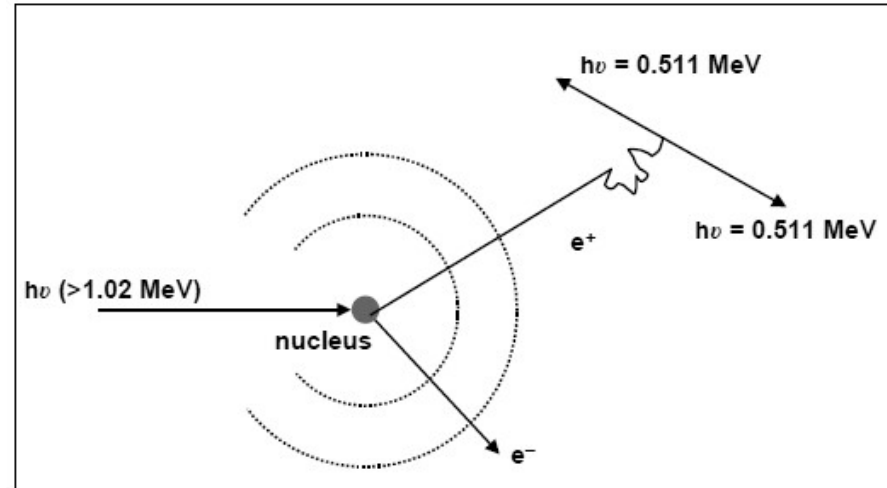
Where,

- E'_γ is the scattered photon energy
- E_γ is the energy of the incident photon
- $\cos\theta$ is the scattering angle in the lab frame
- m_e is the mass of the electron
- c is the speed of light



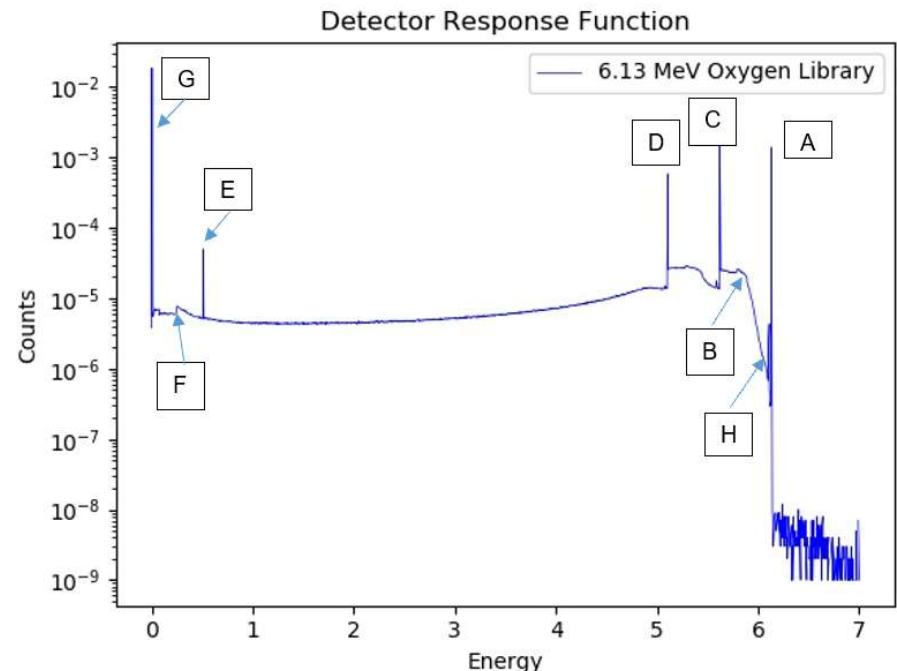
Photon Physics – Pair Production

- When an incoming photon exceeds 1.02 MeV, pair production can occur
- Photon becomes near the nucleus, energy is converted into an electron-positron pair
- Positron will interact with nearby electron creating 2 annihilation 0.511 MeV photons

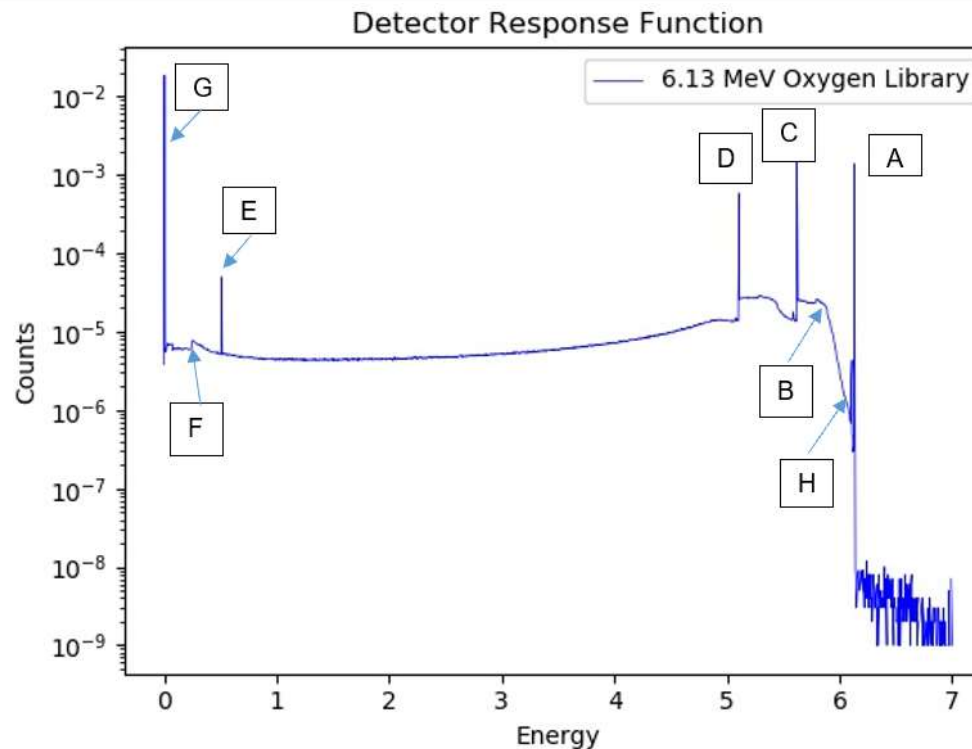


Detector Physics and Features

- MCNP Simulation
 - F8 Tally – energy deposition
 - “Perfect resolution”
- Oxygen-16 activation (N-16 decay)
 - 6.130 MeV photon
 - 7.13 second half life
- Oxygen-16 inelastic scatter
 - 6.13 MeV prompt gamma



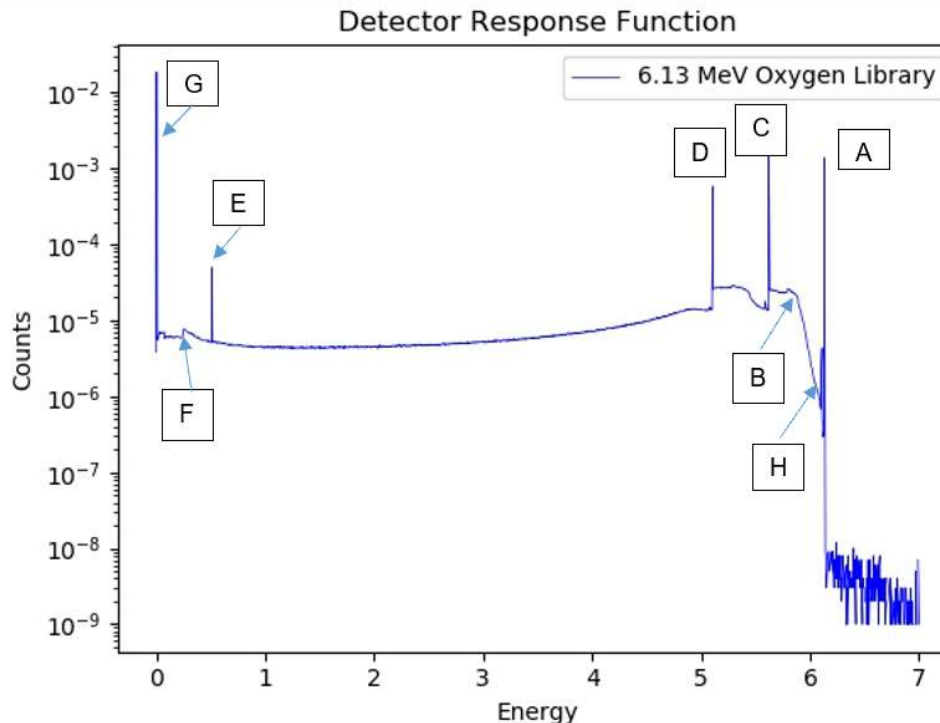
Detector Response Features



A: Full Energy Peak

- The full energy peak is equal to the incoming photon energy, 6.13 MeV for this example. The pulse signals that produce this signature occur when the particle enters the detector and deposits all of its energy with no escaping secondary particles. This can occur in a single photoelectric absorption or by a series of reactions. For this reason, the full energy peak can be referred to as the “photoelectric peak”.

Detector Response Features

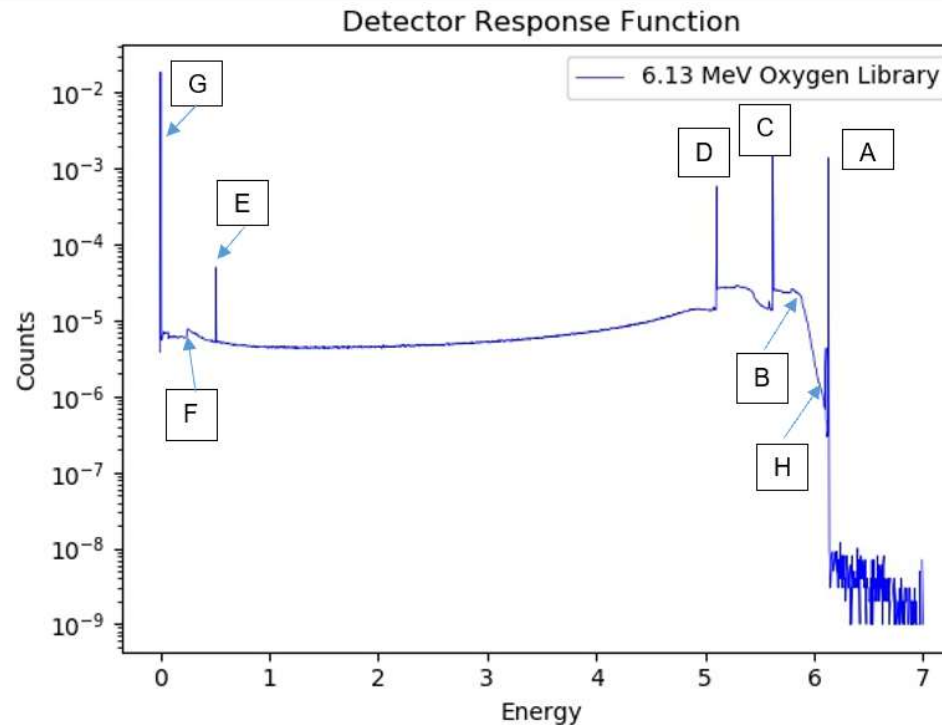


B: Compton Edge

- The Compton edge occurs once a photon undergoes a Compton scattering reaction, and then exits the detector without depositing additional energy. The scattering angle determines the energy that is deposited in the detector, ranging from 0° to 180° . The maximum energy deposited by a Compton scattering identified as the Compton edge is:

$$\Delta E = E_\gamma - E'_\gamma = 6.13 - \frac{6.13}{1 + (1 - \cos\pi) * \frac{6.13}{0.511}} = 5.88 \text{ MeV}$$

Detector Response Features



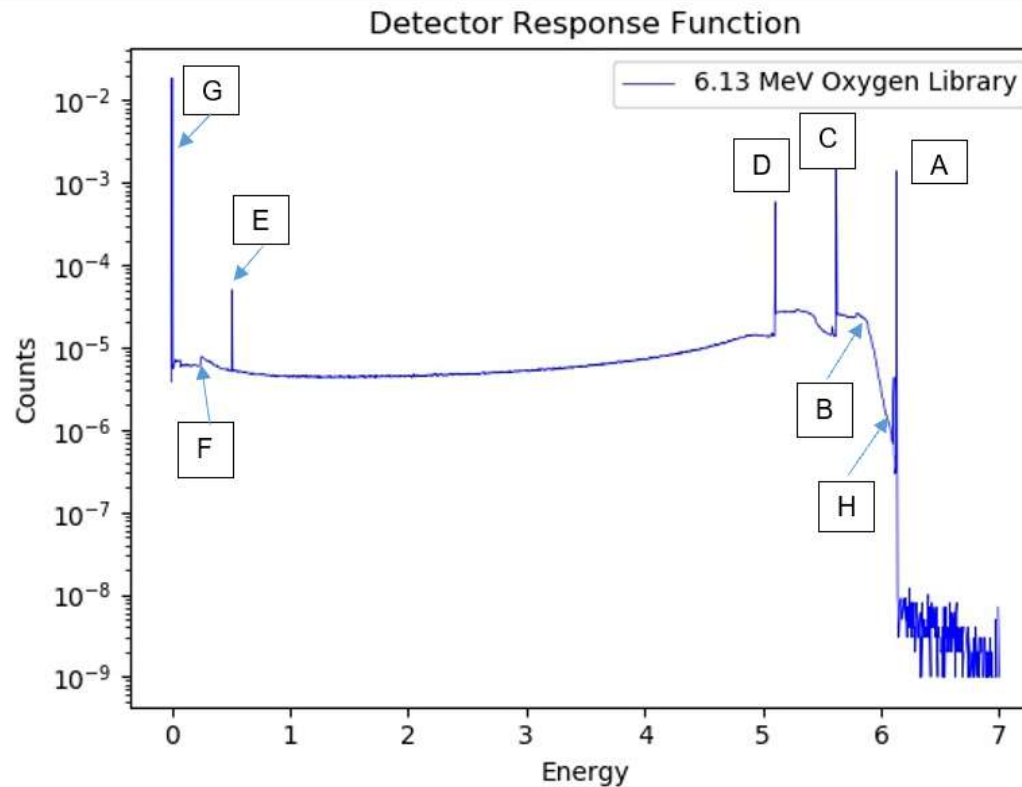
C: Single Escape Peak

- In the event a photon creates a pair production reaction, an electron-positron pair is created. The positron will then annihilate inside the detector, creating a 0.511 MeV photon. If the annihilation photon exits the detector without depositing its energy and the full energy of the incoming photon is deposited inside the detector, the result is the single escape peak. The energy of the peak is equal to the full energy peak minus the resting mass energy of an electron, 0.511 MeV.

D: Double Escape Peak

- The double escape peak is the result of both annihilation photons escape the detector. In this way, the resulting energy is equal to that of the full energy peak minus the resting mass energy of two electrons, 1.022 MeV.

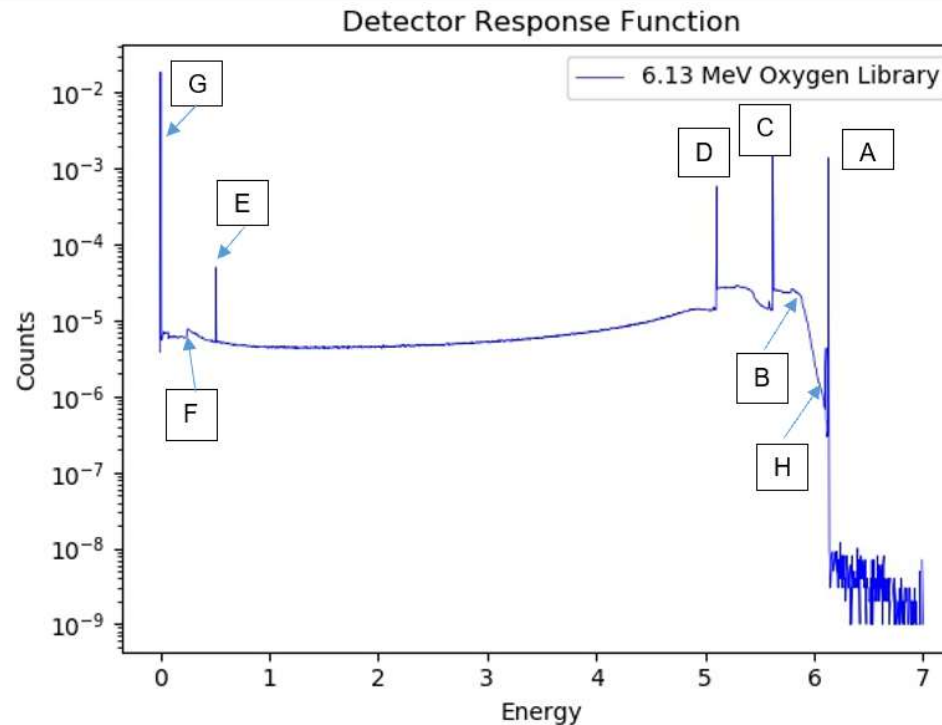
Detector Response Features



E: Annihilation Peak

- In the event that the incoming particle interacts with a material outside of the detector by a pair production reaction, a resulting annihilation photon can enter the detector and deposit its energy. The annihilation peak appears when the detector is surrounded by a dense material and is equal to 0.511 MeV.

Detector Response Features

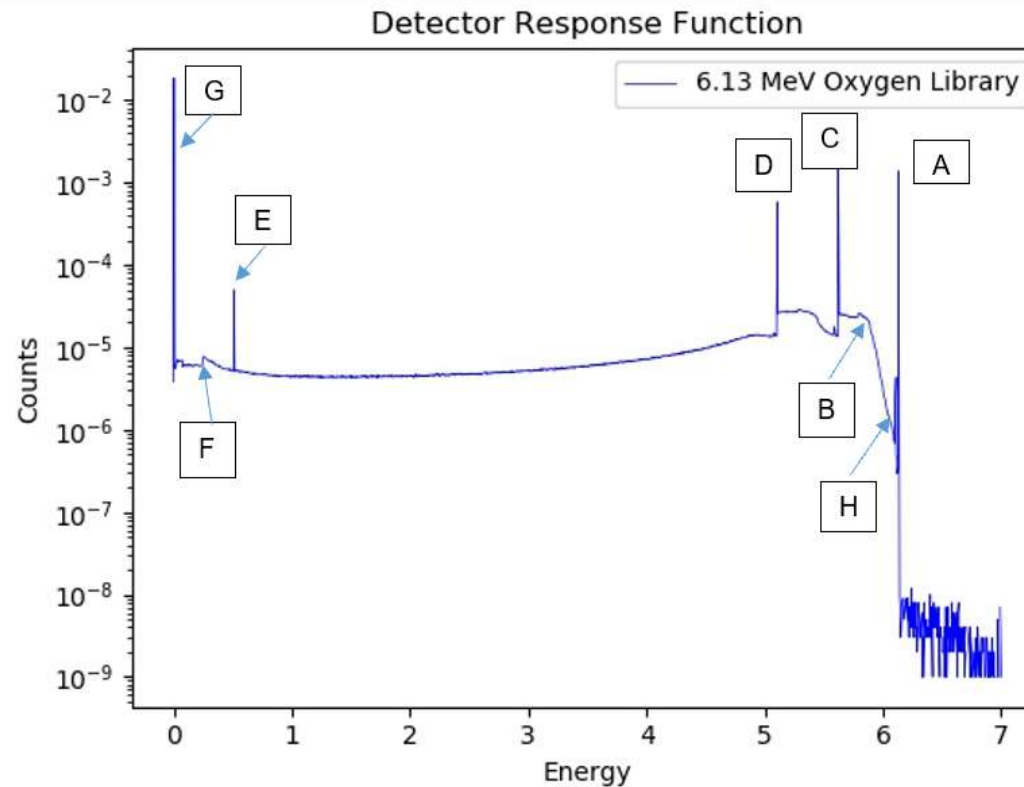


F: Backscattering Peak

- The backscattering peak is created when a Compton scattering even occurs outside the detector and the scattered photon reaches the detector and deposits its full energy. The scattering angle occurs over a small range of angles around 180°. This causes the peak to be a range of energies instead of a singular energy peak. The energy for backscattering peaks is usually between 200 and 300 KeV. For the case of 180° scatter, the energy of the incoming scattered photon would be

$$E'_{\gamma} = \frac{6.13}{1 + (1 - \cos\pi) * \frac{6.13}{0.511}} = 0.245 \text{ MeV}$$

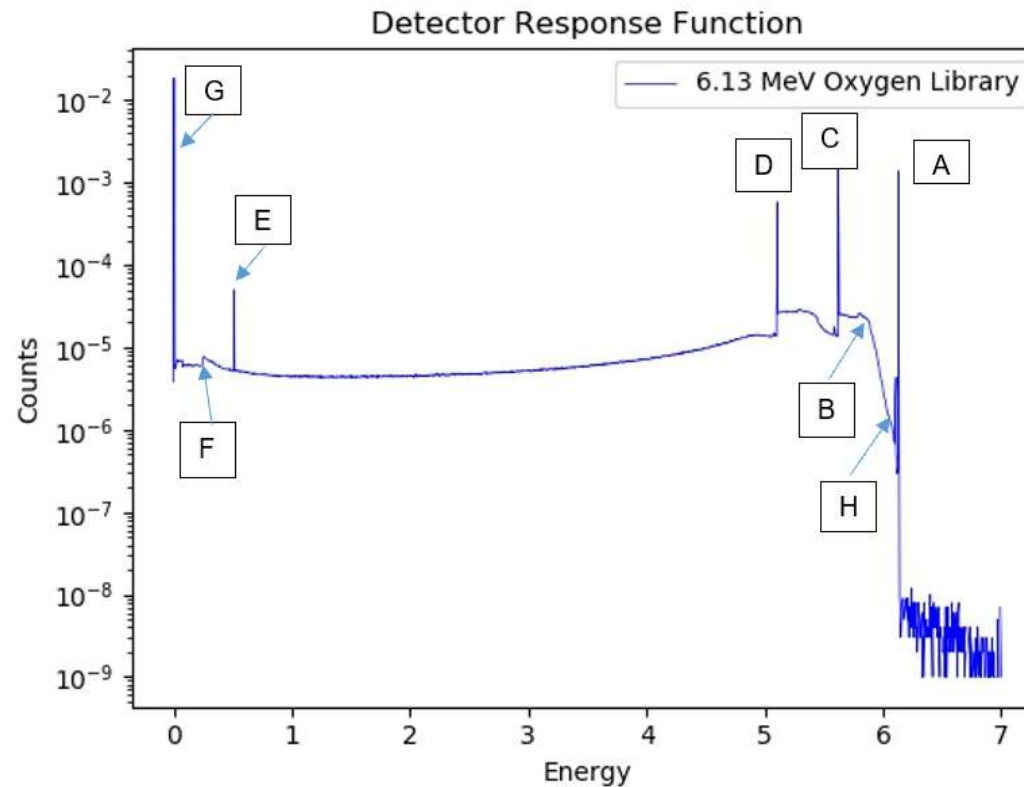
Detector Response Features



G: X-Ray Fluorescence Peaks

- X-ray fluorescence peaks are not of interest to prompt gamma neutron activation analysis and contributes to a collection of noise signatures that collect below 100 KeV. These peaks are generated by interactions that occur in the surrounding medium by exciting the target atom. During the de-excitation, characteristic X-ray photons are emitted and enter the detector and deposit their full energy. These peaks complicate the fitting functions, as they can be orders of magnitude higher than other signatures within the spectrum.

Detector Response Features



H: X-Ray Escape Peaks

- When the excited atoms are generated within the detector, an X-ray photon can exit the detector. The resulting energy response is equal to the full energy peak minus the energy carried by the exited photon. If the detector material is larger than 1", these events happen infrequently and do not affect the total response substantially.

Monte Carlo Library Least Squares

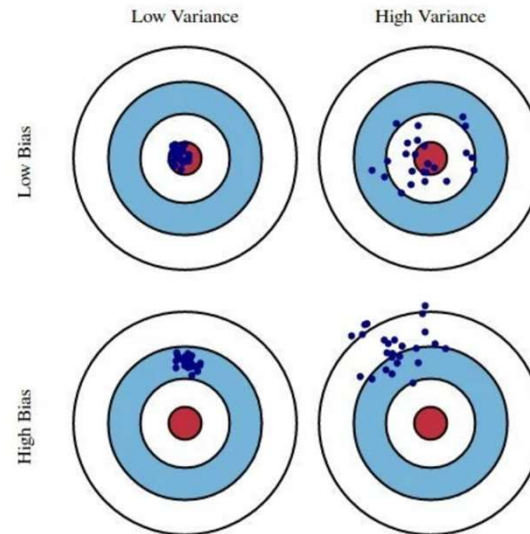
- Same principle as ordinary least squares with library spectra used as the input
- $y_i = \sum_{j=1}^m a_j x_{ij} + E_i, i = 1, n$
 - y_i is the counts per channel i
 - a_j are linear coefficients for each element j
 - x_{ij} are the library spectra, or counts in channel i of element j
 - E_i is random error in counts in channel i
- Error analysis can be performed by reducing Chi-Square:

$$\chi^2_v = \sum_{i=1}^n \frac{e_i^2}{(n-m)\sigma_i^2}$$

- $(n - m)$ is the number of degrees of freedom
- e_i is random error in counts in channel i
- σ_i^2 is the variance of the random error in counts in each channel i
- How to deal with changing environments and unknown compositions?

Supervised Machine Learning

- Ordinary Least Squares traditionally suffers from overfitting
 - Too many model parameters
- Model selection should have the right parameters to accurately predict/fit correct solution
- Adding complexity to the model increases bias while reducing variance
- Supervised machine learning variable selection techniques aim to minimize unnecessary bias and variance simultaneously by selecting the correct parameters



LASSO (Tibshirani, 1996)

- The LASSO (Least Absolute Selection and Shrinkage Operator) is defined as:
 - $\hat{\beta}^{lasso} = \underset{\beta \in \mathbb{R}^p}{\operatorname{argmin}} \|y - X\beta\|_2^2 + \lambda \sum_{j=1}^p |\beta_j|$
 - or $= \underset{\beta \in \mathbb{R}^p}{\operatorname{argmin}} \|y - X\beta\|_2^2 + \lambda \|\beta\|_1$
- Where the first term is the loss function and $\lambda \|\beta\|_1$ serves as a penalty
 - Note: if $\lambda=0$, the equation is identical to that of Ordinary Least Squares (OLS)
- As λ increases, the penalty for each new coefficient grows, allowing variable selection to occur in linear models

Elastic Net (Zou and Hastie, 2005)

- LASSO does not perform well
 - a) In a case where the number of observations (n) are less than the number of parameters (p) LASSO can select at most n variables
 - b) In a case where there are a large number of predictors that are highly correlated, LASSO tends to select only 1, seemingly at random (grouping effect)
 - c) In a case where $n > p$ and the predictors are highly correlated; LASSO is dominated by shrinkage methods like Ridge Regression
- Elastic Net is a modification of LASSO that adds a quadratic penalty as defined below:
 - $\hat{\beta}^{ElasticNet} = \underset{\beta \in \mathbb{R}^p}{\operatorname{argmin}} \|y - X\beta\|_2^2 + \lambda_2 \|\beta\|^2 + \lambda_1 \|\beta\|_1$
 - The quadratic penalty:
 - Removes limitation on the number of selected variables
 - Encourages *grouping effect*
 - Stabilizes the L1 regularization path

Derivation of LASSO and Elastic Net by Coordinate Descent – Linear Model

- The linear model, given a vector of inputs X_j , an output Y can be predicted as :

$$\hat{Y} = \hat{\beta}_0 + \sum_{j=1}^p X_j \hat{\beta}_j$$

- Where,
 - $\hat{\beta}_0$ is the intercept, also known as the bias in machine learning
 - \hat{Y} is the predicted output
- $\hat{\beta}_0$ can be included in the vector coefficients and a constant variable 1 in X, allowing the equation to be rewritten as:

$$\hat{Y} = X^T \hat{\beta} + \varepsilon$$

- Where,
 - X^T is the vector or matrix transpose
 - \hat{Y} is the predicted output
 - $\hat{\beta}$ is the linear coefficient
 - ε is the error

Derivation of LASSO and Elastic Net by Coordinate Descent – Linear Model

- Fitting a linear model to a training data set is popularly done by selecting the β coefficients that minimize the residual sum of squares:

$$\begin{aligned} RSS(\beta) &= \sum_{i=1}^N (y_i - x_i^T \beta)^2 \\ &= \sum_{i=1}^N (y_i - \beta_0 - \sum_{j=1}^p x_{ij} \beta_j)^2 \end{aligned}$$

- The ordinary least squares estimator can be computed by using the following equation

$$\hat{\beta}_{OLS} = (\mathbf{X}^T \mathbf{X})^{-1} \mathbf{X}^T \mathbf{Y}$$

Derivation of LASSO and Elastic Net by Coordinate Descent – Notations (Gauraha, 2018)

- Consider the standard linear regression equation, assume the components of the noise vector are independent and identically distributed. Using subscripts j to denote the j th column of a dataset. Assuming that the design matrix \mathbf{X} is fixed, the data is adjusted to be centered, and the predictors are standardized such that:

$$\sum_{i=1}^n \mathbf{Y}_i = 0, \sum_{i=1}^n (\mathbf{X}_j)_i = 0 \text{ and}$$
$$\frac{1}{n} \mathbf{X}_j^T \mathbf{X}_j = 1 \text{ for all } j = 1, \dots, p.$$

- The $l_{0,1,2}$ -norms are defined as:

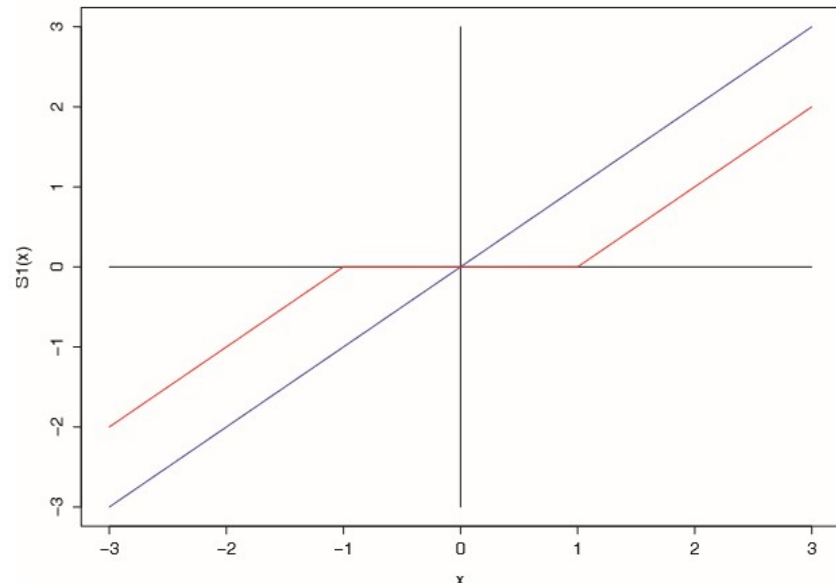
$$\|\beta\|_0 = \sum_{j=1}^p I(\beta_j \neq 0)$$

$$\|\beta\|_1 = \sum_{j=1}^p |\beta_j|$$

$$\|\beta\|_2^2 = \sum_{j=1}^p \beta_j^2$$

- Then, the soft-thresholding operator can be defined as follows:

$$S_\lambda(x) = \begin{cases} x + \lambda & \text{if } x < -\lambda \\ 0 & \text{if } |x| \leq \lambda \\ x - \lambda & \text{if } x > \lambda \end{cases}$$



Derivation of LASSO and Elastic Net by Coordinate Descent – LASSO Univariate Solution

- Before moving to a case involving multiple variables, a single variable case is considered. For this case, $p=1$ and $\mathbf{Y} = \mathbf{X}_1\boldsymbol{\beta}_1 + \varepsilon$, and the optimization problem can be written as:

$$\underset{\boldsymbol{\beta} \in \mathbb{R}^p}{argmin} \frac{1}{n} \|\mathbf{Y} - \mathbf{X}_1\boldsymbol{\beta}_1\|_2^2 + \lambda |\boldsymbol{\beta}_1|$$

- Assuming $\hat{\boldsymbol{\beta}}_1$ is a solution to the equation above, then the sub-differential must contain zero, meaning:

$$-\frac{2}{n} \mathbf{X}_1^T (\mathbf{Y} - \mathbf{X}_1\hat{\boldsymbol{\beta}}_1) + \lambda * sign(\hat{\boldsymbol{\beta}}_1) = 0,$$

Which can be rewritten as:

$$\frac{1}{n} \mathbf{X}_1^T (\mathbf{Y} - \mathbf{X}_1\hat{\boldsymbol{\beta}}_1) = \frac{\lambda}{2} sign(\hat{\boldsymbol{\beta}}_1)$$

Derivation of LASSO and Elastic Net by Coordinate Descent – LASSO Univariate Solution

- Note that since we are assuming the predictors are standardized, $\frac{1}{n} \mathbf{X}_1^T \mathbf{X}_1 = 1$,

$$\hat{\beta}_1 = \begin{cases} \frac{1}{n} \mathbf{X}_1^T \mathbf{Y} - \frac{\lambda}{2} sign(\hat{\beta}_1) & \\ \frac{1}{n} \mathbf{X}_1^T \mathbf{Y} + \frac{\lambda}{2} & \text{if } \frac{1}{n} \mathbf{X}_1^T \mathbf{Y} < -\frac{\lambda}{2} \\ 0 & \text{if } \frac{1}{n} \mathbf{X}_1^T \mathbf{Y} \leq \frac{\lambda}{2} \\ \frac{1}{n} \mathbf{X}_1^T \mathbf{Y} - \frac{\lambda}{2} & \text{if } \frac{1}{n} \mathbf{X}_1^T \mathbf{Y} > \frac{\lambda}{2} \end{cases}$$

- An alternative interpretation is that $\hat{\beta}_1 = \frac{1}{n} \mathbf{X}_1^T \mathbf{Y}$ is soft-thresholded by $\frac{\lambda}{2}$ such that:

$$\hat{\beta}_1 = S_{\frac{\lambda}{2}} \left(\frac{1}{n} \mathbf{X}_1^T \mathbf{Y} \right)$$

- Therefore, the LASSO estimator for a single variable case can be computed by soft-thresholding the OLS estimator by $\frac{\lambda}{2}$ or

$$\hat{\beta}_1 = S_{\frac{\lambda}{2}} (\hat{\beta}_{OLS})$$

- Where $\hat{\beta}_{OLS} = \frac{1}{n} \mathbf{X}_1^T \mathbf{Y}$.

Derivation of LASSO and Elastic Net by Coordinate Descent – LASSO Full Solution

- Coordinate descent is an iterative method that solves one variable iteratively, while holding all other variables constant. For each coordinate sub-problem, each component of β is fixed except for the j th component β_j . By denoting \mathbf{X}_j as the j th column of \mathbf{X} and \mathbf{X}_{-j} denote all of the columns except for the j th column, then the problem can be rewritten as:

$$\underset{\beta \in \mathbb{R}^p}{\operatorname{argmin}} \left\{ \frac{1}{n} \|\mathbf{Y} - \mathbf{X}_{-j}\beta_{-j} - \mathbf{X}_j\beta_j\|_2^2 + \lambda |\beta_j| + \lambda \sum_{l \neq j} |\beta_l| \right\}$$

- Next, we define $r_j := \mathbf{Y} - \mathbf{X}_{-j}\beta_{-j}$ as the partial residual or the difference between the actual response \mathbf{Y} and the fitted model that excludes variable \mathbf{X}_j . The solution above becomes the univariate LASSO problem with vector r_j as the response variable:

$$\underset{\beta \in \mathbb{R}^p}{\operatorname{argmin}} \left\{ \frac{1}{n} \|r_j - \mathbf{X}_j\beta_j\|_2^2 + \lambda |\beta_j| + \lambda \sum_{l \neq j} |\beta_l| \right\}$$

- Now suppose $\hat{\beta}_j$ is a solution to the optimization problem above. Then the stationary condition yields the following:

$$\begin{aligned} -\frac{2}{n} \mathbf{X}_j^T (r_j - \mathbf{X}_j \hat{\beta}_j) + \lambda * sign(\hat{\beta}_j) &= 0, \\ \frac{1}{n} r_j^T \mathbf{X}_j - \hat{\beta}_j &= \frac{\lambda}{2} sign(\hat{\beta}_j) \end{aligned}$$

- The OLS estimator for the j th variable can then be computed as $\hat{\beta}_{OLS,j} = \frac{1}{n} r_j^T \mathbf{X}_j$. The univariate LASSO solution can then be computed by soft-thresholding the OLS estimator as:

$$\hat{\beta}_j = S_{\frac{\lambda}{2}}((\hat{\beta}_{OLS})_j)$$

Derivation of LASSO and Elastic Net by Coordinate Descent – LASSO Full Solution

LASSO Coordinate Descent Algorithm

Input: dataset (\mathbf{Y} , \mathbf{X})

Output: $\hat{\beta}$: =LASSO estimated vector of regression coefficients

Initialize $\beta = 0$

repeat

for each $j \in \{1, \dots, p\}$ **do**

 Compute the partial residual r_j , where

$$r_j = \mathbf{Y} - \sum_{l \neq j} \mathbf{X}^l \beta_l$$

 Compute the OLS coefficient for single predictor

$$(\hat{B}_{OLS})_j = \frac{1}{n} r_1^T \mathbf{X}_j$$

 Update β_j (LASSO solution: single variable case)

$$\beta_j = S_{\frac{\lambda}{2}}((\hat{B}_{OLS})_j)$$

end

until convergence;

$\hat{\beta} = \beta$

Return $\hat{\beta}$

Derivation of LASSO and Elastic Net by Coordinate Descent – Elastic Net Full Solution

- The derivation and steps to calculate the Elastic Net penalty via coordinate descent are similar to those taken to calculate the LASSO penalty (Yang, 2013). The second order penalty adds an additional term to the LASSO solution such that:

$$\underset{\beta \in \mathbb{R}^p}{\operatorname{argmin}} \frac{1}{n} \|Y - X_1\beta_1\|_2^2 + P_{\lambda,\alpha}(\beta)$$

- Where $P_{\lambda,\alpha}(\beta)$ is the Elastic Net penalty defined as:

$$P_{\lambda,\alpha}(\beta) = \lambda \sum_{j=1}^p p_\alpha(\beta_j) = \lambda \sum_{j=1}^p \left[\frac{1}{2} (1 - \alpha) \beta_j^2 + \alpha |\beta_j| \right]$$

- Note that when $\alpha = 1$, the Elastic Net reduces to the LASSO equation. When each predictor shows a strong correlation, some $\alpha < 1$ should be used. For each fixed λ , coordinate descent is used to solve the Elastic Net. Once again, we define a current residual $r_j := Y - X_{-j}\beta_{-j}$ that excludes the jth term from each calculation. To update the estimate for β_j , the univariate Elastic Net problem is solved by:

$$\hat{\beta}_j = \underset{\beta \in \mathbb{R}^p}{\operatorname{argmin}} \left\{ \frac{1}{n} \|r_j - X_j\beta_j\|_2^2 + \lambda p_\alpha(\beta_j) \right\}$$

- The soft threshold is applied, leading to:

$$\hat{\beta}_j = \frac{S\left(\frac{1}{n} r^T X_j + \beta_j, \lambda\alpha\right)}{1 + \lambda(1 - \alpha)}$$

Derivation of LASSO and Elastic Net by Coordinate Descent – Elastic Net Full Solution

Elastic Net Coordinate Descent Algorithm

Input: dataset (\mathbf{Y} , \mathbf{X})

Output: $\hat{\beta}$: =Elastic Net estimated vector of regression coefficients

Initialize $\beta = 0$

repeat

for each $j \in \{1, \dots, p\}$ **do**

 Compute the partial residual r_j , where

$$r_j = \mathbf{Y} - \sum_{l \neq j} \mathbf{X}^l \beta_l$$

 Update β_j (Elastic Net solution: single variable case)

$$\hat{\beta}_j = \frac{S(\frac{1}{n} r^T \mathbf{X}_j + \beta_j, \lambda\alpha)}{1 + \lambda(1 - \alpha)}$$

end

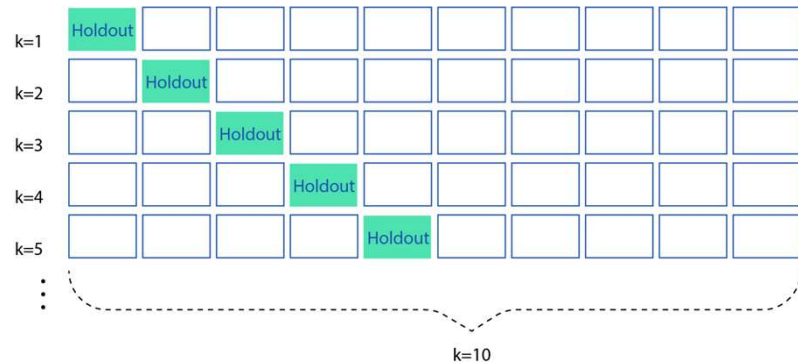
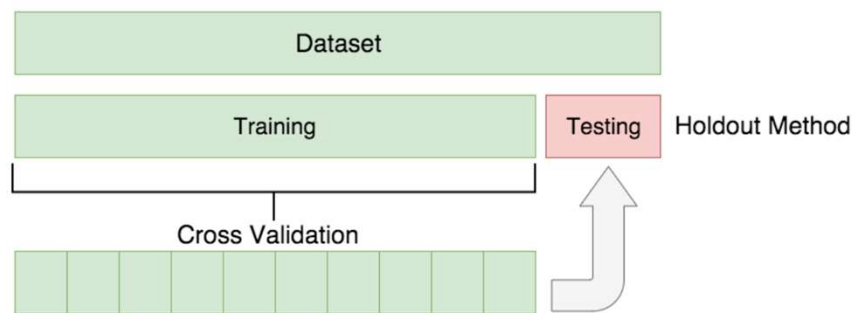
until *convergence*;

$$\hat{\beta}_j = \beta_j$$

Return $\hat{\beta}$

Cross Validation

- Each method relies on test/train split to tune model parameters
- This step introduces bias from selecting some data over others (random)
- Cross validation performs the test/train split multiple times, reducing randomness from the model training

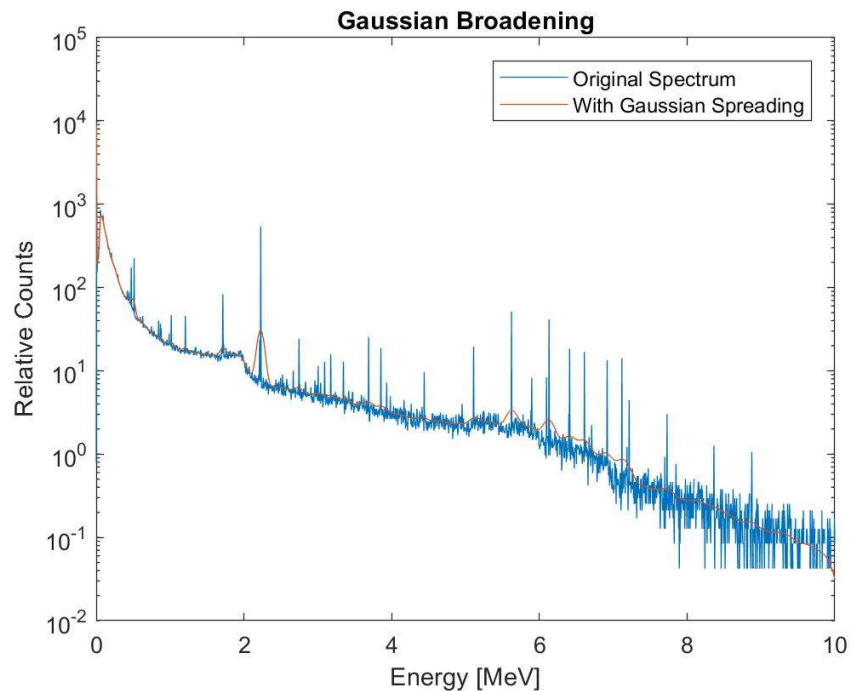


Library Generation

- Extensive MCNP simulations
 - Center for Engineering Applications of Radioisotopes (CEAR) cluster – reduced run times from 1.5-3 days to ~1 hour
 - F8 tally for gamma detection
 - No GEB
- Detector Response Function (Gardner and Sood, 2004)
 - Expected response generated in a detector from incident radiation
 - Non-linearities resolved to treat problem as a linear combination of library inputs
 - Gaussian broadening fit of full width/half max using calibration sources
 - Energy to channel conversion (2nd order polynomial in the following examples)

Processing of Data

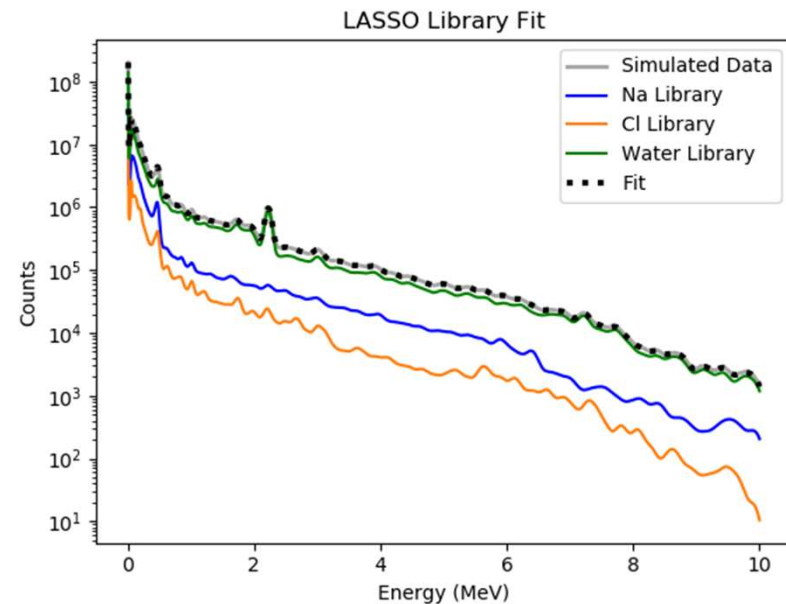
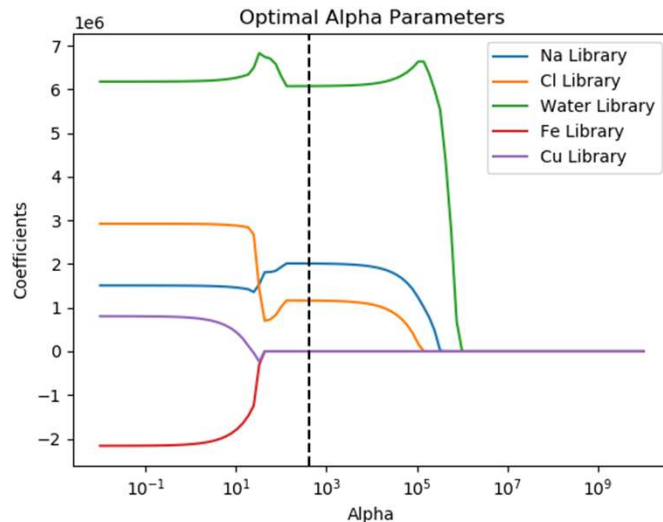
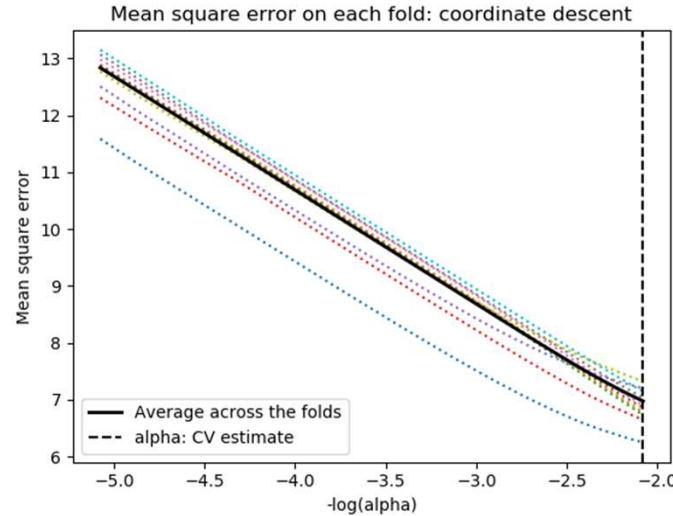
- MCNP simulations are broadened post processing (faster than GEB tally)
- Nonlinear NaI response requires adjustment during channel to energy conversion
- $Energy = a + b * channel + c * channel^2$



Simulated Example

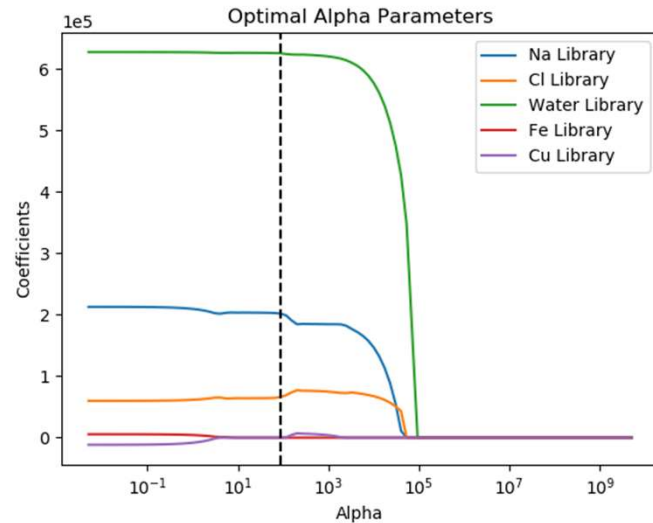
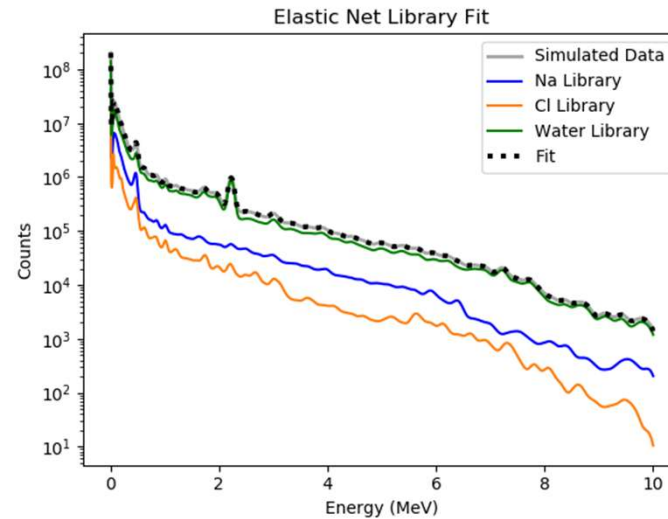
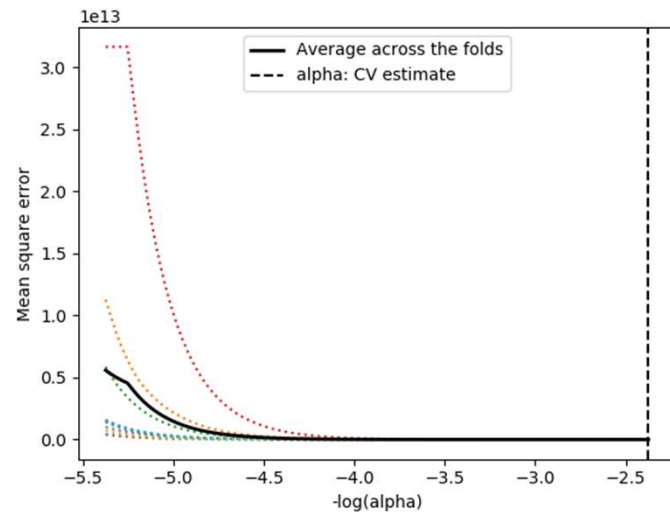
- Saltwater simulated response
 - 3.6% saltwater
- 5 total libraries used for fitting – water, sodium, chlorine, iron, and copper
 - Only water, sodium, and chlorine contribute to the spectrum
- Demonstrates
 - Cross validation curves
 - Regularization paths
 - Final fitting

LASSO Simulated Example



Note: 5 libraries are used. Fe and Cu do not contribute to the total spectrum, are given a 0 contribution and selected out of the final model.

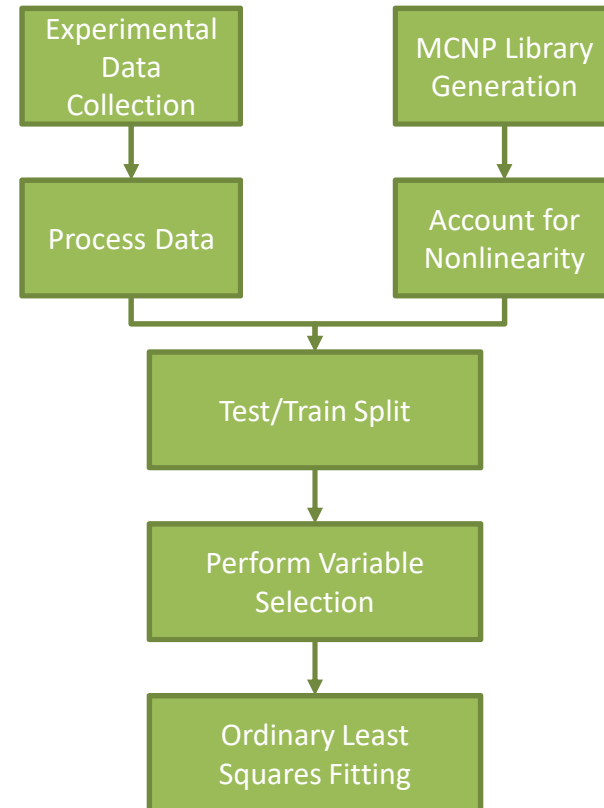
Elastic Net Simulation and Comparison



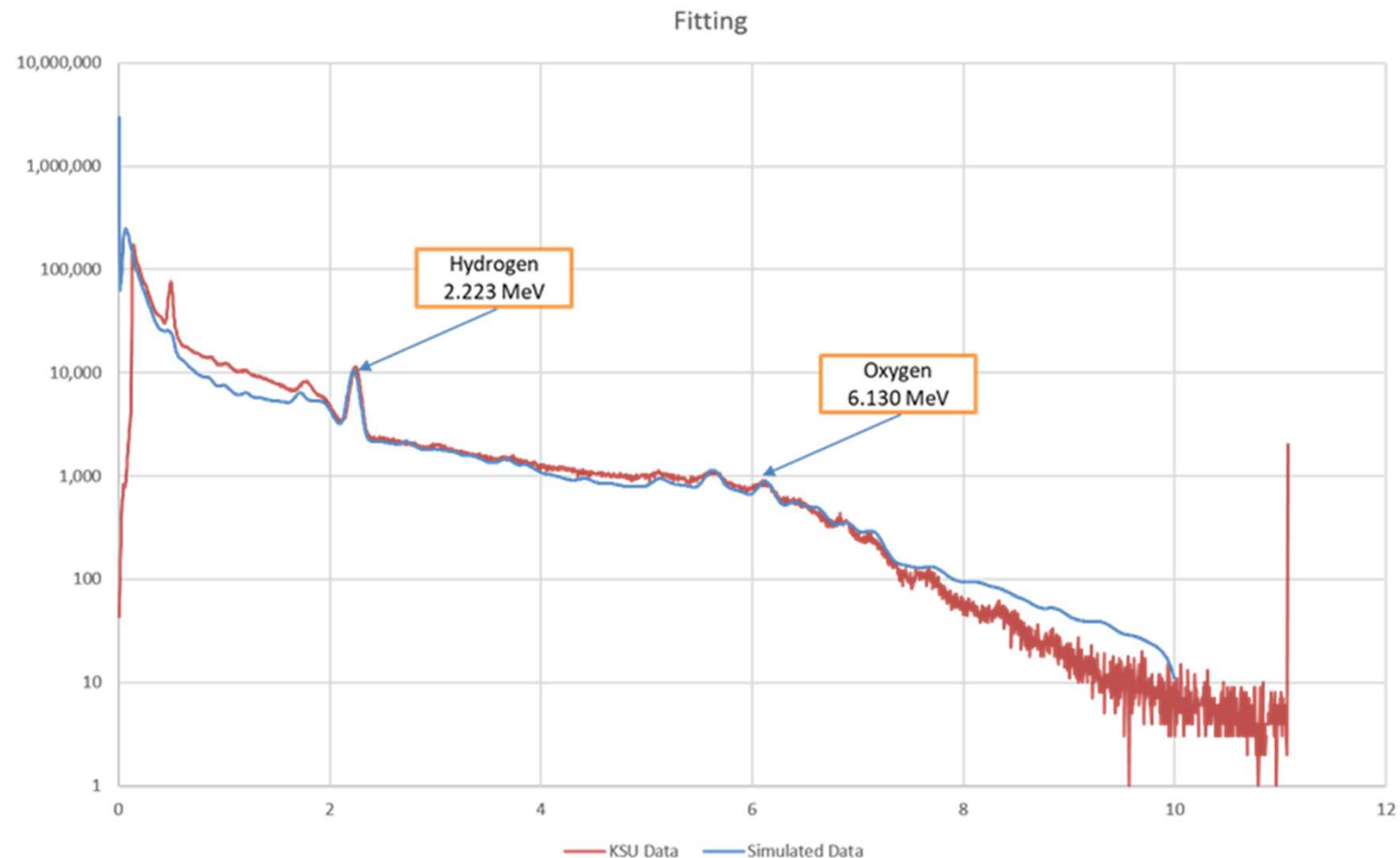
Relative Error		
	Elastic Net	LASSO
Water	5.01%	0.07%
Na	2.95%	1.32%
Cl	7.95%	3.65%

Full Run Flow Chart

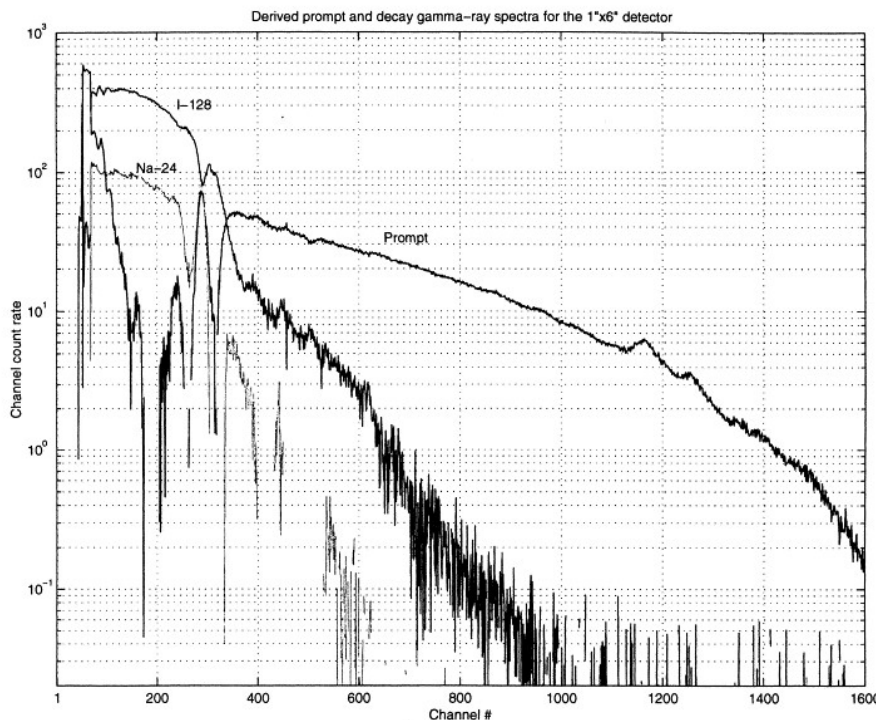
- Simulated and experimental data is generated
- Each set is processed
 - Nonlinearities removed
 - **Prompt/delayed responses are extracted**
- Test/train split data for model selection
- Variable selection through LASSO or Elastic Net remove unnecessary model parameters and provides initial guesses
- Final ordinary least squares fitting to reduce bias from model selection procedure



First Experimental Fit - Water

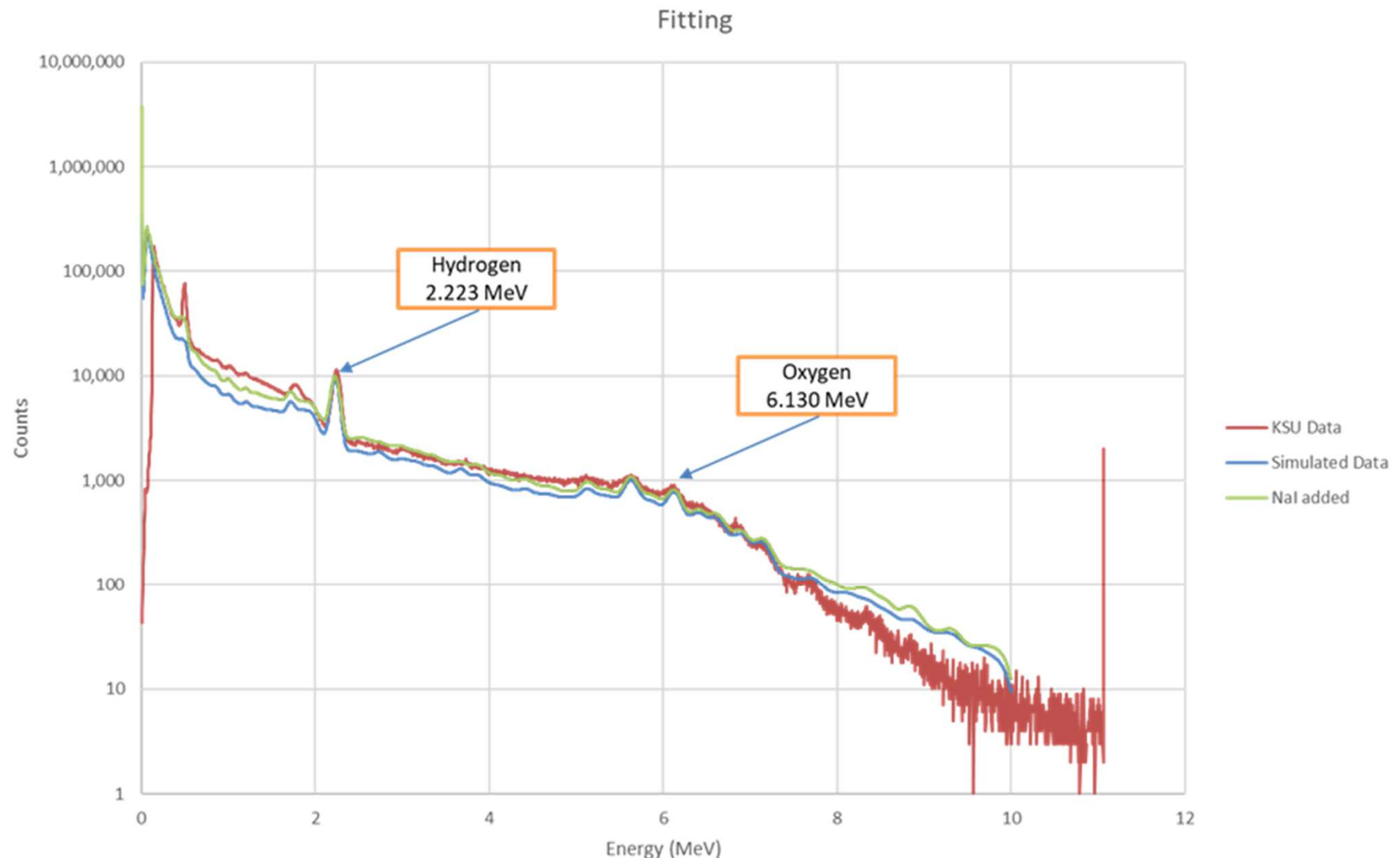


Gardner and Mayo, 2000

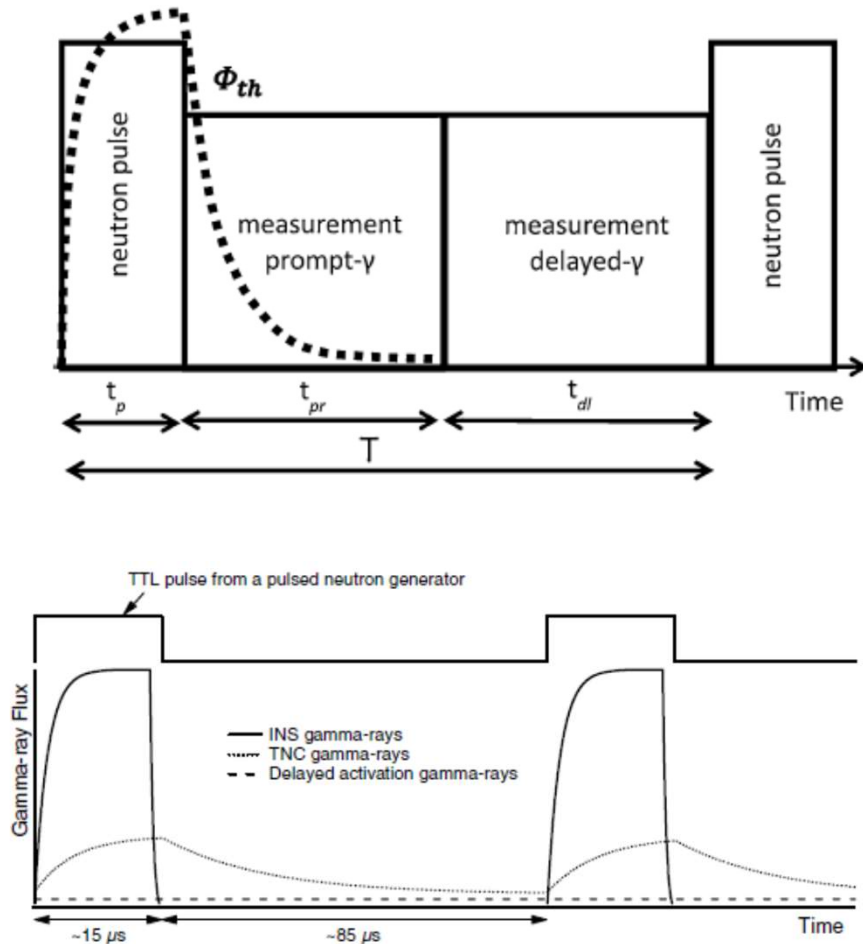


- Activated NaI detector using NC State PULSTAR reactor
- Detector activation is common during PGNAA
- I-128 more sensitive than Na-24
- β particle emission difficult to simulate using MCNP

Results With NaI Activation - Water



Pulsed Neutron Generator (PNG) die-off time

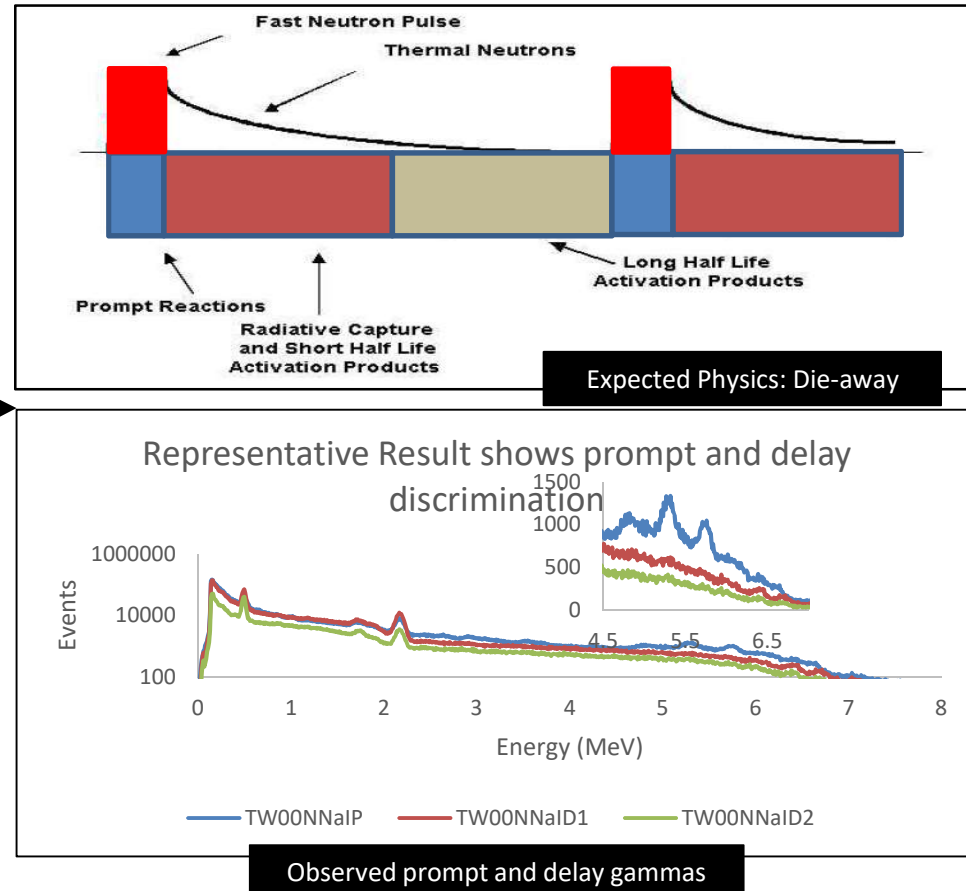
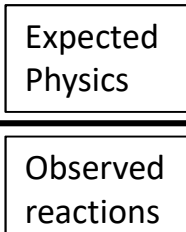


- Pulse from PNG
- Increase in gamma rays from inelastic scatter and neutron capture
- After 15-20 microseconds, inelastic gamma rays no longer contribute to total spectrum
- Neutron capture gamma rays continue exponential decrease until next pulse

Representative Test Results: Water Sample

Events list	
1	990985713 2374
2	1204979649 2726
3	1305476485 2932
4	1342423986 416
5	1670964547 -32768
6	1972904434 215
7	229908075 397
8	393453902 2391
9	467451720 2658
10	813441274 -32768

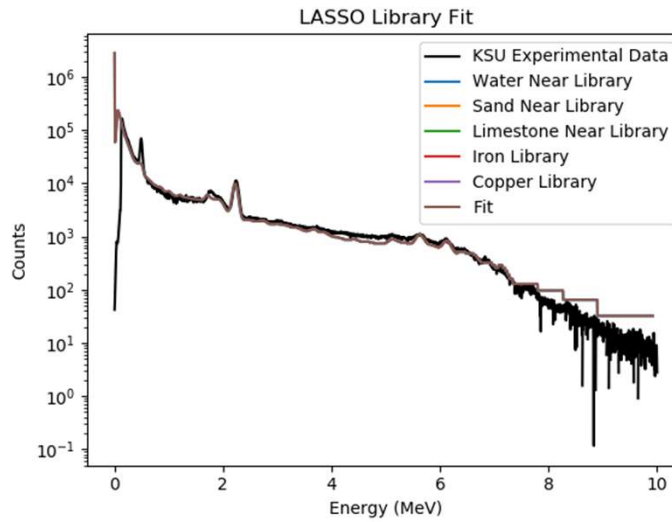
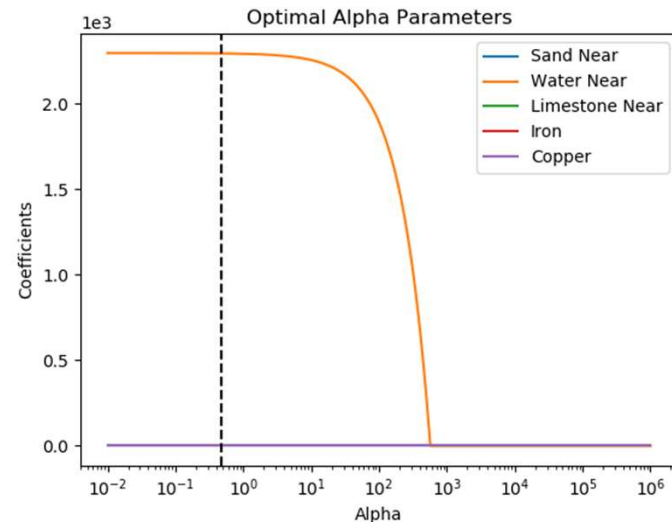
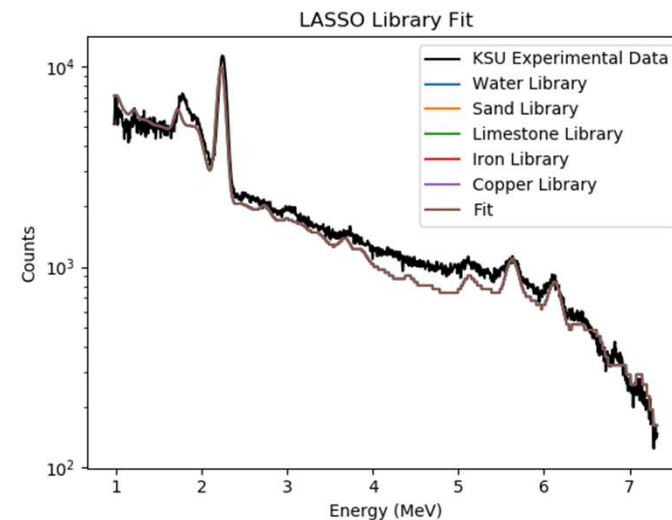
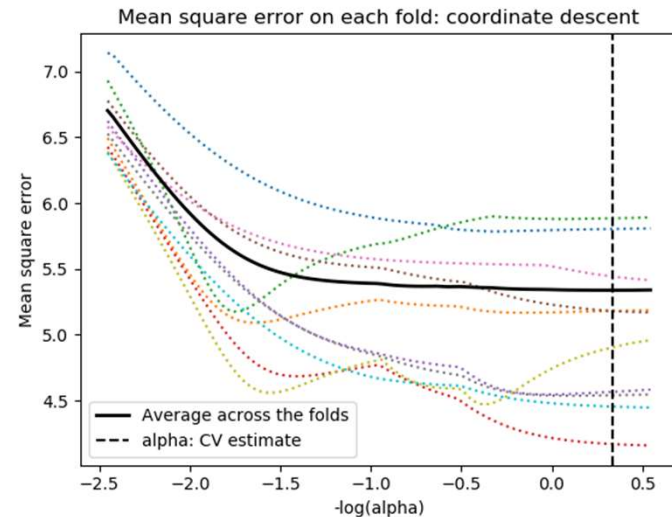
Triggers list	
1	65175 6773
2	565160 6768
3	1065144 6767
4	1565128 6769
5	2065113 6770
6	2565097 6771
7	3065082 6768
8	3565066 6771
9	4065051 6772
10	4565035 6772



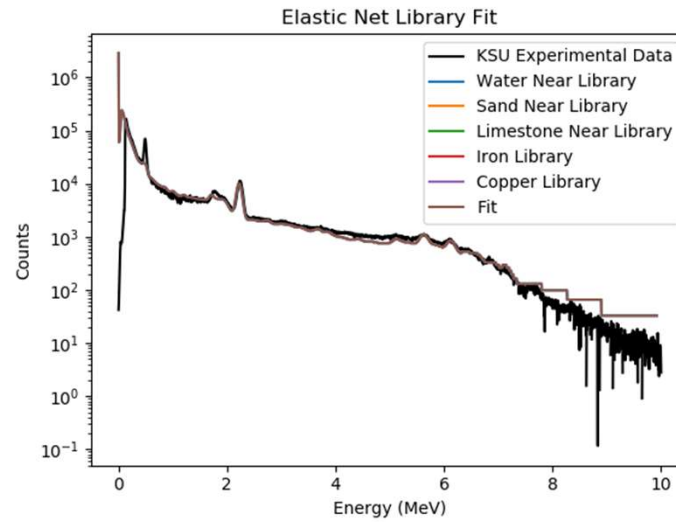
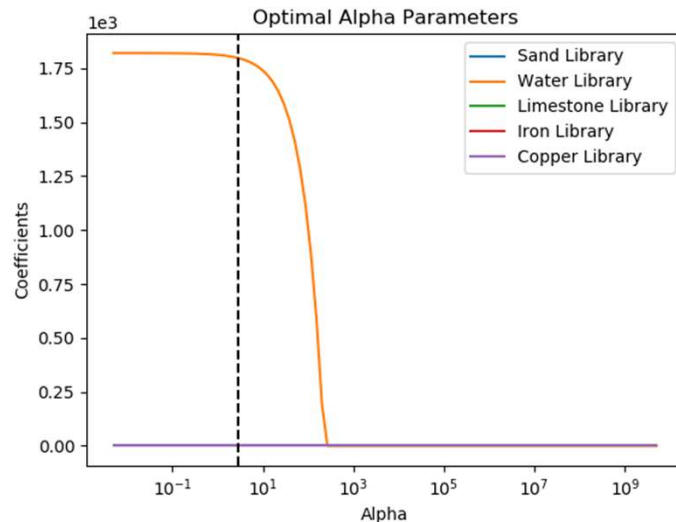
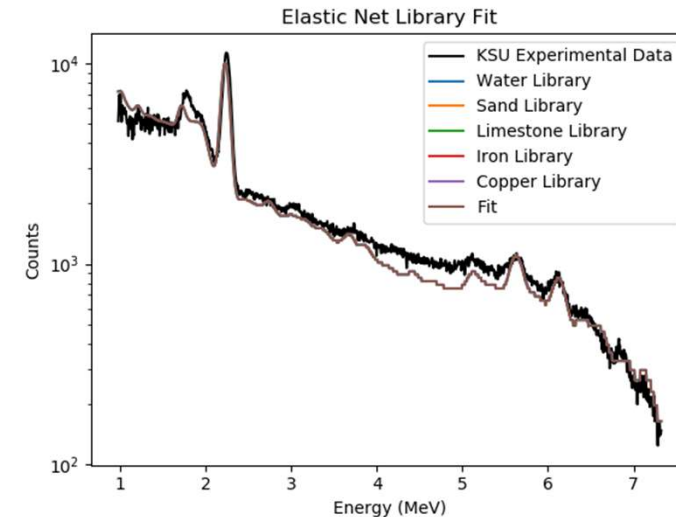
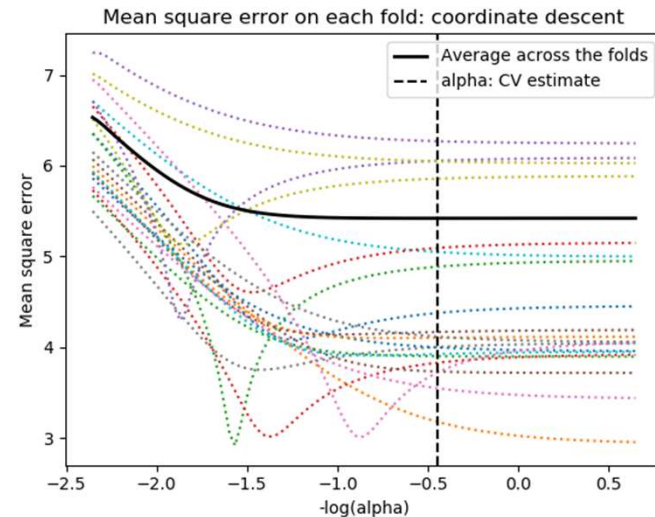
Kansas State Experiment Results

- 5 separate tests were conducted with both near and far gamma detectors
 - Water-H₂O
 - Sand-SiO₂
 - Sand with water
 - Limestone-CaCO₃
 - Limestone with water
- Data is truncated to remove low energy noise, and high energy “low statistics counts”
- Ill conditions were set by:
 - Slightly shifting experiment calibrations for sand measurements
 - Known cross sectional problems with calcium
- Each figure shown for each case is an entire random sample run

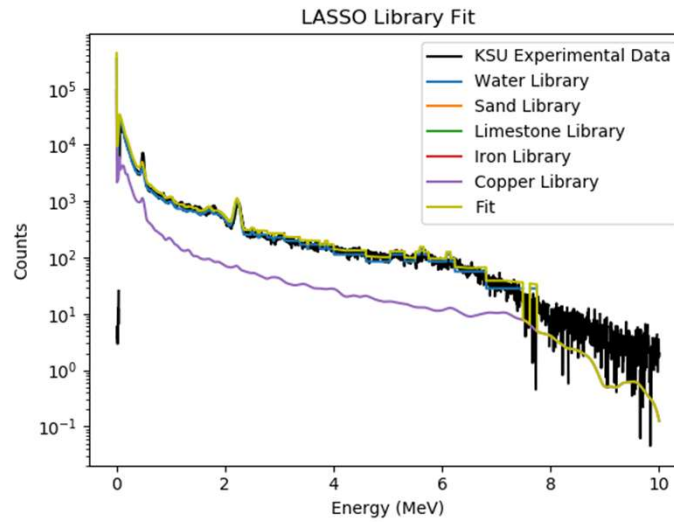
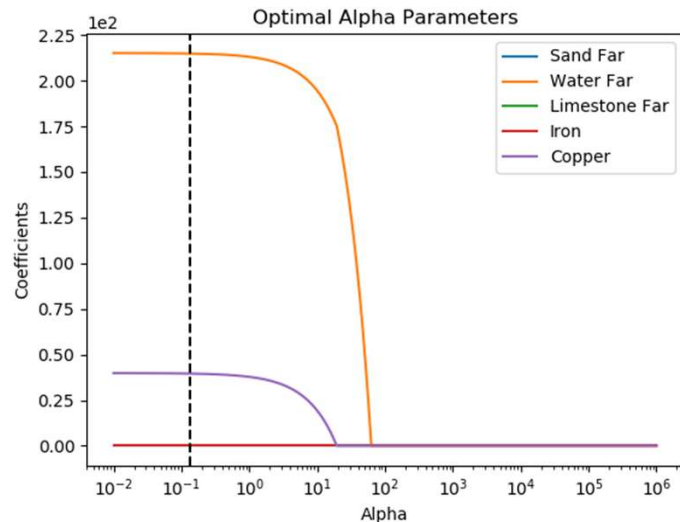
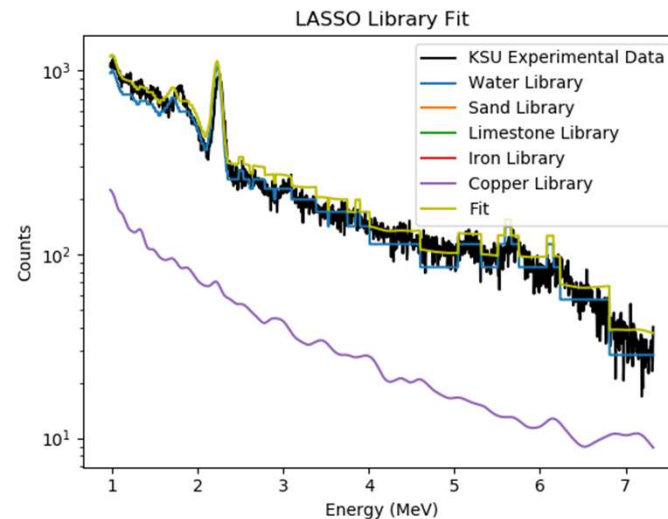
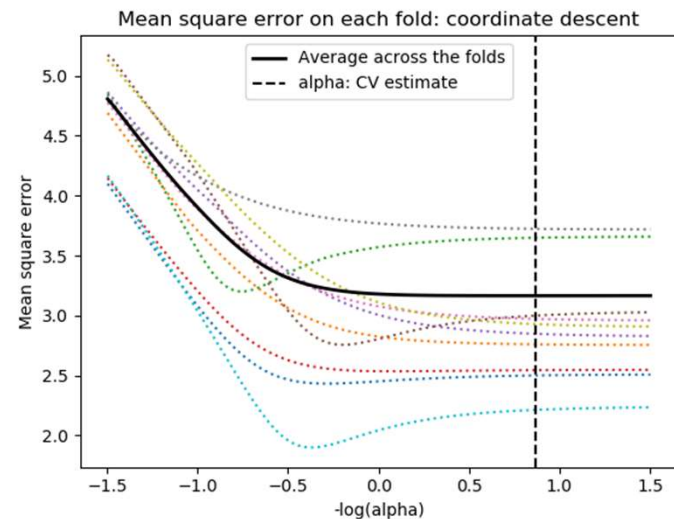
Water Trial Near - LASSO



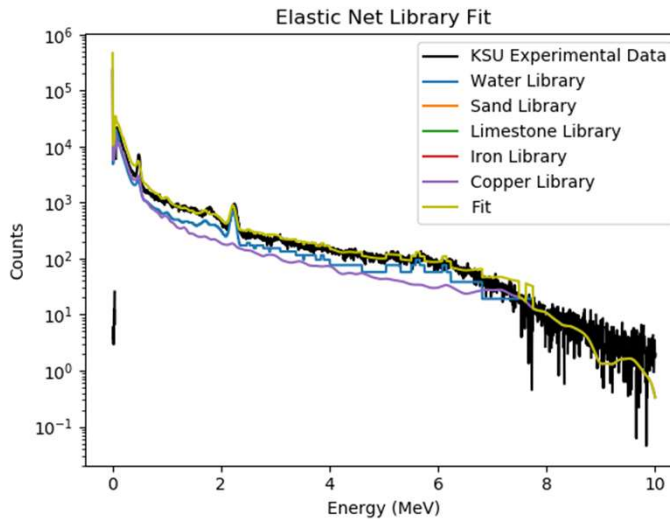
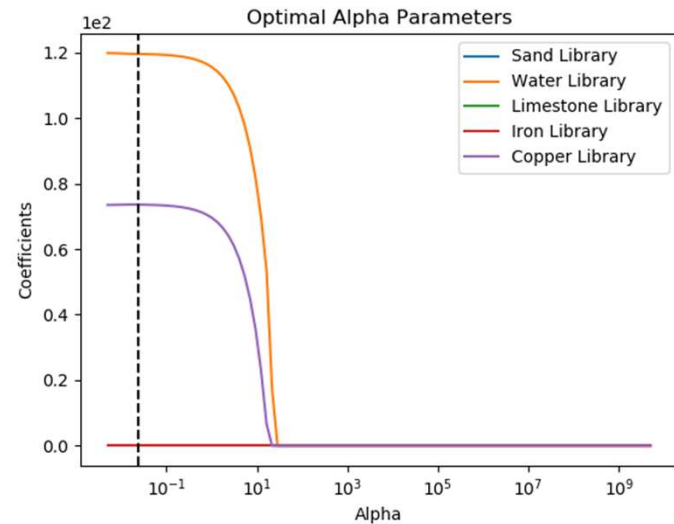
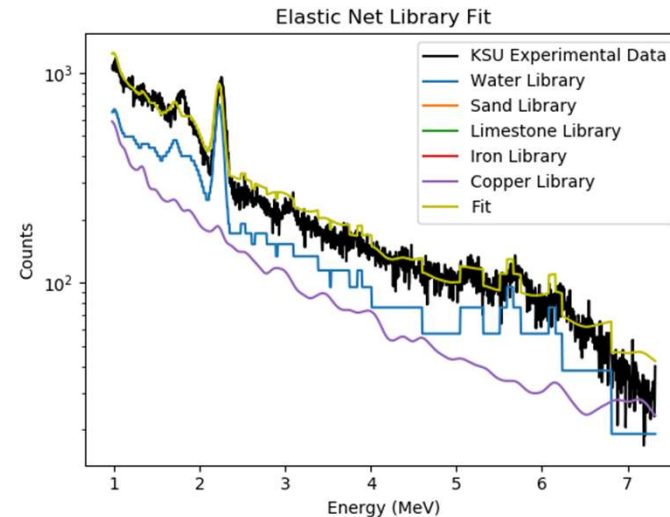
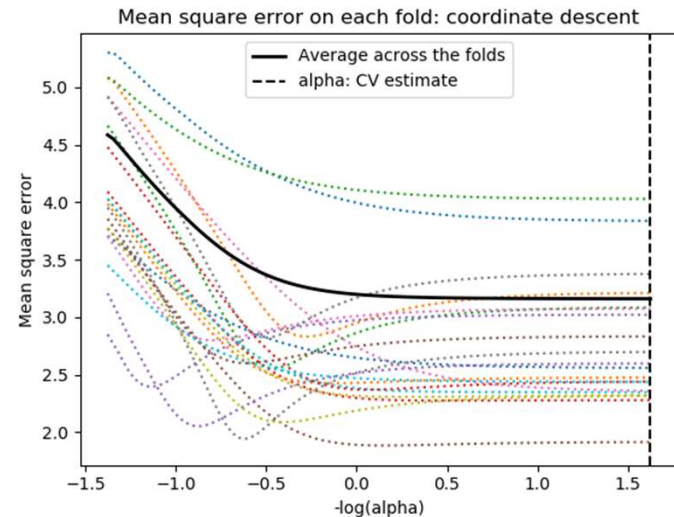
Water Trial Near – Elastic Net



Water Trial Far - LASSO

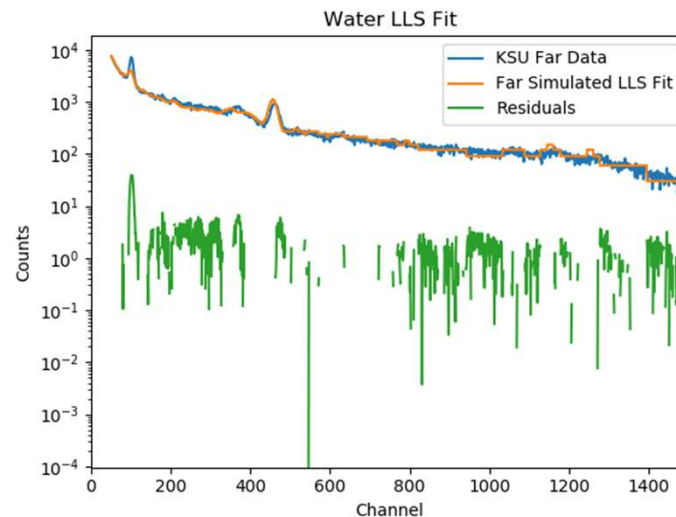
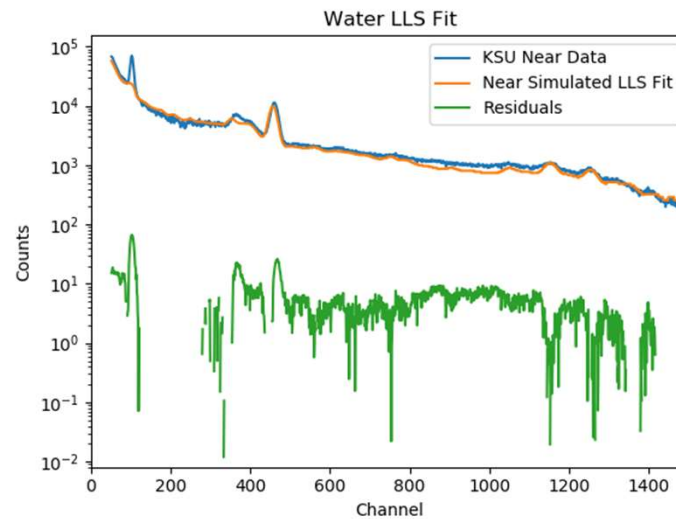


Water Trial Far – Elastic Net

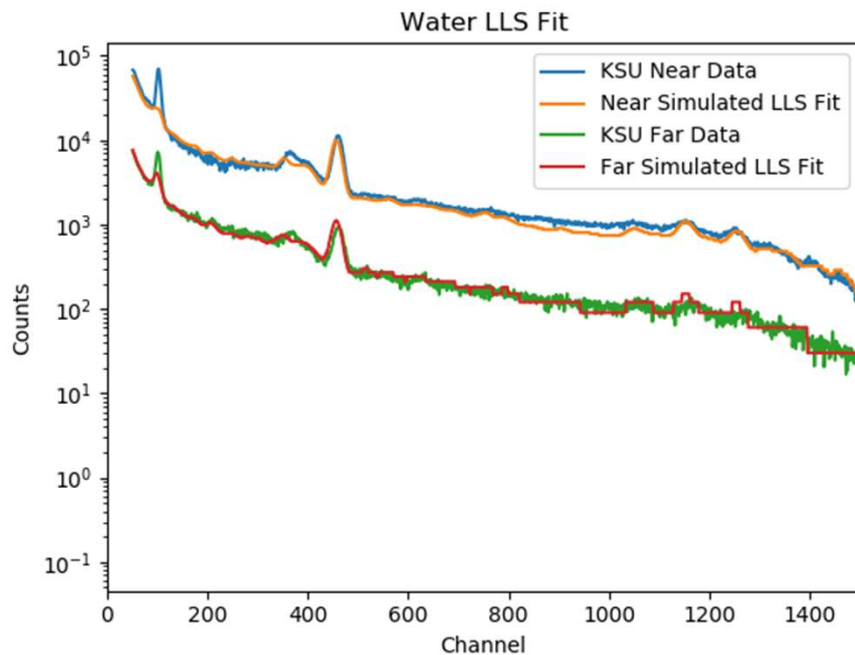


Water Trial LLS Analysis

Water Normalization Parameters		
	Near Detector	Far Detector
LASSO	0.464	0.136
Elastic Net	2.783	0.024



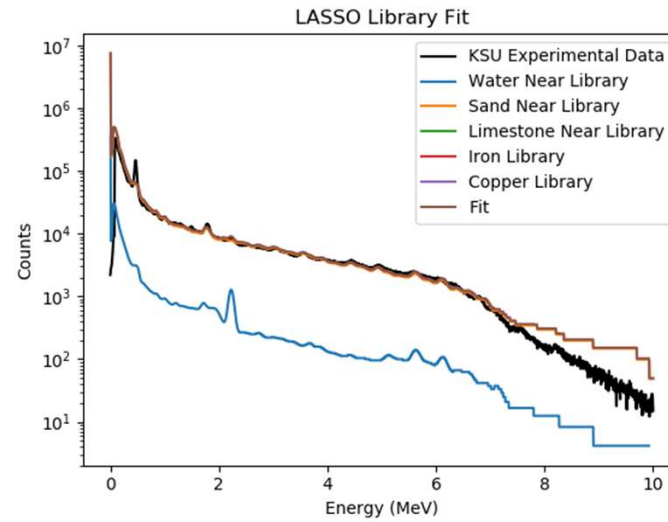
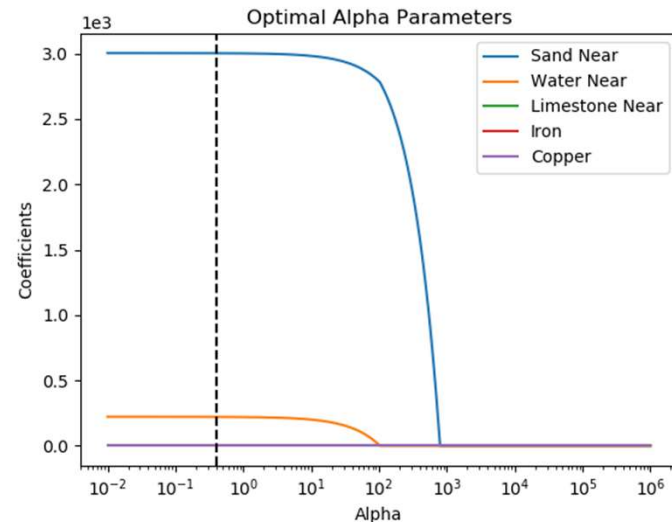
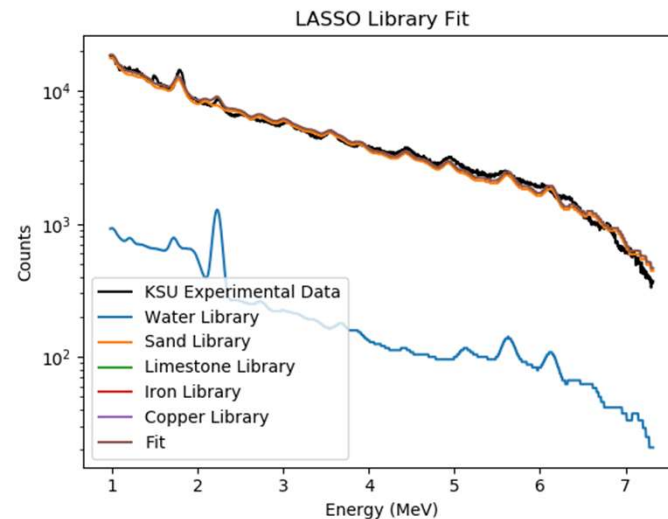
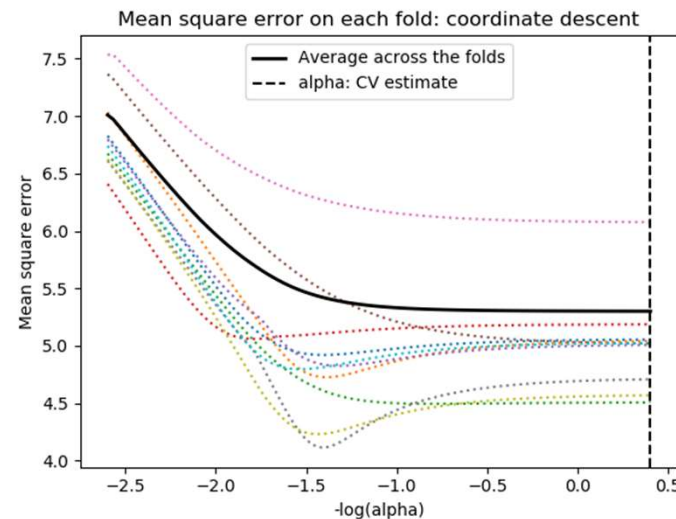
Water Trial LLS Analysis



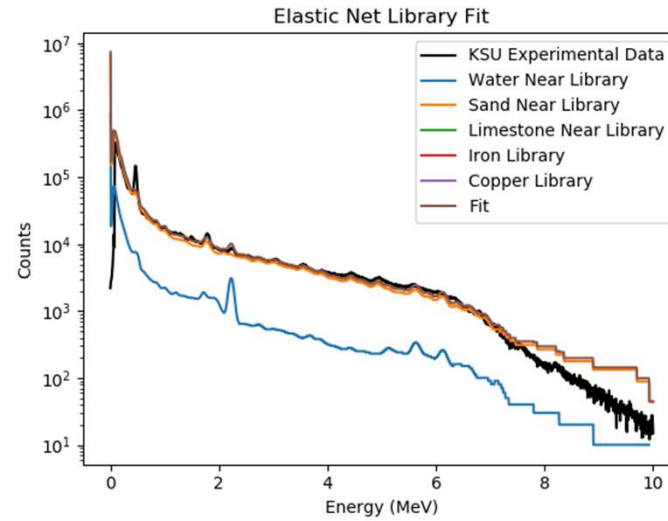
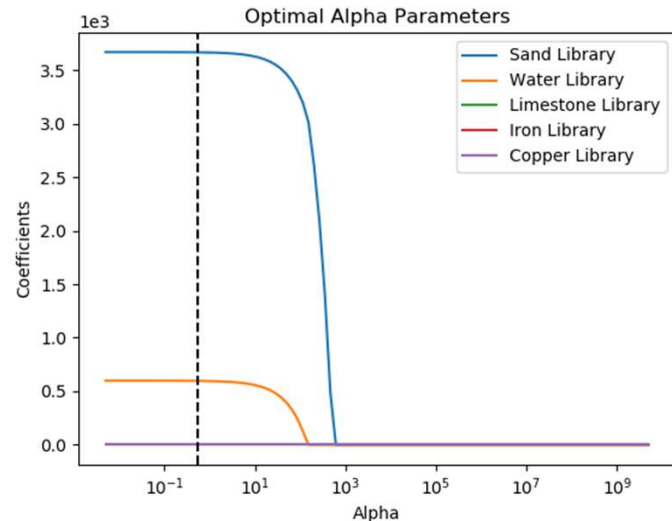
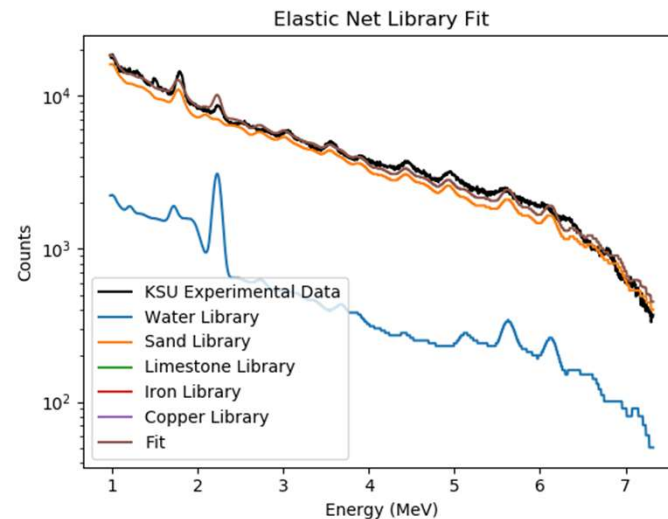
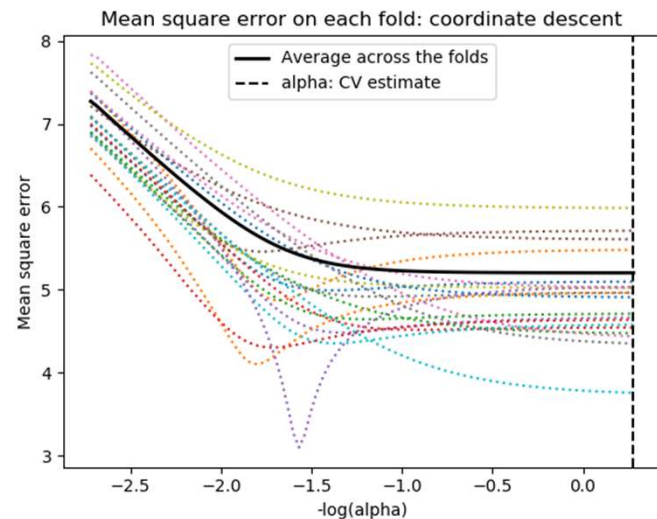
Water Linear Least Squares Results – Near Detector		
Chi-Squared = 99.3	Coefficients	Error
Water	322.62	0.05
Sand	NA	NA
Limestone	NA	NA
Iron	NA	NA
Copper	NA	NA

Water Linear Least Squares Results – Far Detector		
Chi-Squared = 13.3	Coefficients	Error
Water	301.94	0.12
Sand	NA	NA
Limestone	NA	NA
Iron	NA	NA
Copper	NA	NA

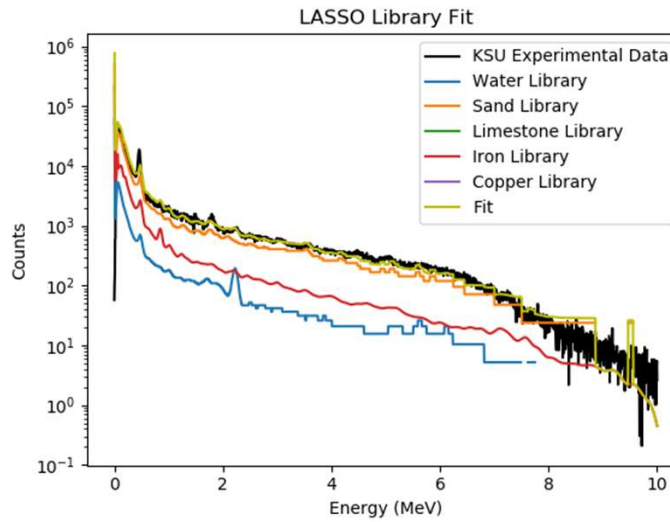
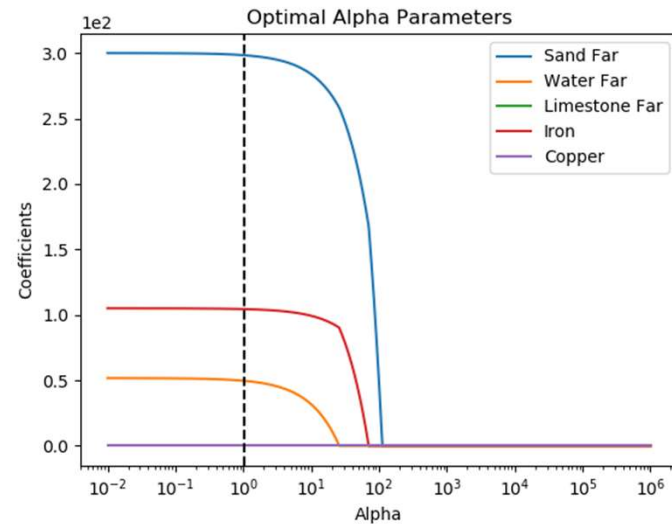
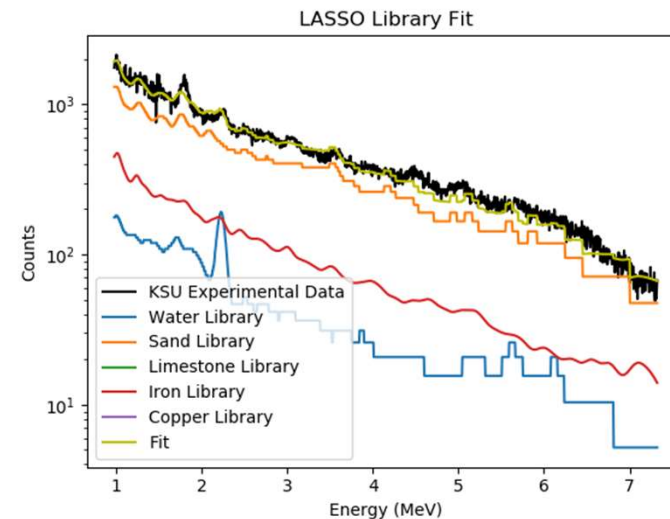
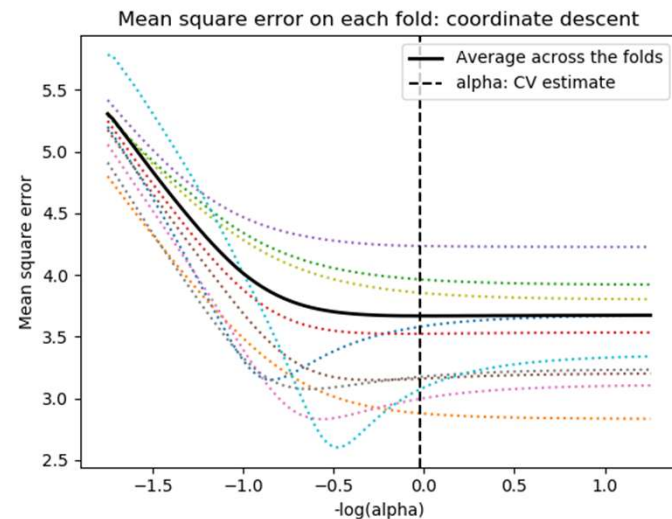
Sand Trial Near - LASSO



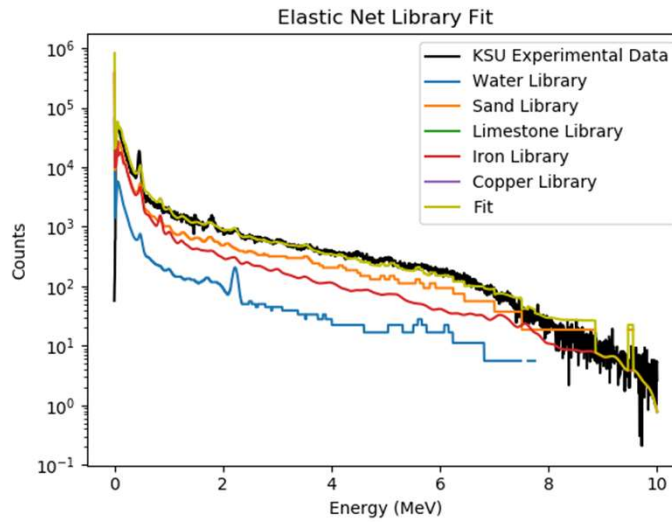
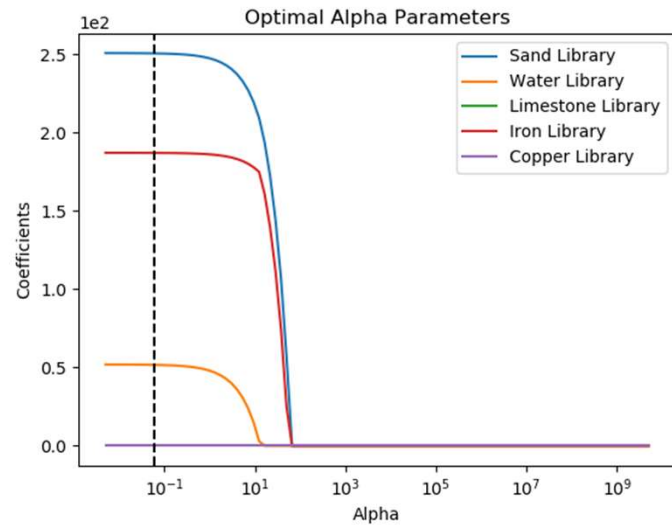
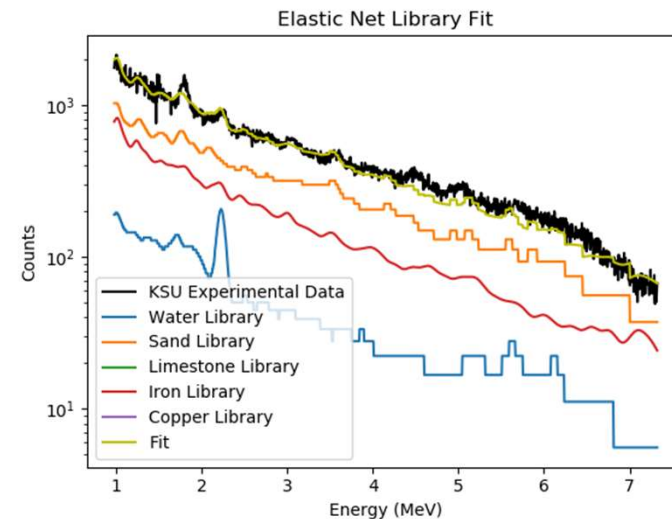
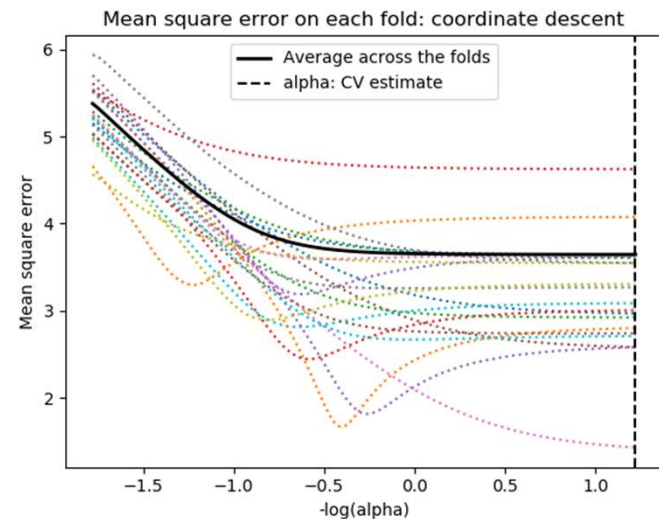
Sand Trial Near – Elastic Net



Sand Trial Far - LASSO

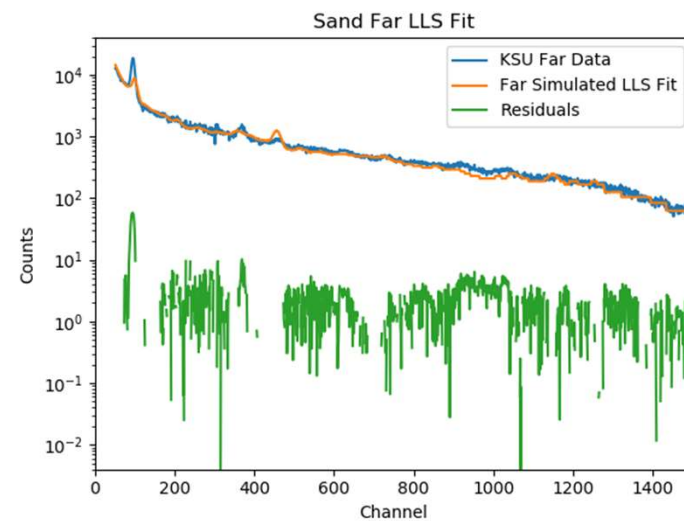
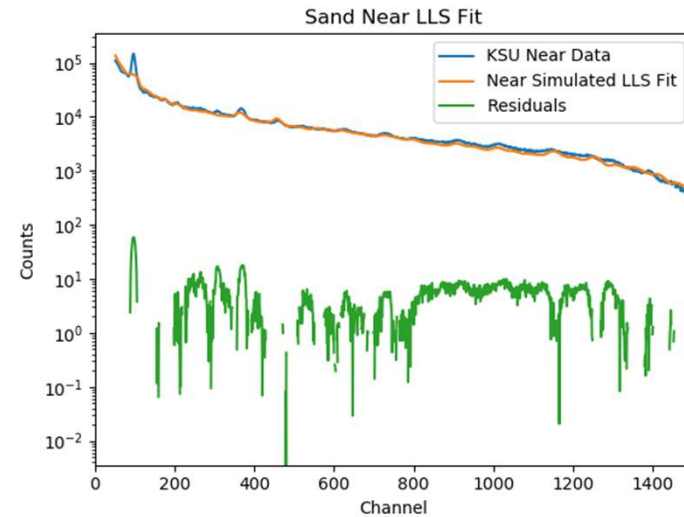


Sand Trial Far – Elastic Net

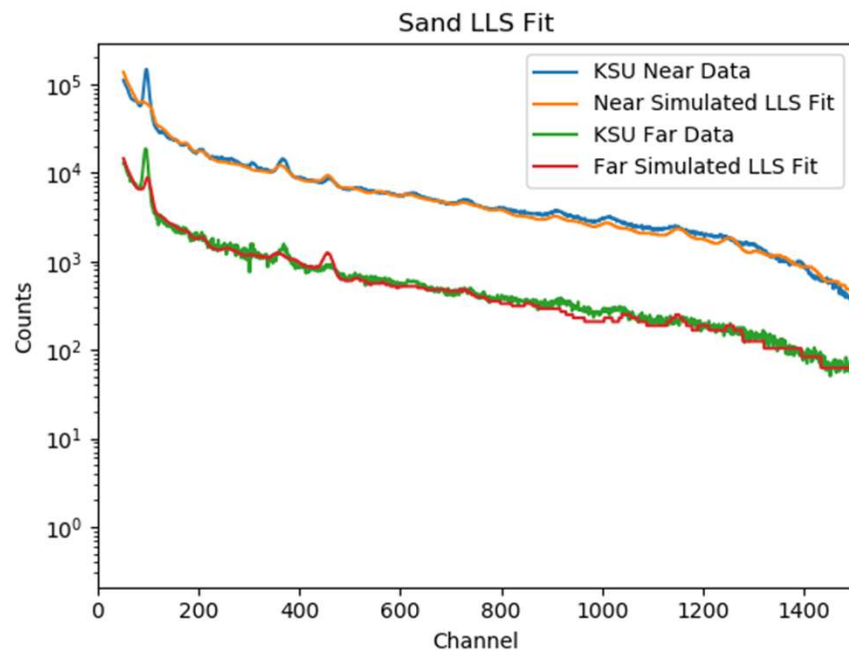


Sand Trial LLS Analysis

Sand Normalization Parameters		
	Near Detector	Far Detector
LASSO	0.396	1.050
Elastic Net	0.526	0.060



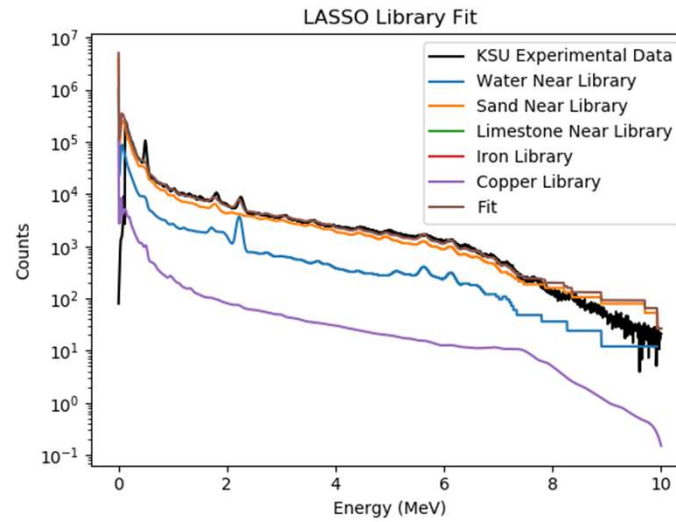
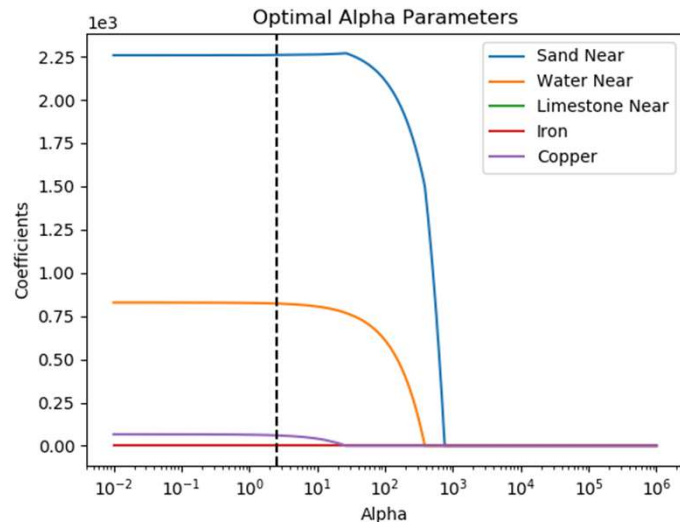
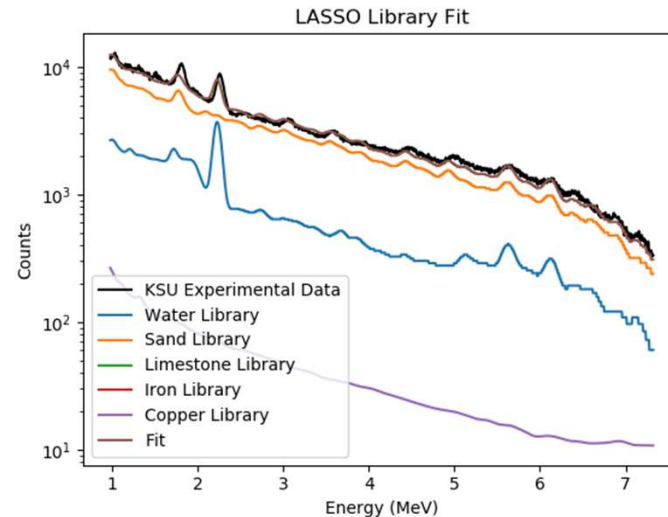
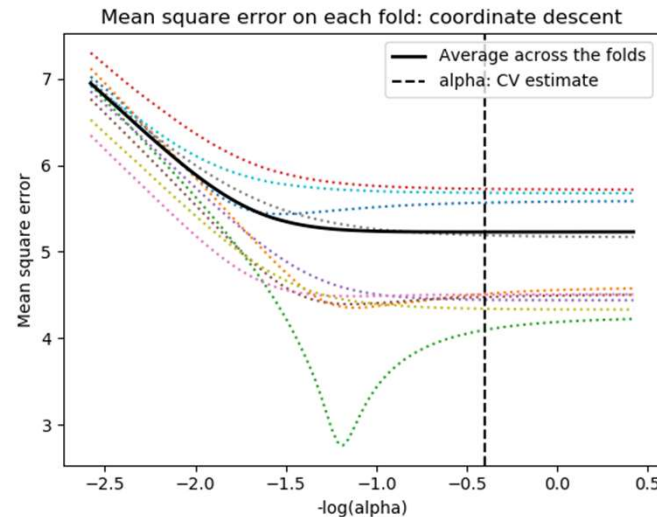
Sand Trial LLS Analysis



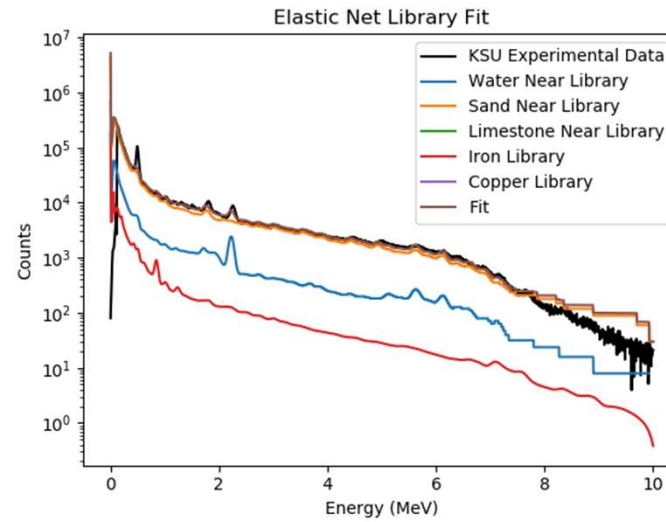
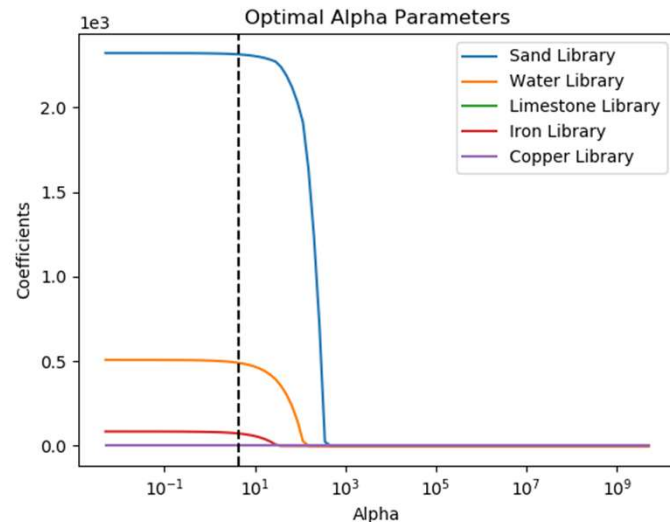
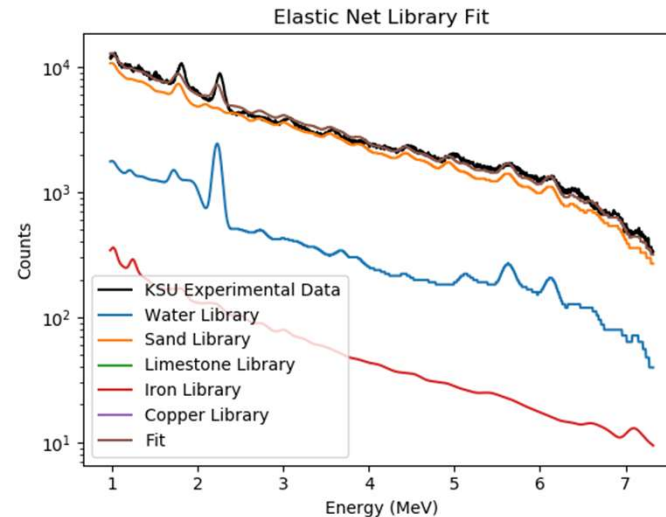
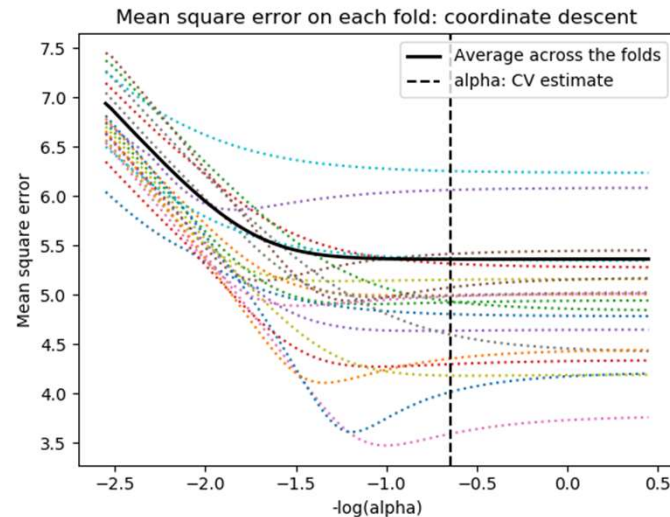
Water Linear Least Squares Results – Near Detector		
Chi-Squared = 88.4	Coefficients	Error
Water	79.94	1.10
Sand	437.37	0.13
Limestone	NA	NA
Iron	NA	NA
Copper	NA	NA

Water Linear Least Squares Results – Far Detector		
Chi-Squared = 27.6	Coefficients	Error
Water	203.90	0.90
Sand	210.55	0.49
Limestone	NA	NA
Iron	NA	NA
Copper	NA	NA

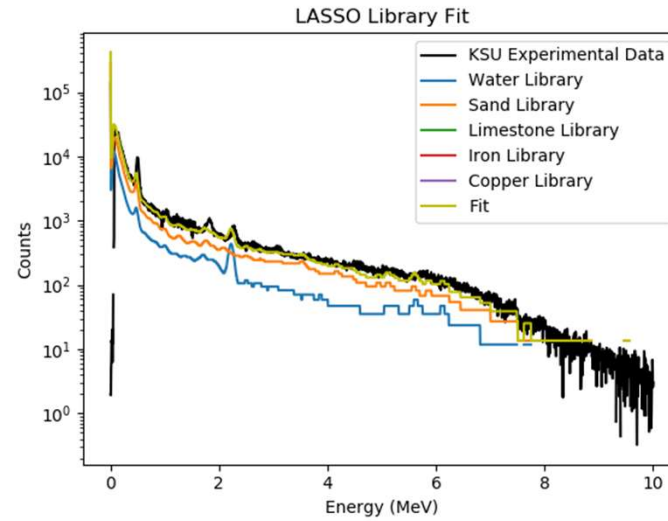
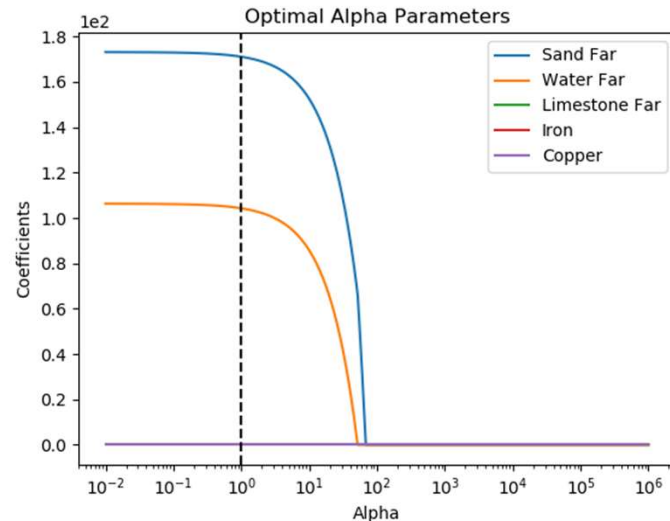
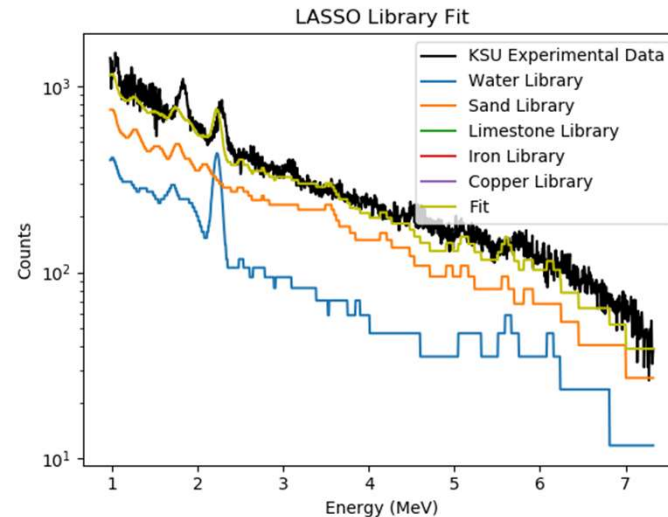
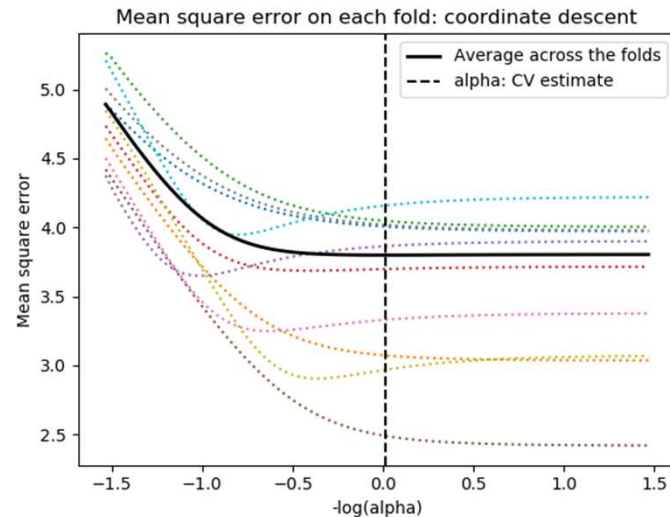
Sand with Water Trial Near - LASSO



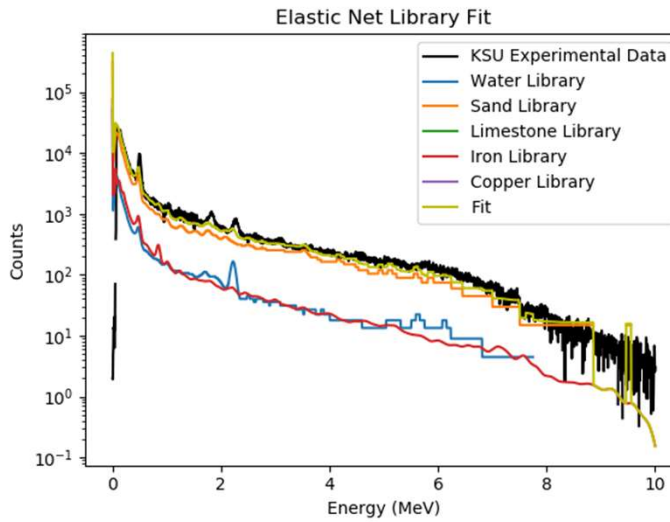
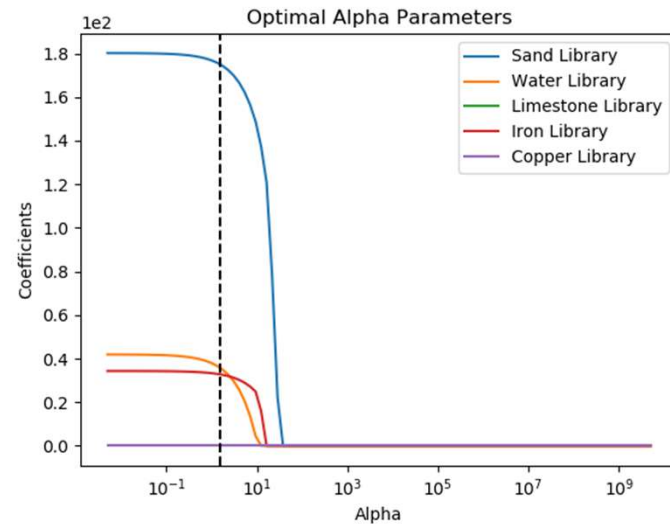
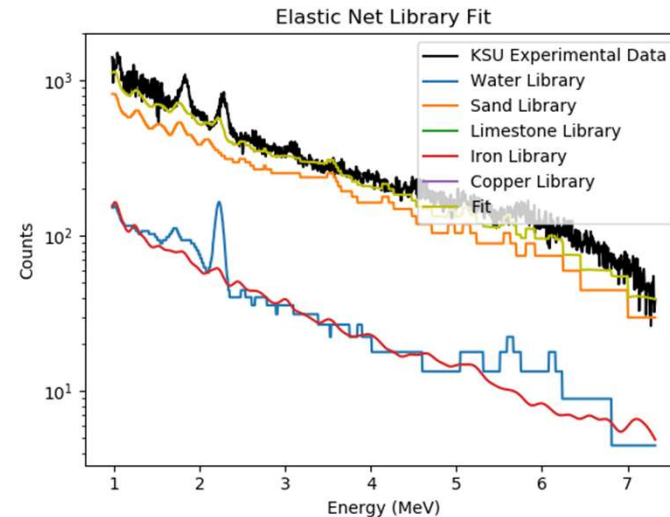
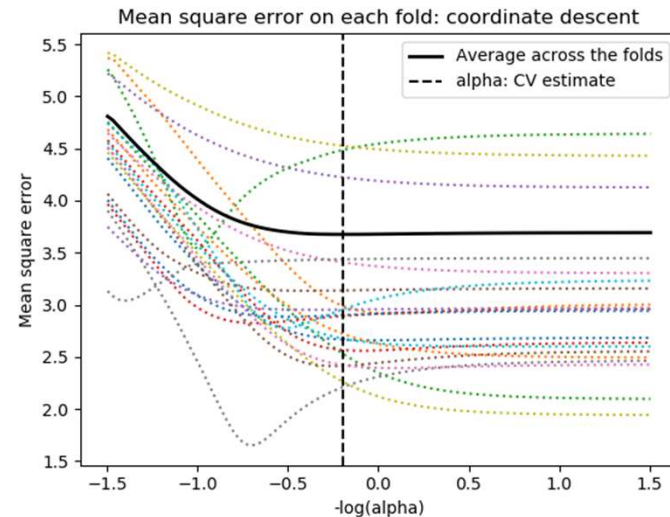
Sand with Water Trial Near – Elastic Net



Sand with Water Trial Far - LASSO

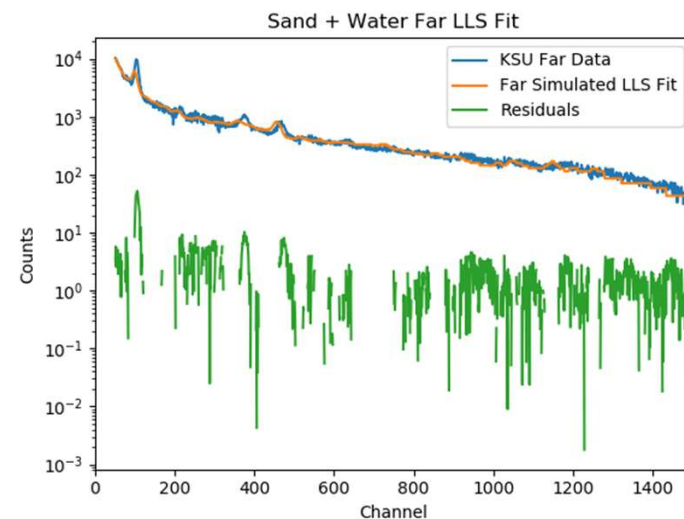
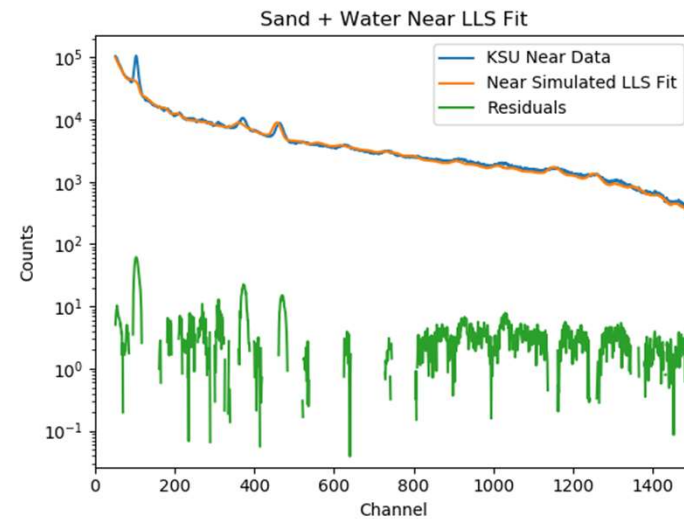


Sand with Water Trial Far – Elastic Net

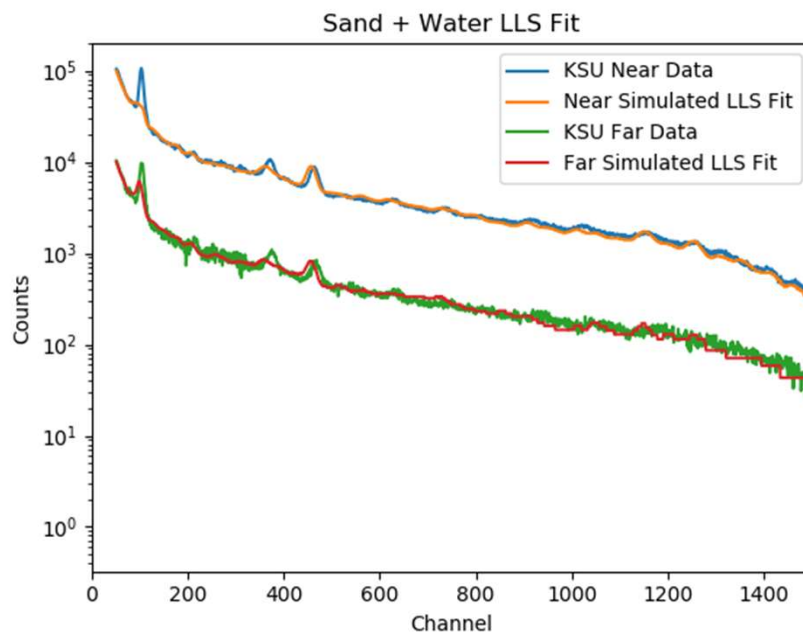


Sand with Water Trial LLS Analysis

Sand and Water Normalization Parameters		
	Near Detector	Far Detector
LASSO	2.495	0.972
Elastic Net	4.385	1.561



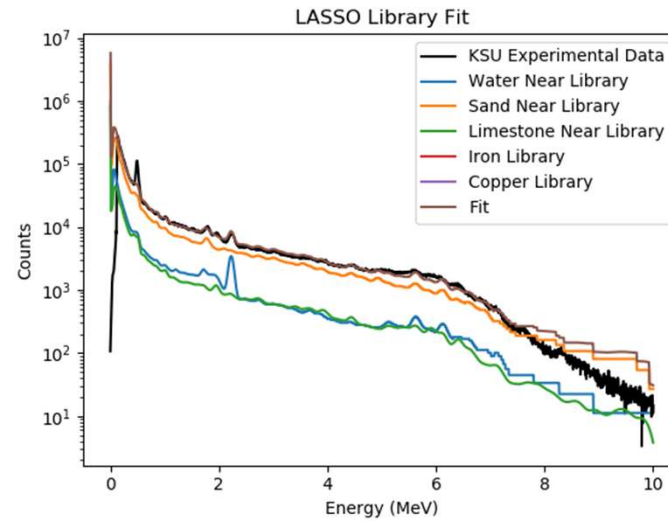
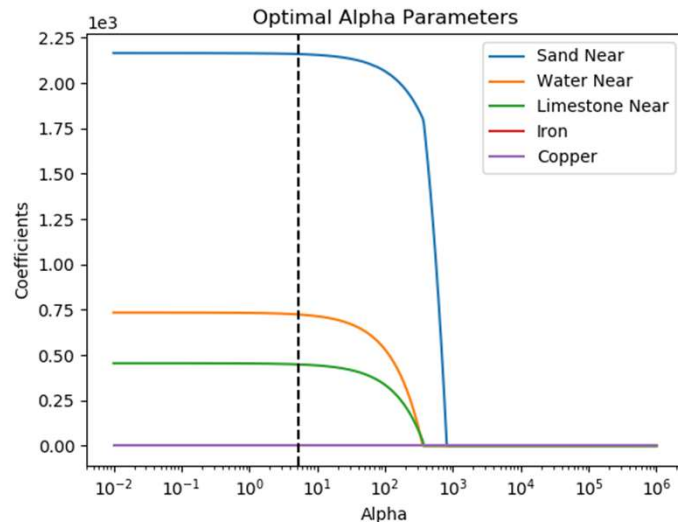
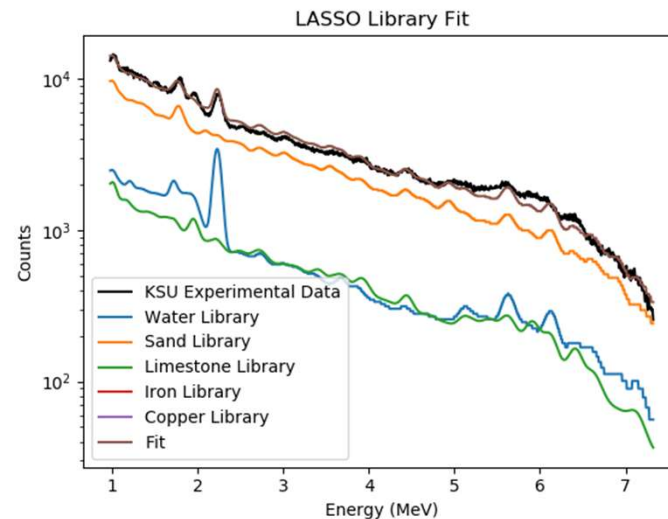
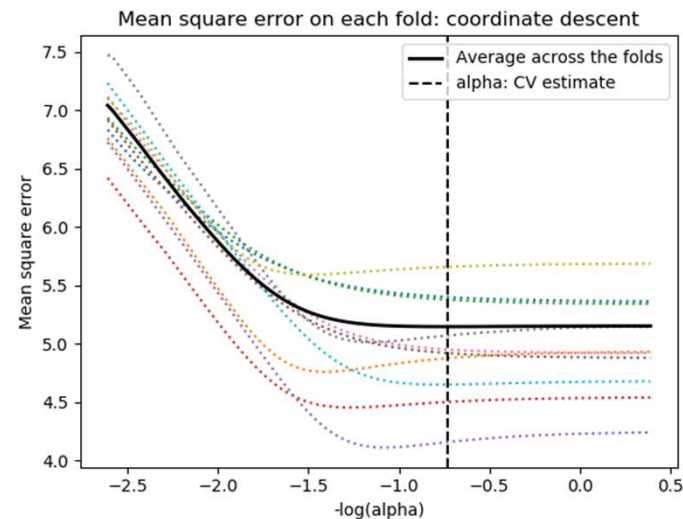
Sand with Water Trial LLS Analysis



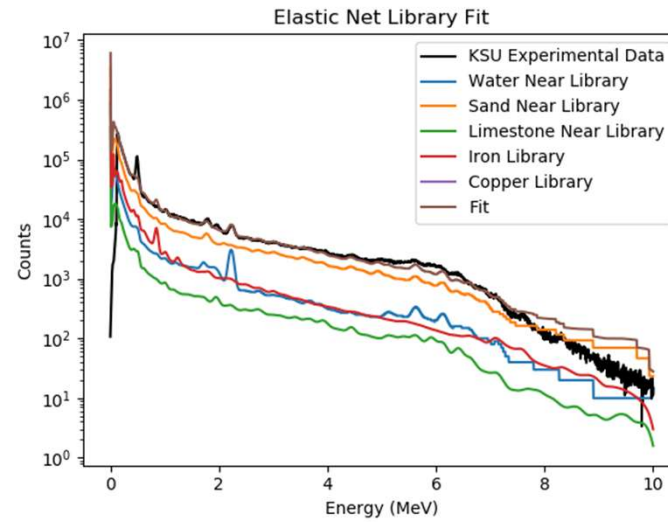
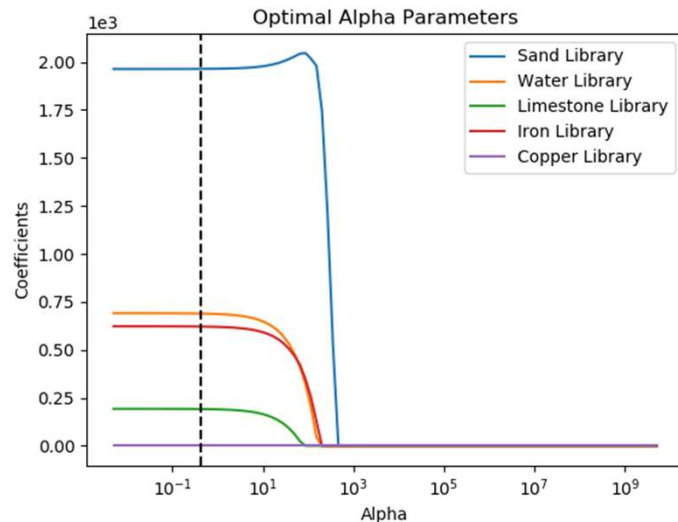
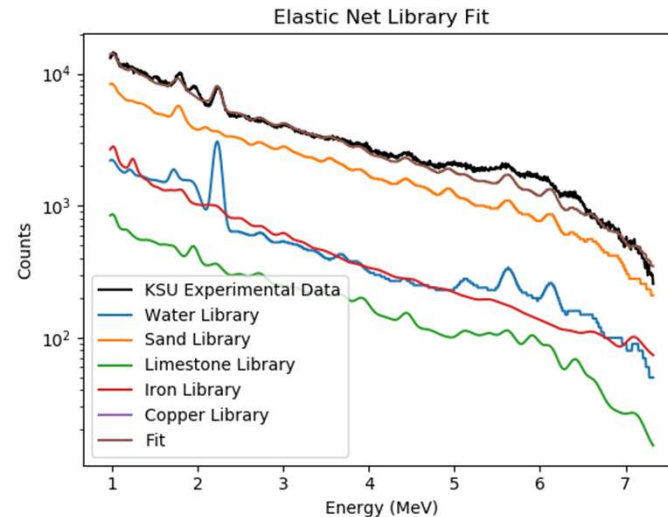
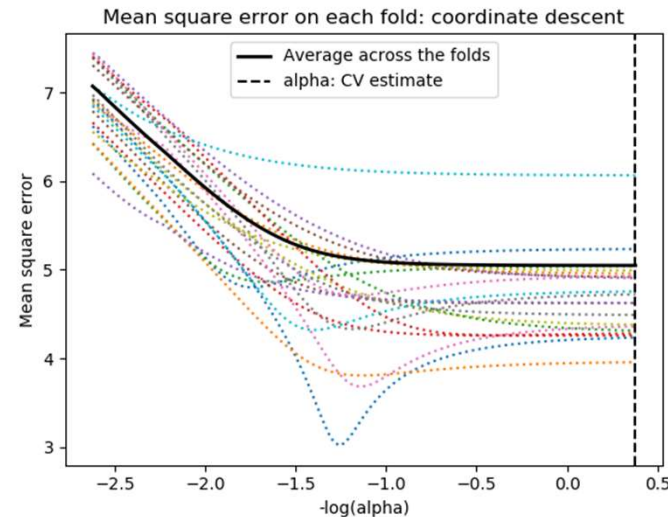
Sand and Water Linear Least Squares Results – Near Detector		
Chi-Squared = 51.8	Coefficients	Error
Water	164.20	0.48
Sand	247.83	0.20
Limestone	NA	NA
Iron	NA	NA
Copper	NA	NA

Sand and Water Linear Least Squares Results – Far Detector		
Chi-Squared = 18.2	Coefficients	Error
Water	125.89	1.34
Sand	152.51	0.62
Limestone	NA	NA
Iron	NA	NA
Copper	NA	NA

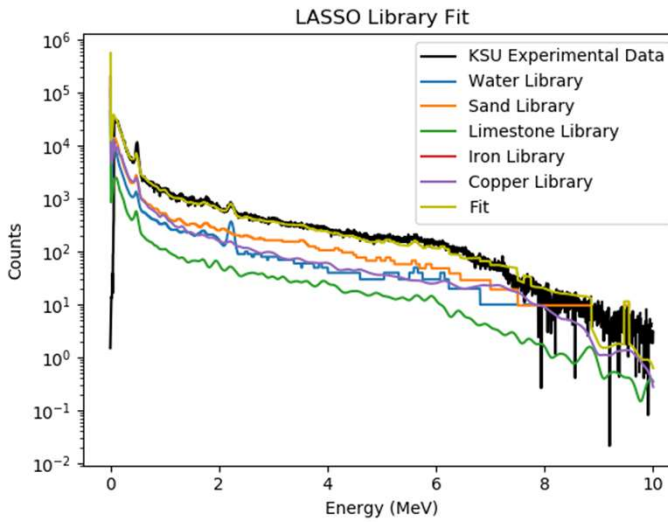
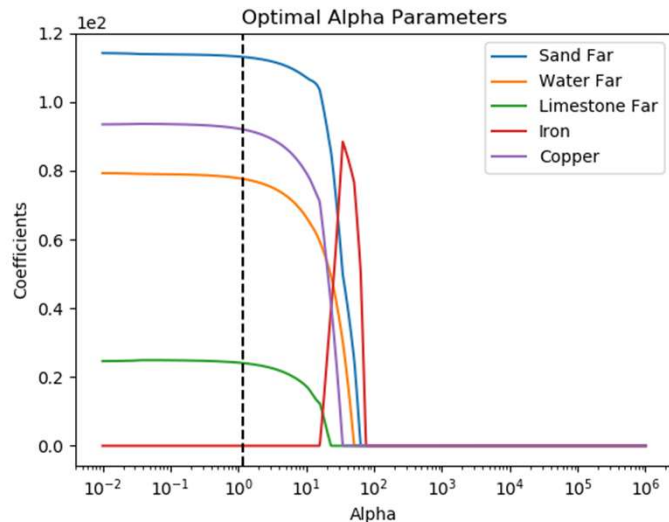
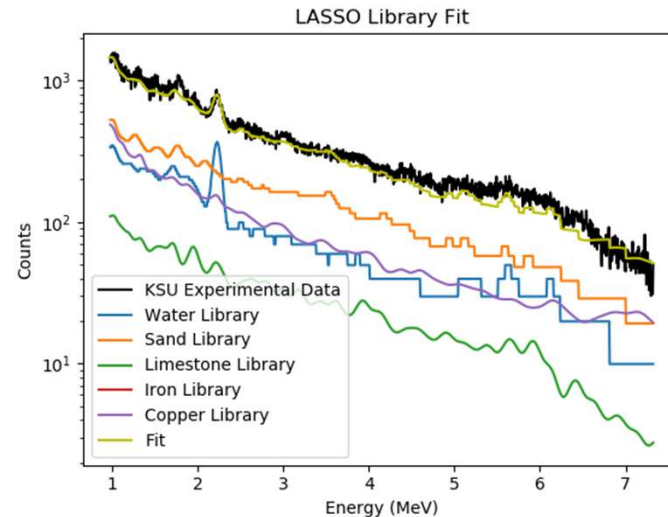
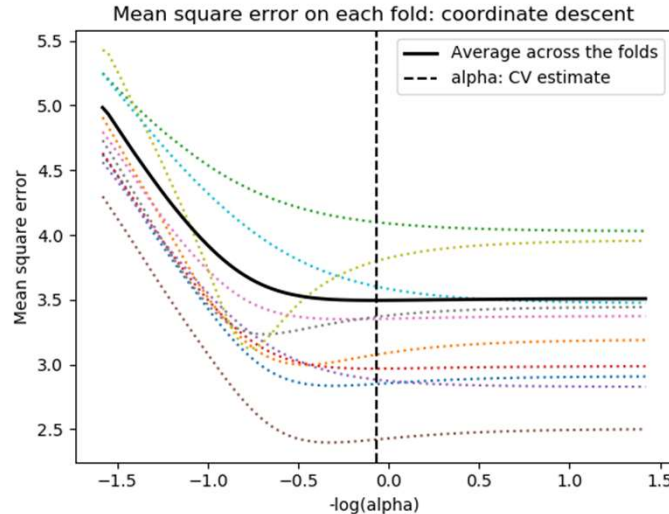
Limestone Trial Near - LASSO



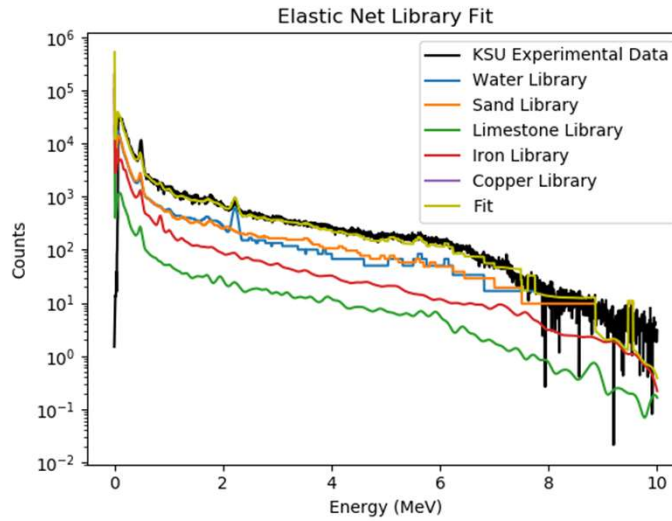
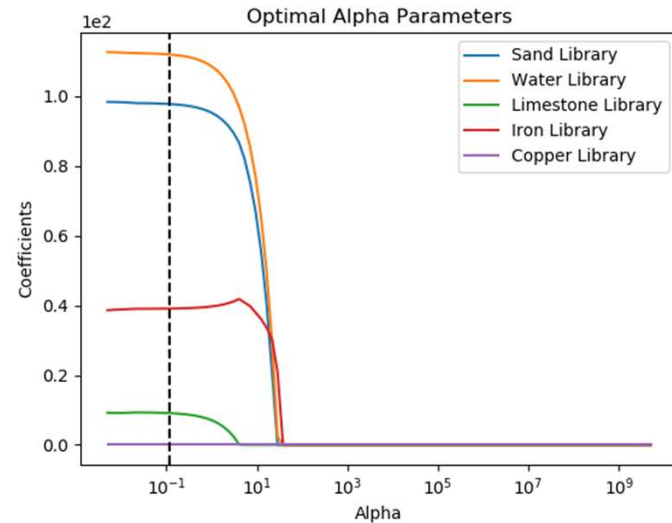
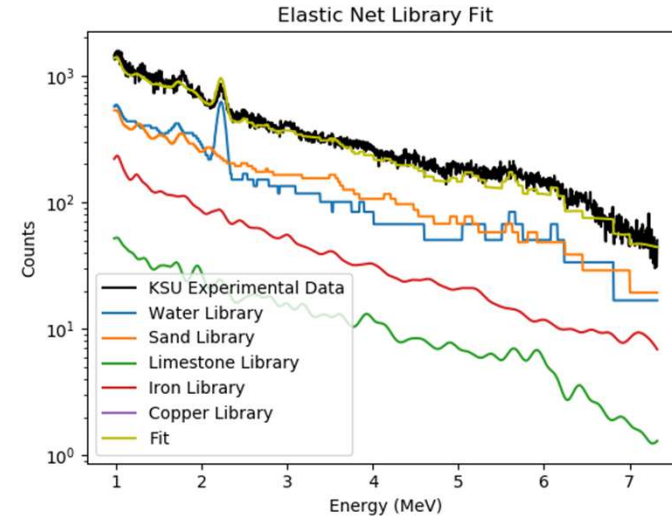
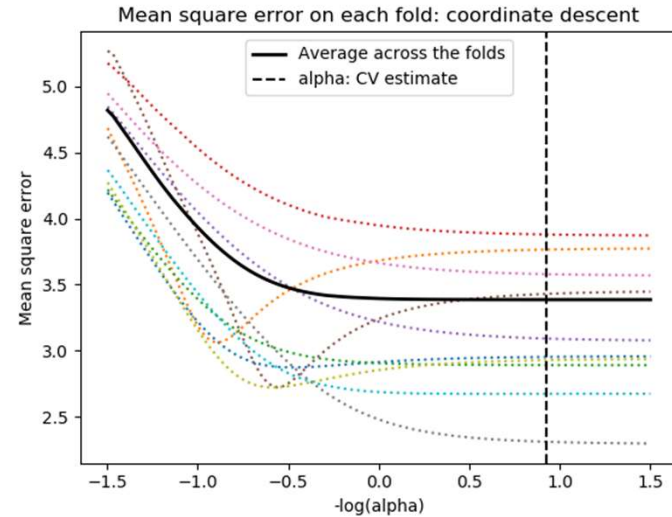
Limestone Trial Near – Elastic Net



Limestone Trial Far - LASSO

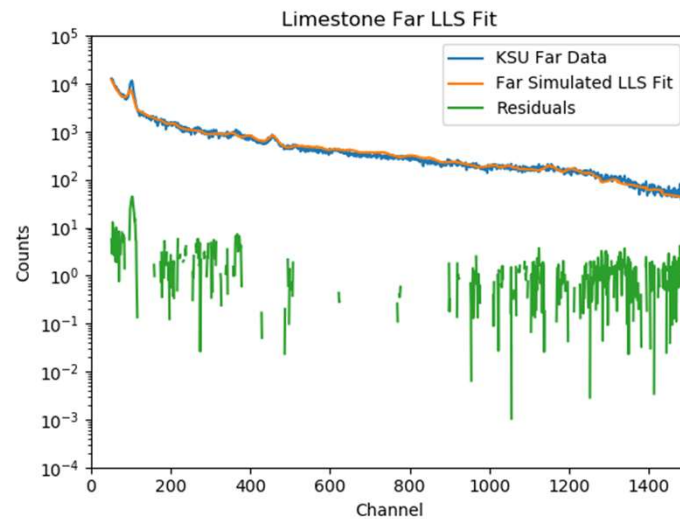
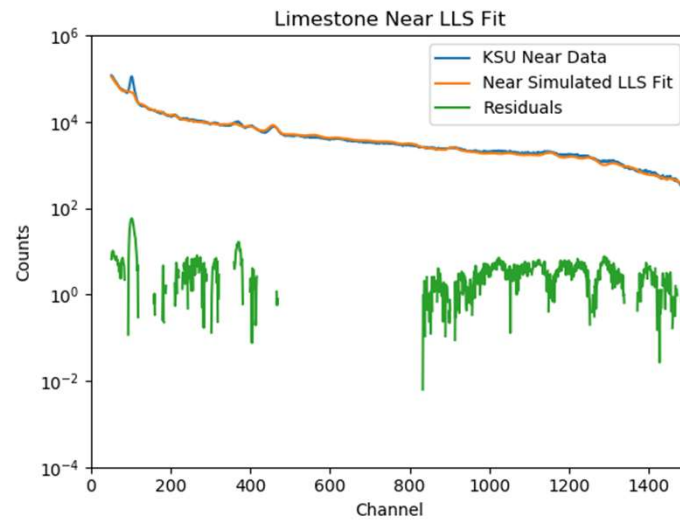


Limestone Trial Far – Elastic Net

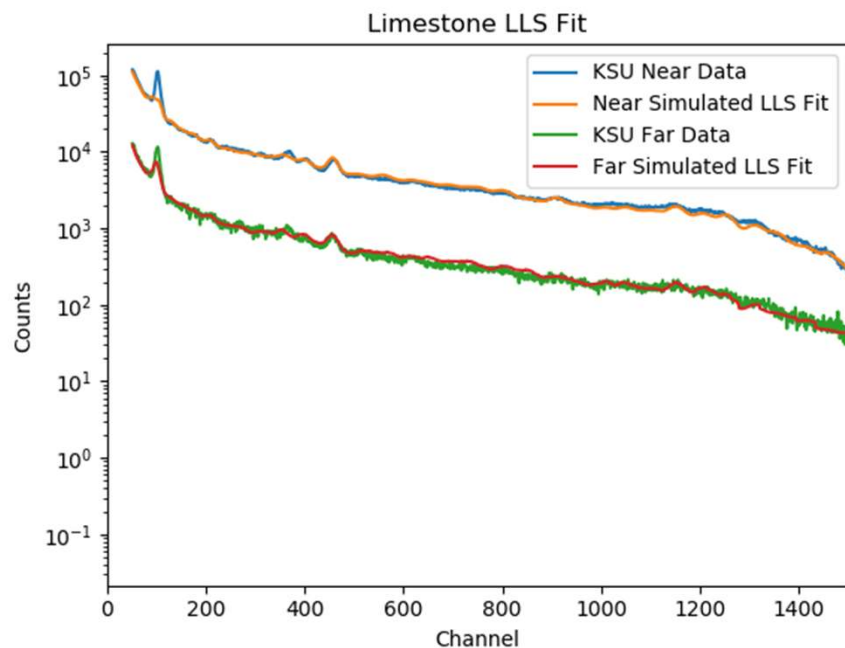


Limestone Trial LLS Analysis

Limestone Normalization Parameters		
	Near Detector	Far Detector
LASSO	5.384	1.163
Elastic Net	0.419	0.118



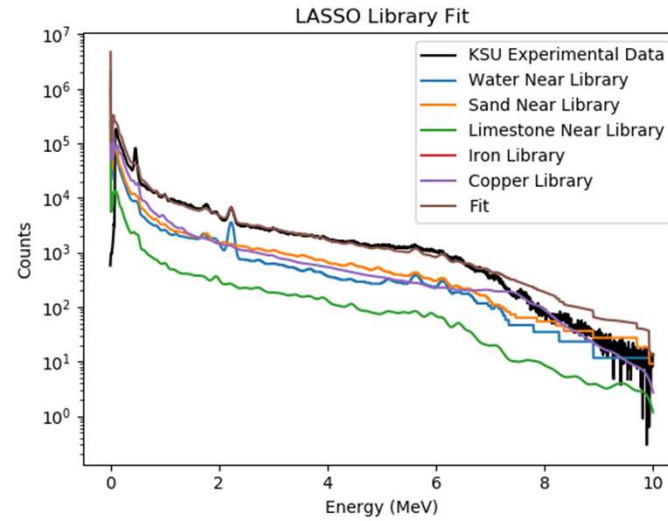
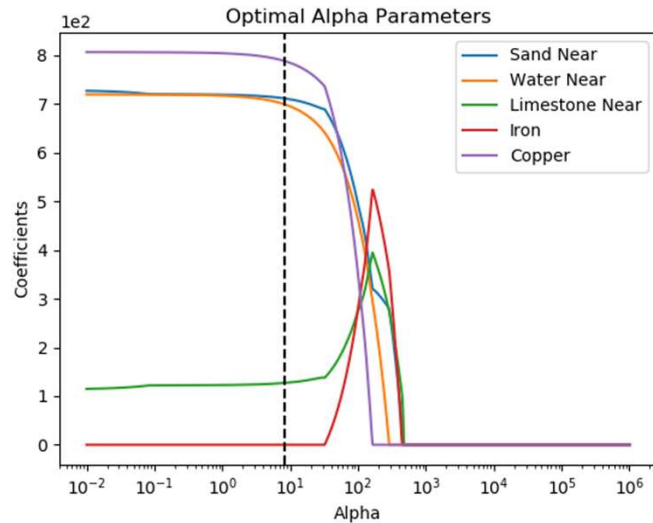
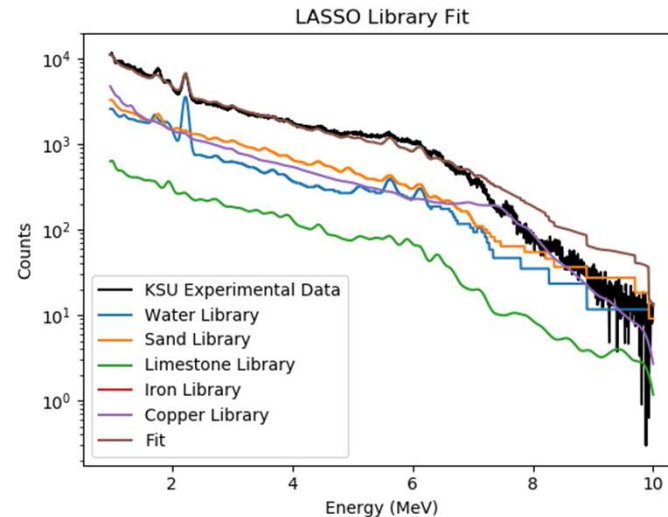
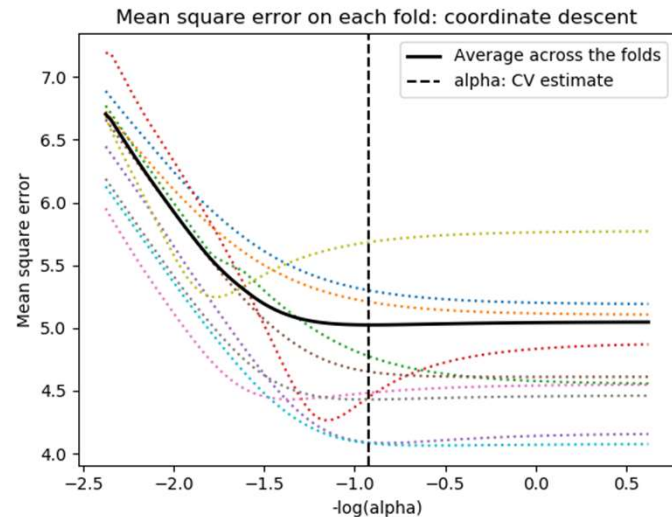
Limestone Trial LLS Analysis



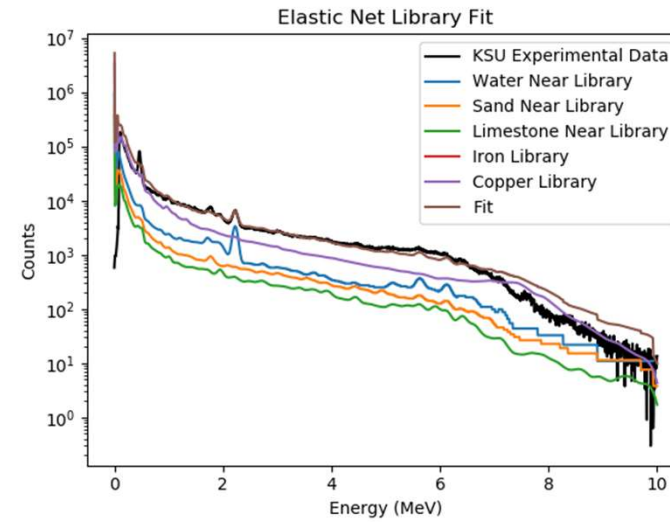
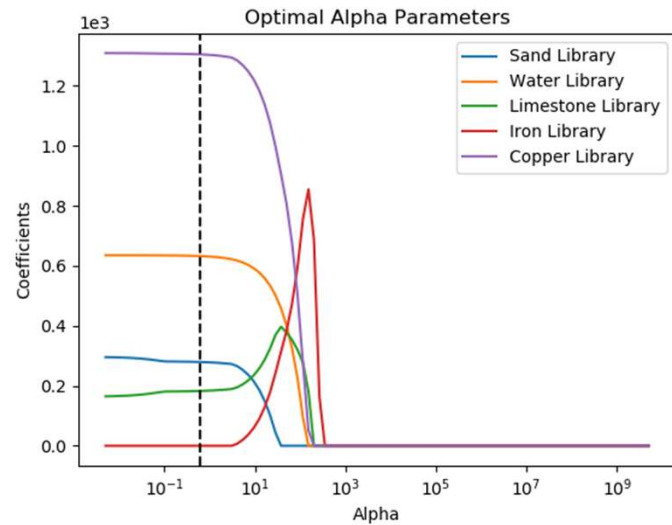
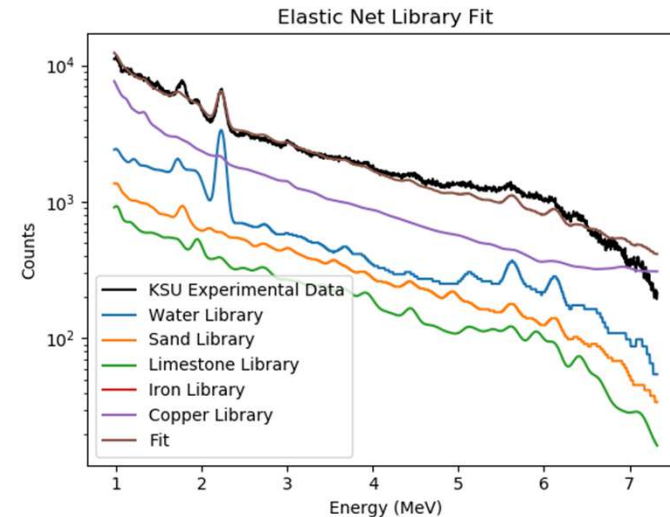
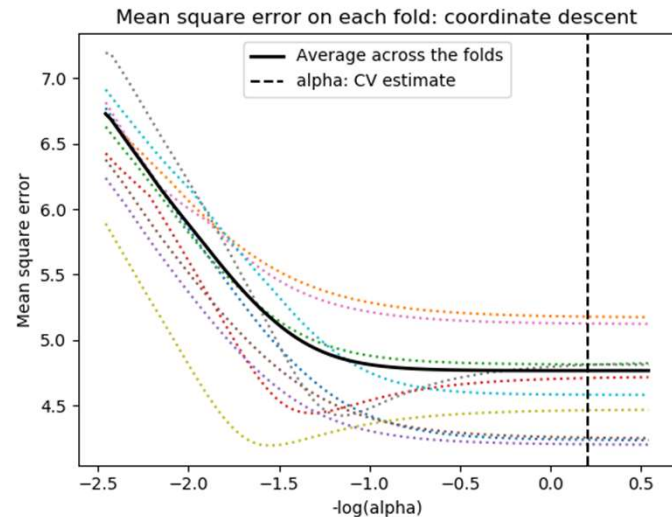
Limestone Linear Least Squares Results – Near Detector		
Chi-Squared = 26.7	Coefficients	Error
Water	104.44	0.79
Sand	139.82	1.42
Limestone	230.1	1.08
Iron	NA	NA
Copper	NA	NA

Limestone Linear Least Squares Results – Far Detector		
Chi-Squared = 18.2	Coefficients	Error
Water	75.14	2.88
Sand	90.42	3.14
Limestone	171.14	2.31
Iron	NA	NA
Copper	NA	NA

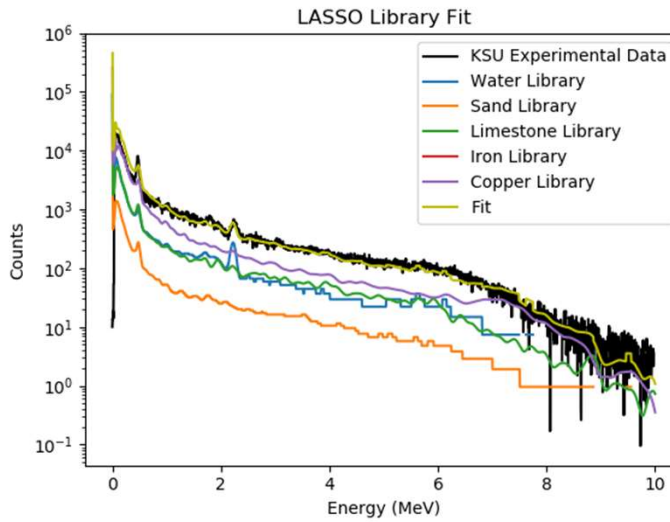
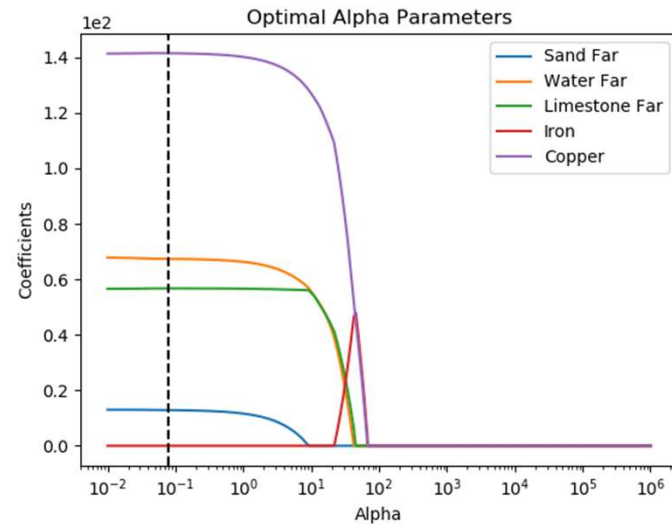
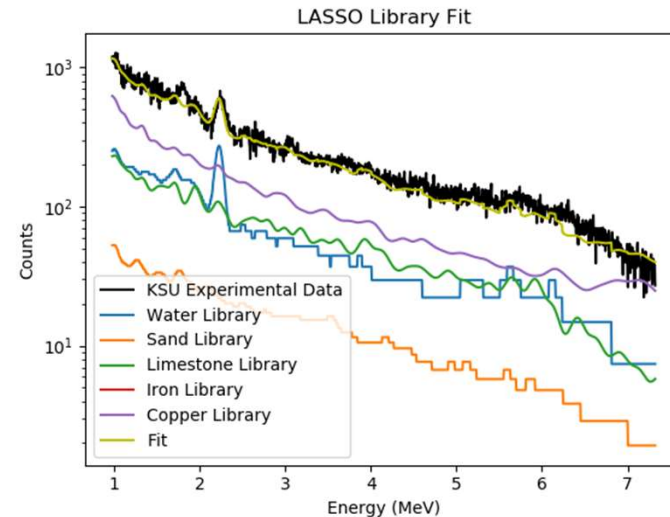
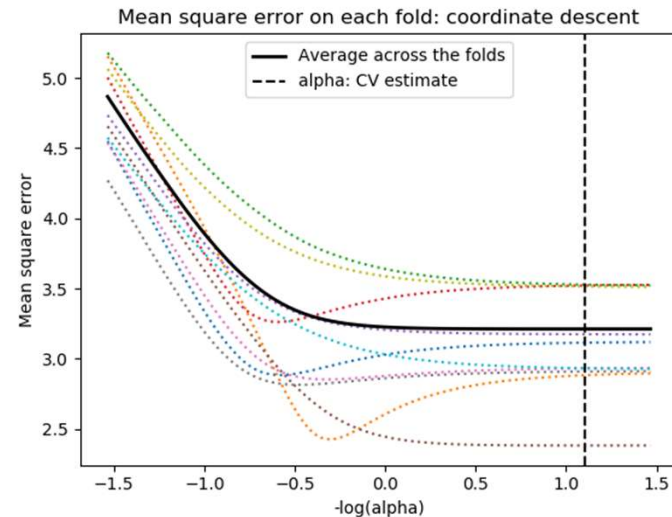
Limestone with Water Trial Near - LASSO



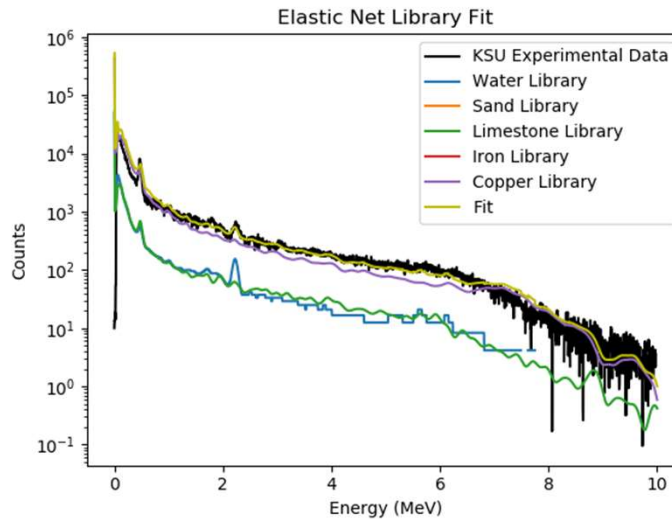
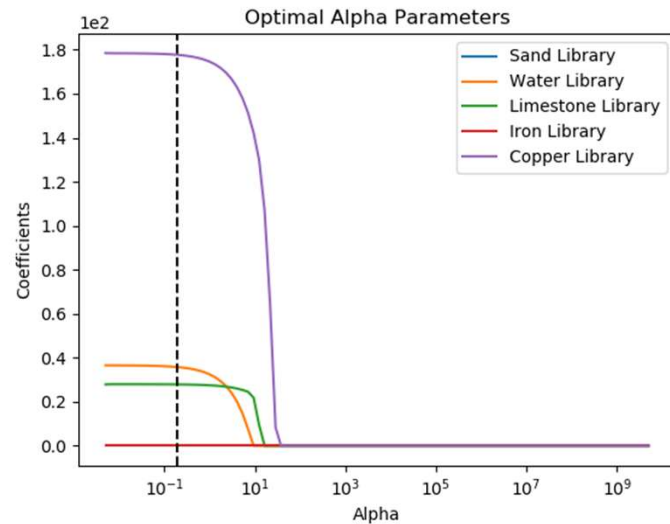
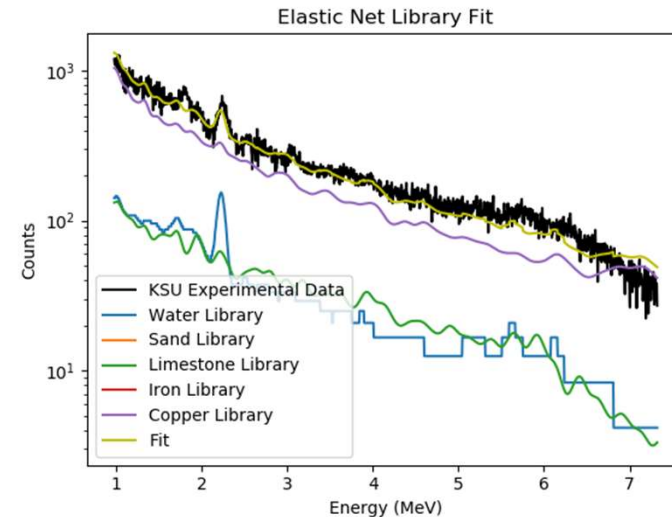
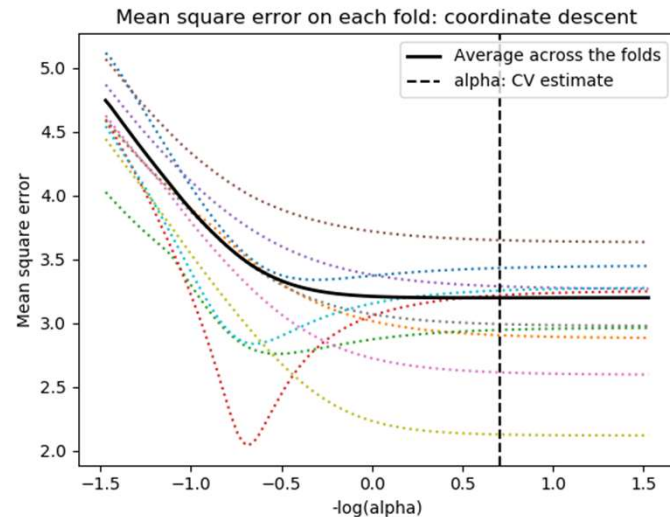
Limestone with Water Trial Near – Elastic Net



Limestone with Water Trial Far - LASSO

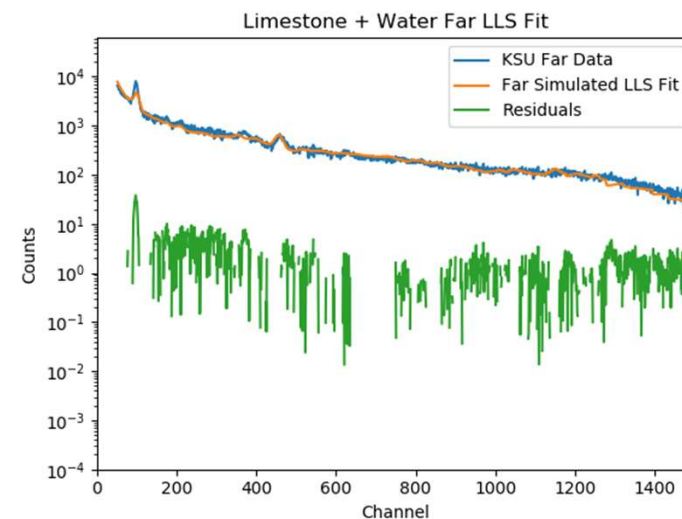
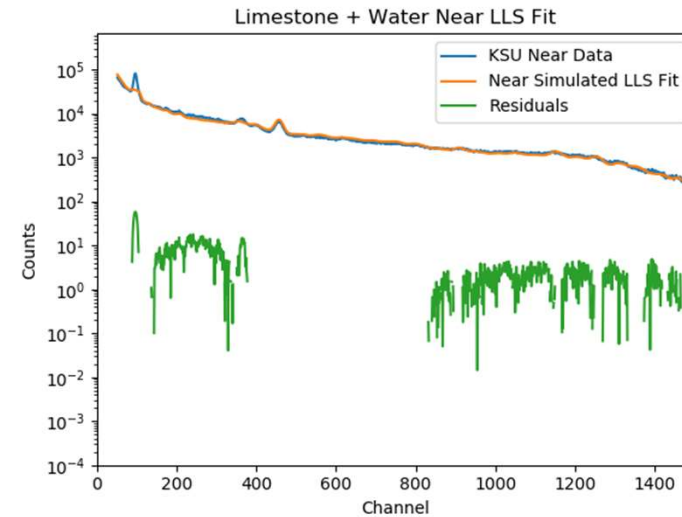


Limestone with Water Trial Far – Elastic Net

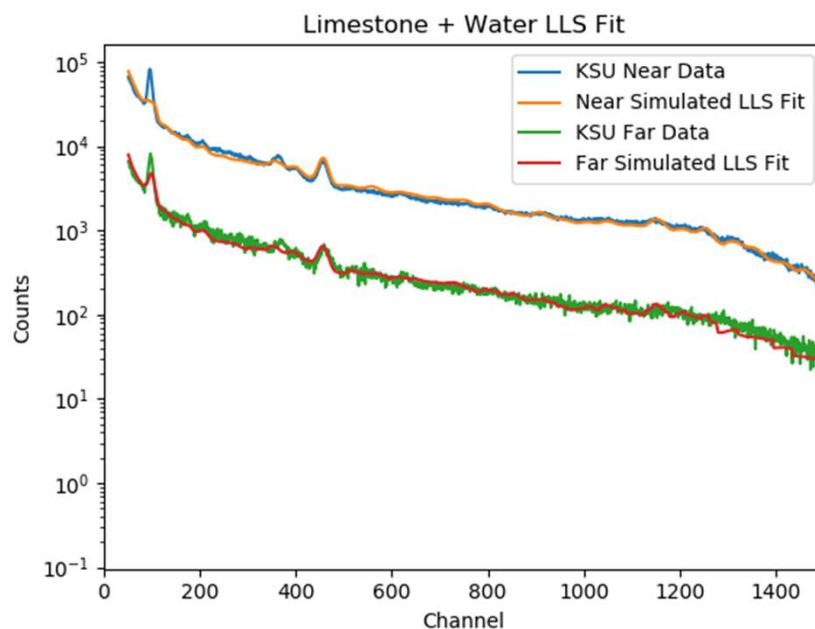


Limestone with Water Trial LLS Analysis

Limestone with Water Normalization Parameters		
	Near Detector	Far Detector
LASSO	8.362	0.079
Elastic Net	0.619	0.195



Limestone with Water Trial LLS Analysis



Limestone With Water Linear Least Squares Results – Near Detector		
Chi-Squared = 34.2	Coefficients	Error
Water	140.80	0.51
Sand	90.48	1.77
Limestone	114.66	1.76
Iron	NA	NA
Copper	NA	NA

Limestone With Water Linear Least Squares Results – Far Detector		
Chi-Squared = 10.2	Coefficients	Error
Water	96.77	1.91
Sand	64.89	3.64
Limestone	71.21	4.61
Iron	NA	NA
Copper	NA	NA

Discussion of KSU Benchmarking Tool

- Met with oil well logging industry experts during Dr. Gardner's retirement ceremony
 - Indicated they have abandoned far gamma detectors, citing there are more effective means of determining density
 - Many expressed interest in variable selection techniques after describing the capabilities
 - Mentioned the need for improved cross-sectional data on Calcium and other isotopes
- D-T pulsed neutron generators have advantages
 - Increased energy allows for more inelastic scattering signatures
 - Pulsing times can be used to extract a more accurate background
 - Natural background and delayed/activation gammas
- Improvements can be made by incorporating work from Aaron Feinberg and Long Vo
 - Bayesian approach to fit all non-linear components
 - Time dependent digitizer data
- Detailed chemical analysis should be performed to test against the known makeup on future experiments (Water content from known and unknown origin as well)

RIID Simulation Tests

Variable selection via RIVAL (removing irrelevant variables amidst Lasso iterations) and its application to nuclear material detection[☆]

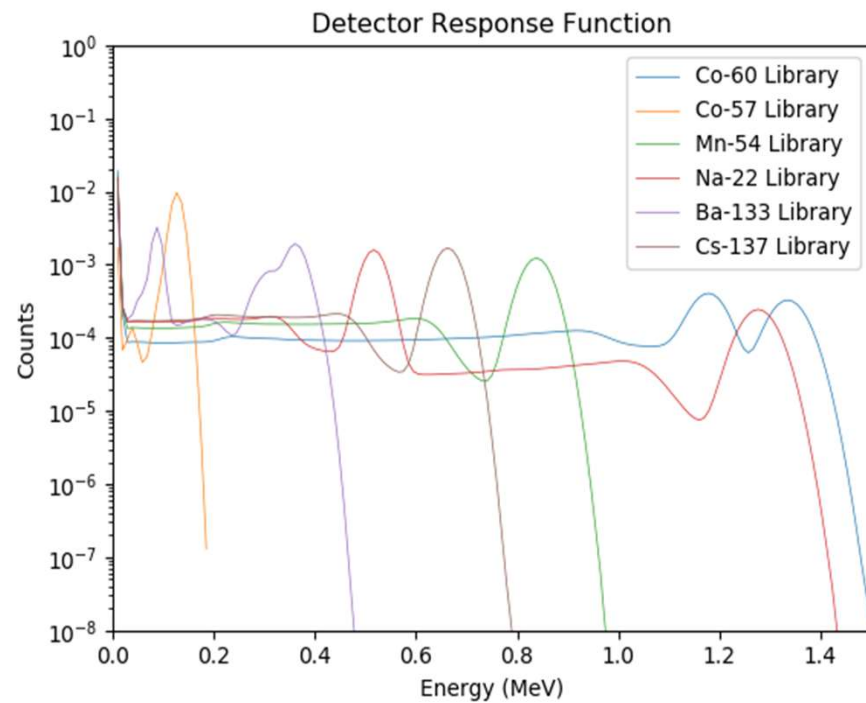
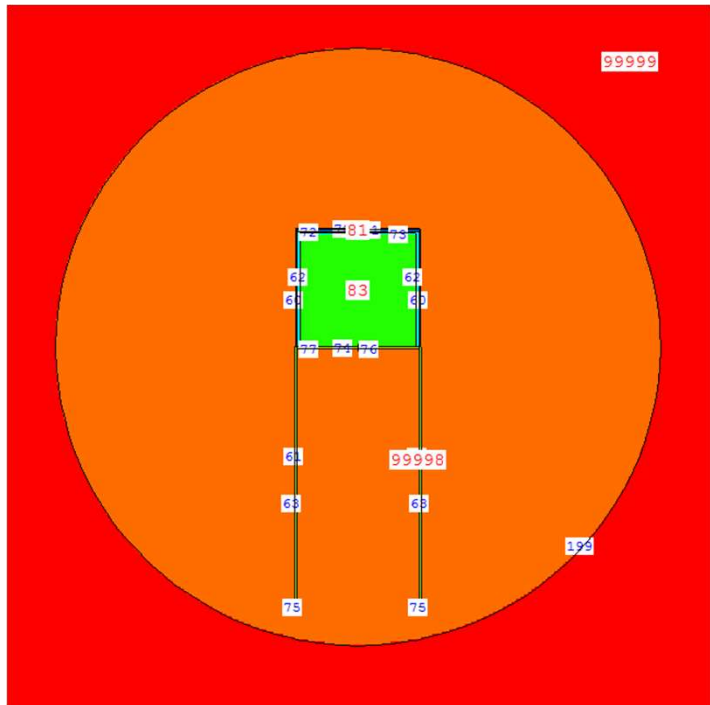
Paul Kump^a, Er-Wei Bai^{a,d,1}, Kung-sik Chan^b, Bill Eichinger^c, Kang Li^d

Detection of radionuclides from weak and poorly resolved spectra using Lasso and subsampling techniques

Er-Wei Bai^{a,*}, Kung-sik Chan^b, William Eichinger^c, Paul Kump^a

- 2 papers on using LASSO technique on radiation detectors, 0 on Elastic Net
- Test the accuracy of LASSO and Elastic Net using RIID simulations on 20 runs for:
 - High, medium, low counting situations
 - Masking and convolved spectra
 - Shielding and non-shielding situations

RIID Simulation Example



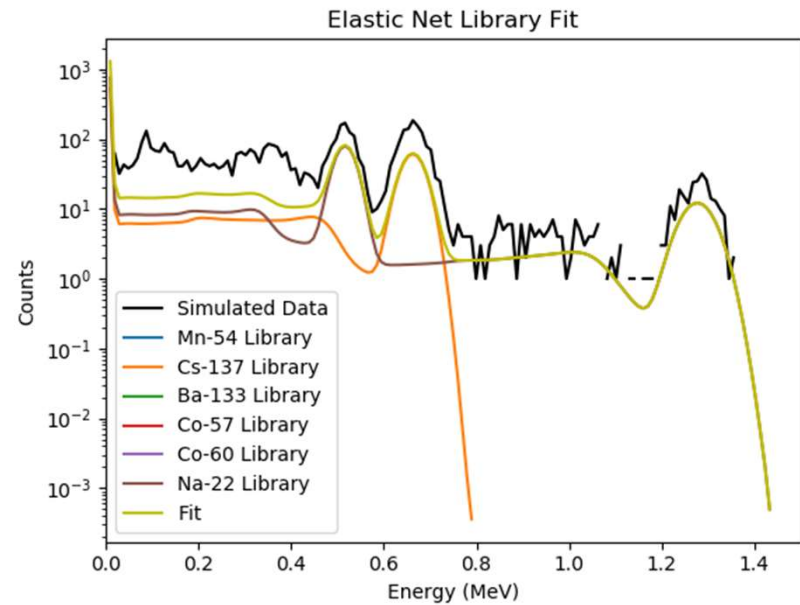
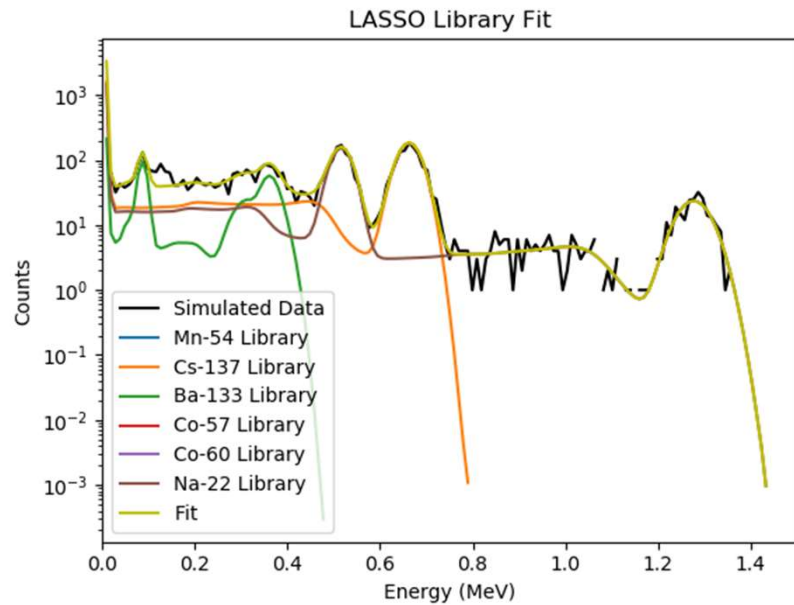
- Testing situations with combination of 6 radionuclides:
Co-60, Co-57, Ba-133, Mn-54, Cs-137, Na-22

Masking without Shielding

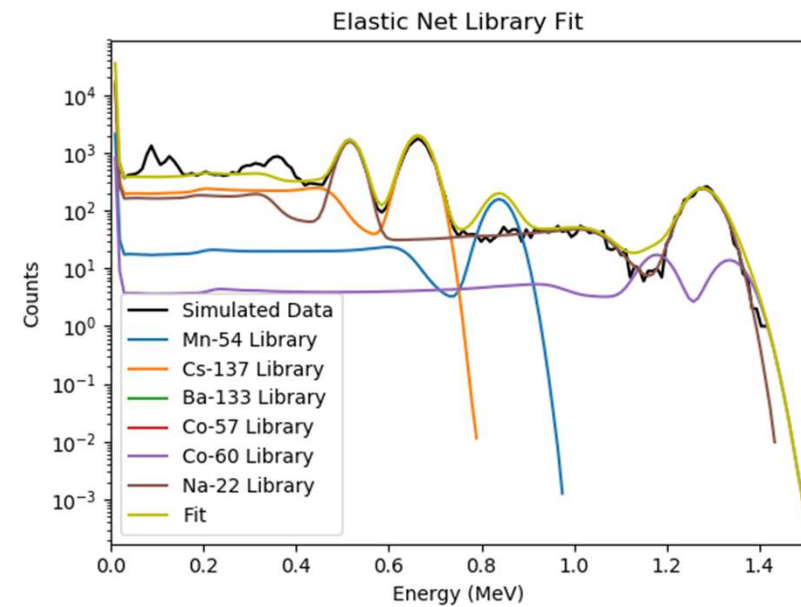
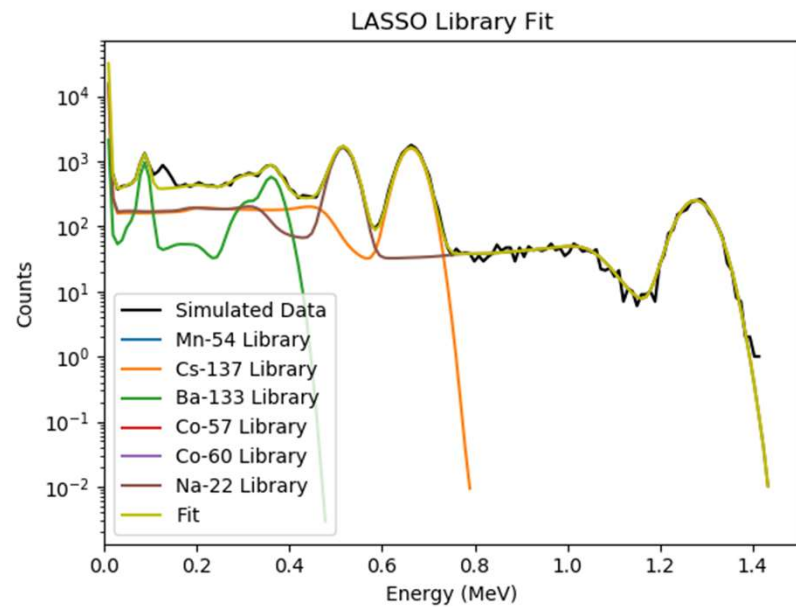
- Masking is a term used for a situation where higher energy radioisotopes “mask” the signature of a lower energy source
- Small amounts of Co-57 are used to demonstrate the effectiveness of LASSO and Elastic Net on this problem type
- Each figure is a random test run

Masking Linear Coefficients			
Ba-133	30,000	300,000	3,000,000
Na-22	100,000	1,000,000	10,000,000
Mn-54	0	0	0
Cs-137	100,000	1,000,000	10,000,000
Co-60	0	0	0
Co-57	5,000	50,000	500,000
Total Counts	4,997	50,790	510,348

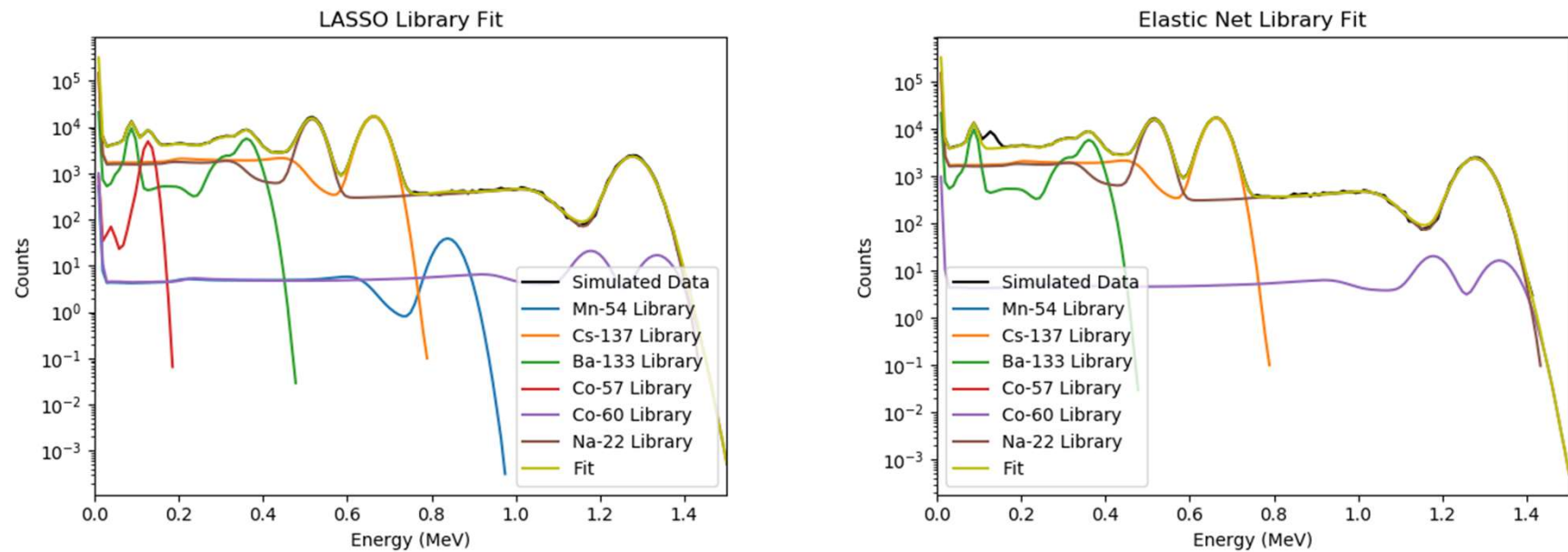
Masking without Shielding – Low Counts



Masking without Shielding – Medium Counts



Masking without Shielding – High Counts



Masking without Shielding – Summary

- LASSO outperforms Elastic Net for every counting rate
- At the highest count rate, LASSO correctly identifies Co-57 contributions 70% of the time, with a false positive rate for Mn-54 and Co-60 25% of the time

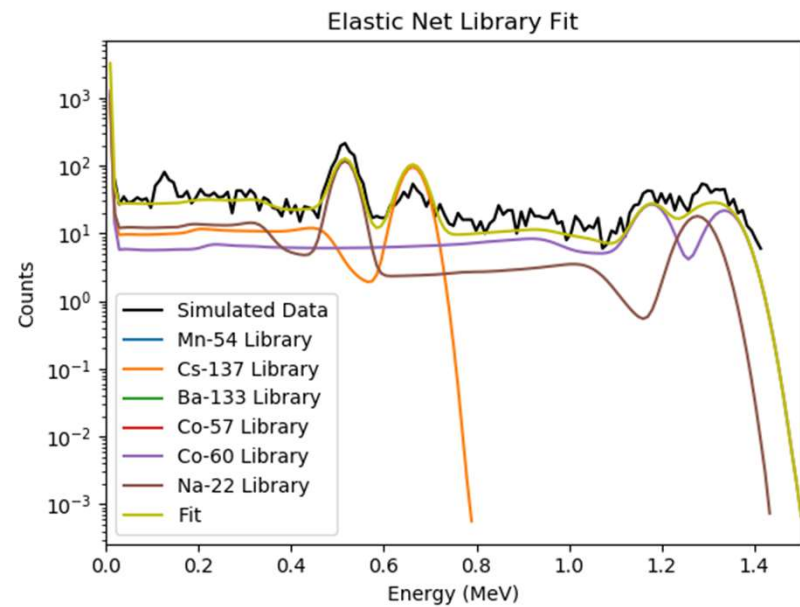
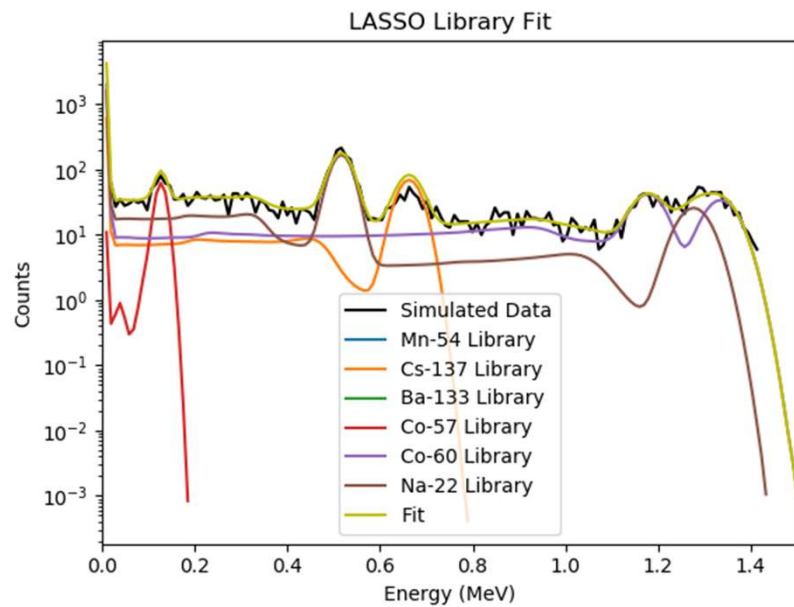
Masking Without Shielding Prediction Accuracy						
	Lasso-Low	EN-Low	Lasso-Med	EN-Med	LASSO-High	Elastic Net-High
Ba-133	0.85	0.65	0.95	0.75	1.00	0.85
Na-22	0.95	0.90	1.00	0.95	1.00	1.00
Mn-54	0.65	0.60	0.55	0.55	0.75	0.50
Cs-137	0.95	0.75	1.00	0.90	1.00	0.85
Co-60	0.55	0.40	0.60	0.75	0.75	0.70
Co-57	0.40	0.35	0.50	0.30	0.70	0.40

Convolution without Shielding

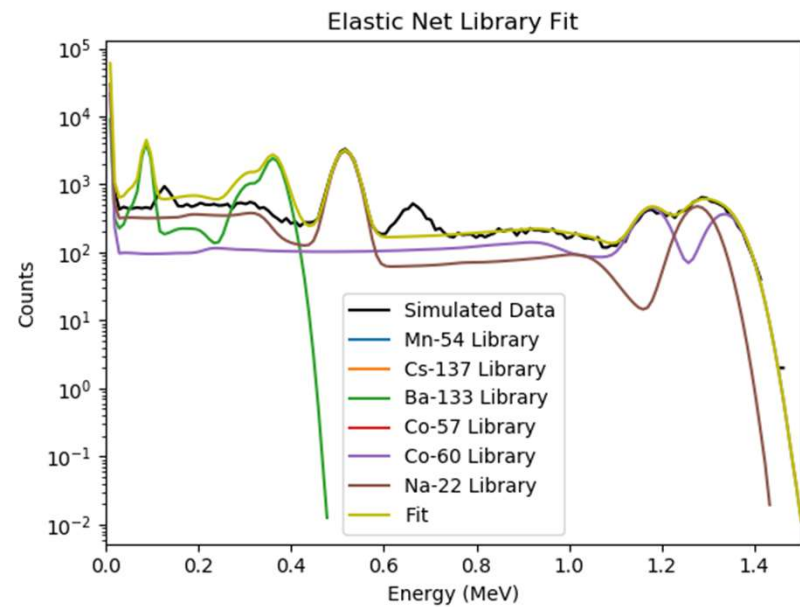
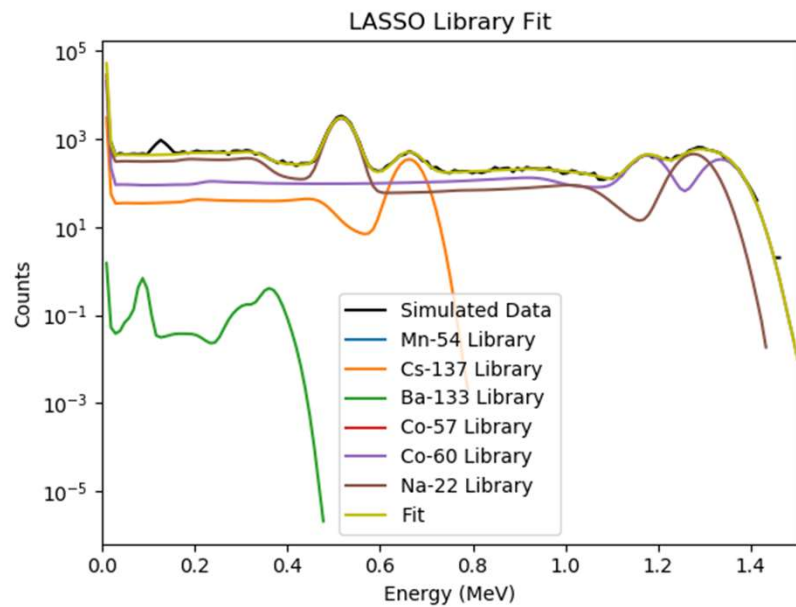
- Convolved peaks involve a situation where two or more radioisotopes have broadened peak energies that overlap
- Single peak analysis techniques have a difficult time with this problem
- LASSO and Elastic Net are full spectrum analysis techniques
- Large contributions of both Na-22 and Co-60 are used to simulate a convolution problem
- Small amounts of Co-57 are again used to test the detection of low contributing sources
- Each figure is a random test run

Convolution Linear Coefficients			
Ba-133	0	0	0
Na-22	125,000	2,000,000	20,000,000
Mn-54	0	0	0
Cs-137	20,000	200,000	2,000,000
Co-60	100,000	1,000,000	10,000,000
Co-57	5,000	50,000	500,000
Total Counts	4,817	64,407	646,974

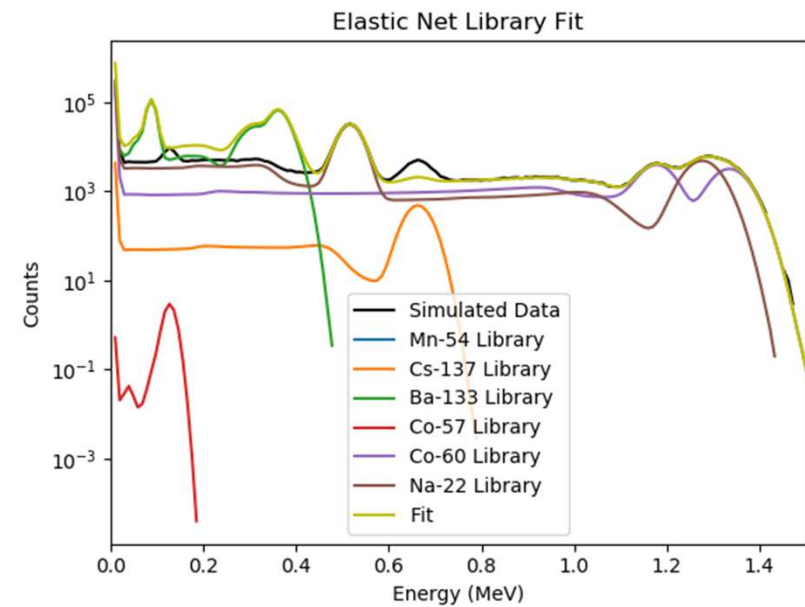
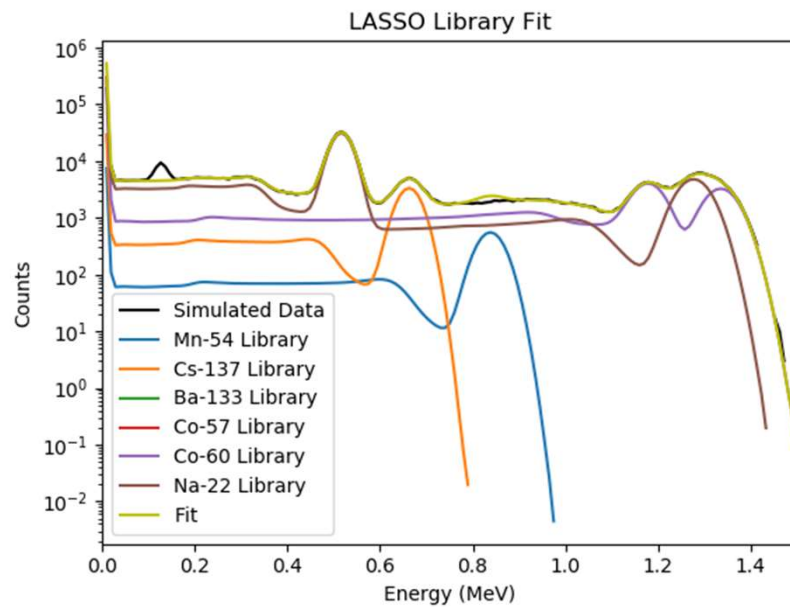
Convolution without Shielding – Low Counts



Convolution without Shielding – Medium Counts



Convolution without Shielding – High Counts



Convolution without Shielding – Summary

- LASSO outperforms Elastic Net for most count rates
- At each counting rate, LASSO correctly identified both Na-22 and Co-60
- False positive rates increased with higher count rates for this trial
- Co-57 contributions may be close to detectable limit for each method, as the false negative rate was >50% for 4 of the 6 cases

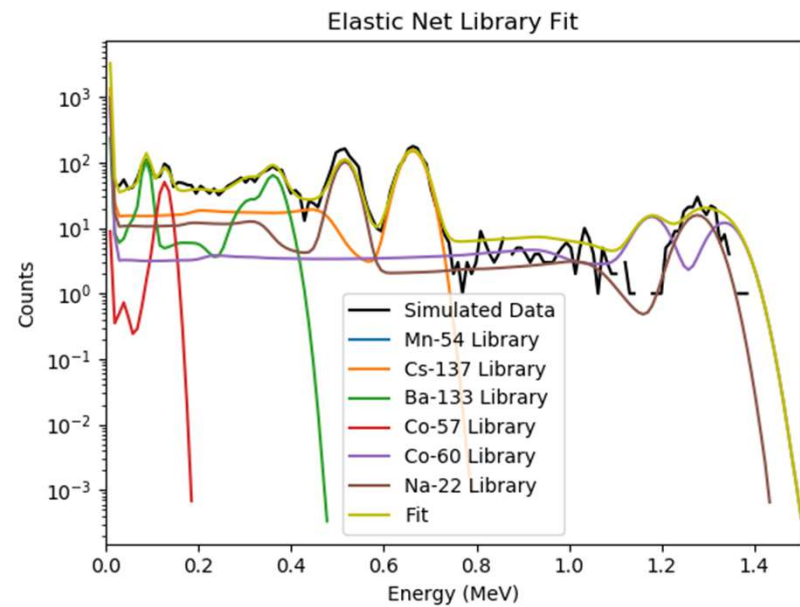
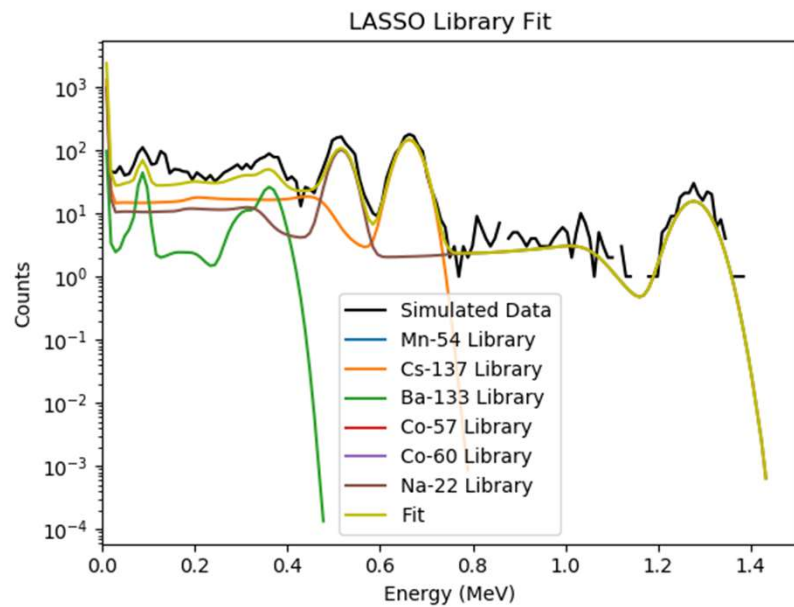
Convolution Without Shielding Prediction Accuracy						
	Lasso-Low	EN-Low	Lasso-Med	EN-Med	LASSO-High	Elastic Net-High
Ba-133	0.90	0.90	0.75	0.80	0.60	0.80
Na-22	1.00	0.95	1.00	1.00	1.00	1.00
Mn-54	0.75	0.95	0.80	0.65	0.65	0.65
Cs-137	0.85	0.75	0.90	0.75	1.00	0.95
Co-60	1.00	0.95	1.00	1.00	1.00	1.00
Co-57	0.15	0.10	0.60	0.35	0.45	0.50

Masking with Shielding

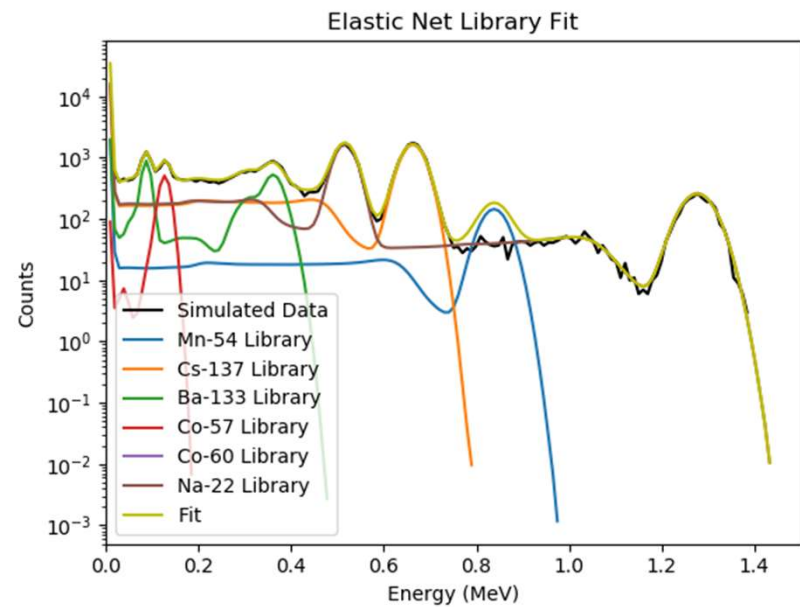
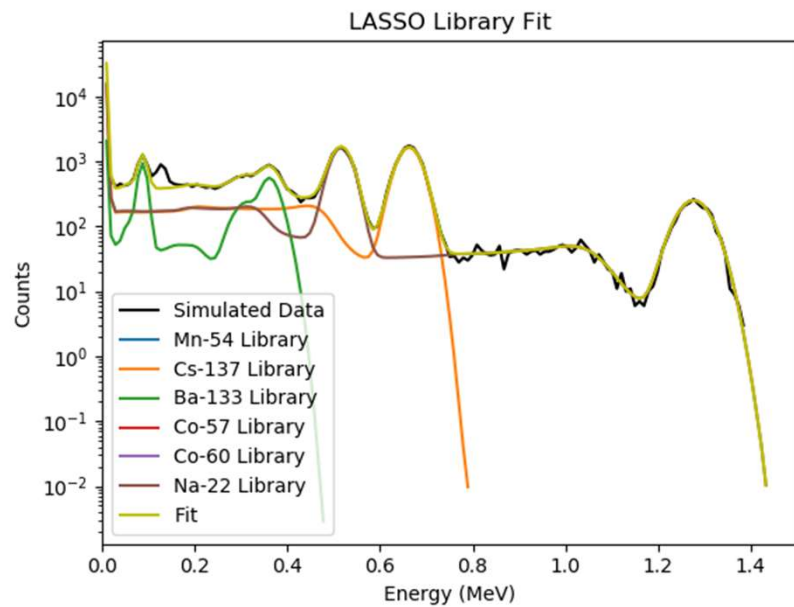
- Masking is a term used for a situation where higher energy radioisotopes “mask” the signature of a lower energy source
- Small amounts of Co-57 are used to demonstrate the effectiveness of LASSO and Elastic Net on this problem type
- A 1-inch aluminum shield is placed between the detector and source
- All coefficients are held the same
- Libraries used for fitting are generated without the shielding, with the combination spectrum consisting of the shielded libraries
- Each figure is a random test run

Masking with Shielding Linear Coefficients			
Ba-133	30,000	300,000	3,000,000
Na-22	100,000	1,000,000	10,000,000
Mn-54	0	0	0
Cs-137	100,000	1,000,000	10,000,000
Co-60	0	0	0
Co-57	5,000	50,000	500,000
Total Counts	4956	50,625	509,744

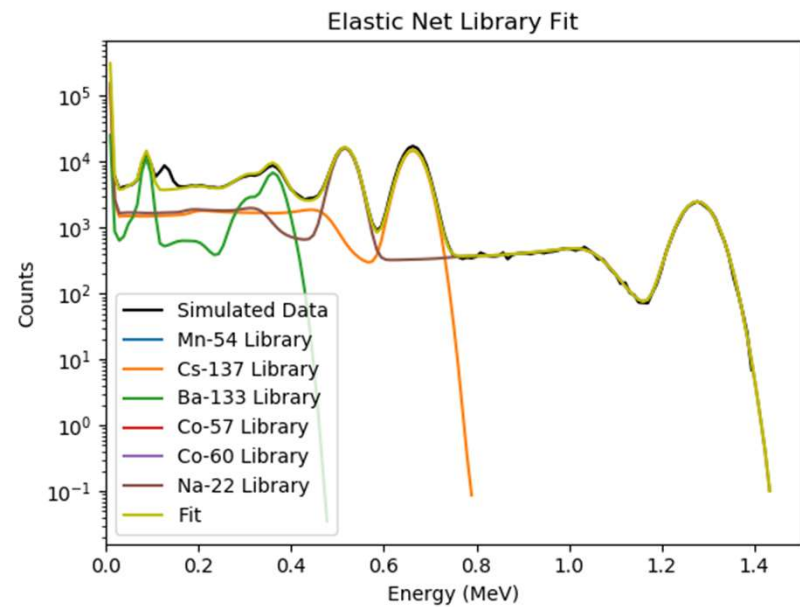
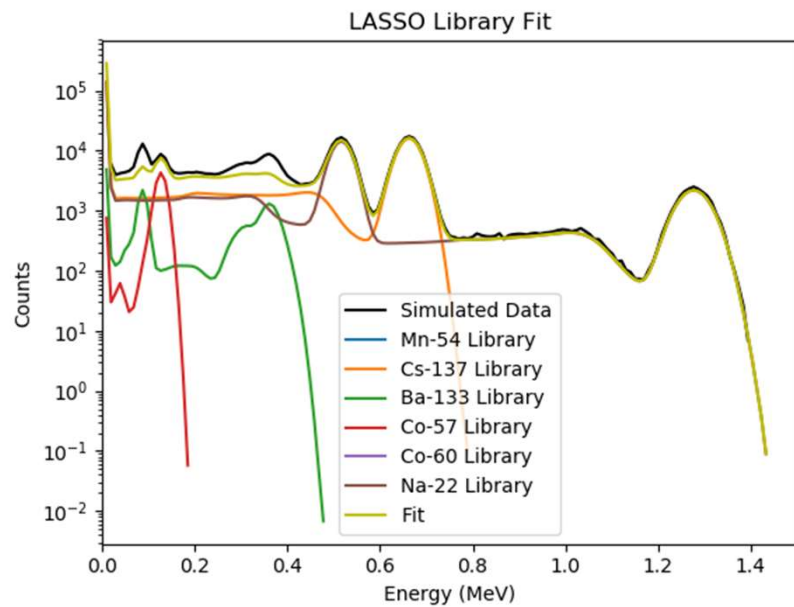
Masking with Shielding – Low Counts



Masking with Shielding – Medium Counts



Masking with Shielding – High Counts



Masking with Shielding – Summary

- LASSO again outperforms Elastic Net for every counting rate
- At the highest count rate, LASSO correctly identifies Co-57 contributions only 55% of the time, with a false positive rate for Mn-54 and Co-60 20-30% of the time
- As expected, the false positive and false negative rates increased with added shielding
- Each figure is a random test run

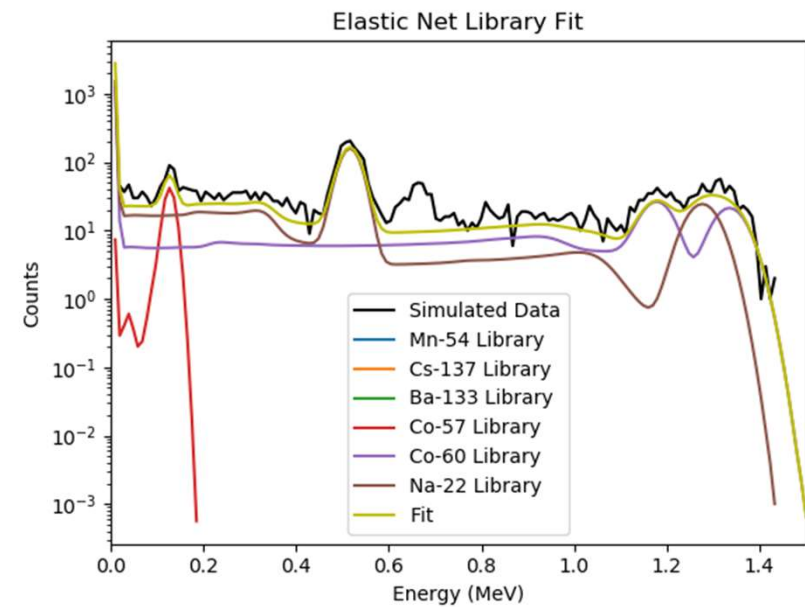
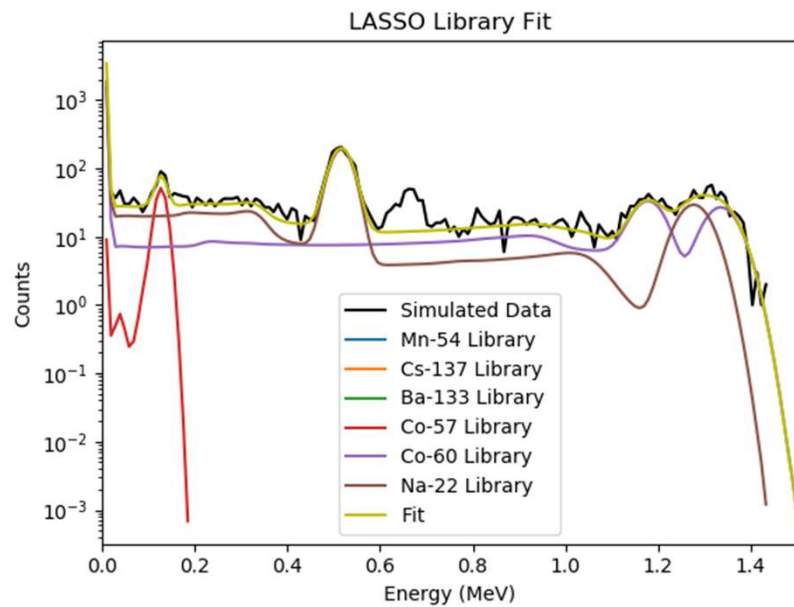
Masking with Shielding Prediction Accuracy						
	Lasso-Low	EN-Low	Lasso-Med	EN-Med	LASSO-High	Elastic Net-High
Ba-133	0.80	0.55	0.90	0.70	1.00	0.80
Na-22	1.00	0.90	1.00	0.90	1.00	1.00
Mn-54	0.55	0.55	0.60	0.65	0.70	0.65
Cs-137	0.85	0.75	0.95	0.80	1.00	0.85
Co-60	0.70	0.30	0.60	0.75	0.80	0.70
Co-57	0.35	0.30	0.35	0.25	0.55	0.35

Convolution with Shielding

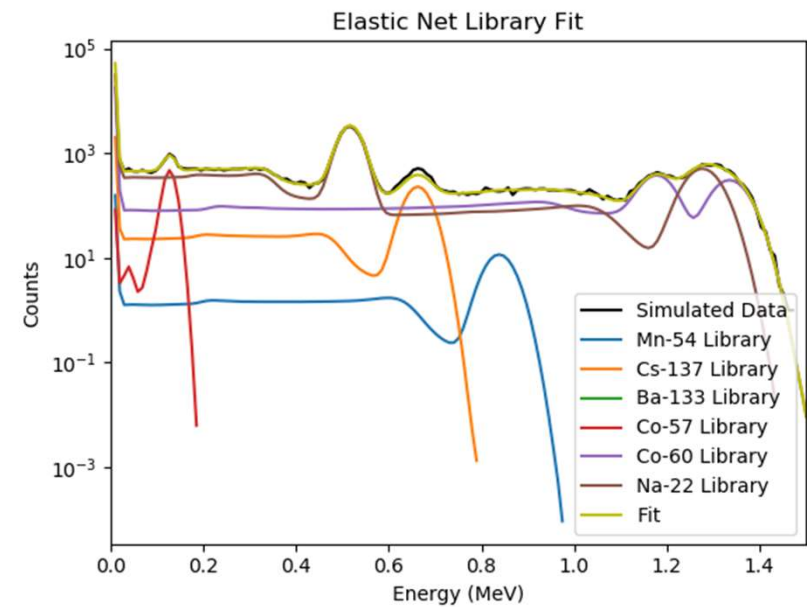
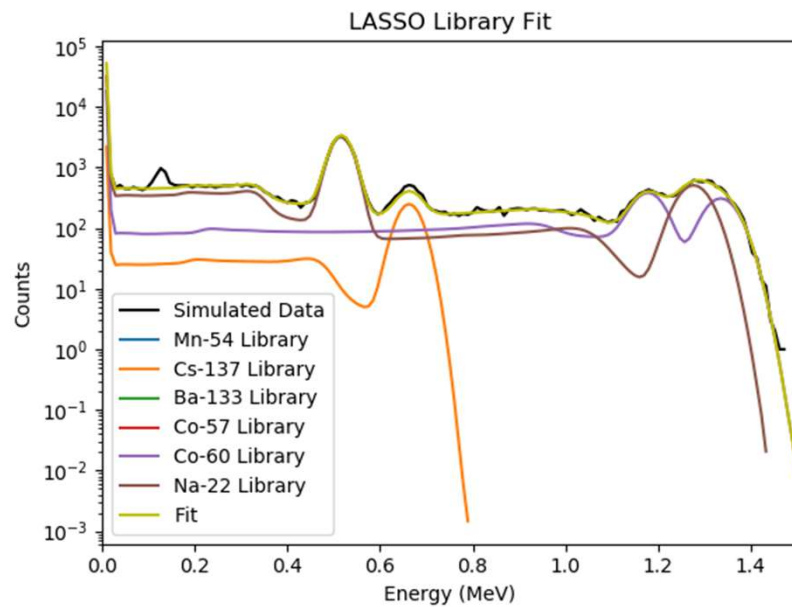
- Convolved peaks involve a situation where two or more radioisotopes have broadened peak energies that overlap
- Single peak analysis techniques have a difficult time with this problem
- LASSO and Elastic Net are full spectrum analysis techniques
- Large contributions of both Na-22 and Co-60 are used to simulate a convolution problem
- A 1-inch aluminum shield is placed between the detector and source
- All coefficients are held the same
- Libraries used for fitting are generated without the shielding, with the combination spectrum consisting of the shielded libraries

Convolution with Shielding Linear Coefficients			
Ba-133	0	0	0
Na-22	125,000	2,000,000	20,000,000
Mn-54	0	0	0
Cs-137	20,000	200,000	2,000,000
Co-60	100,000	1,000,000	10,000,000
Co-57	5,000	50,000	500,000
Total Counts	4,387	61,327	61,756

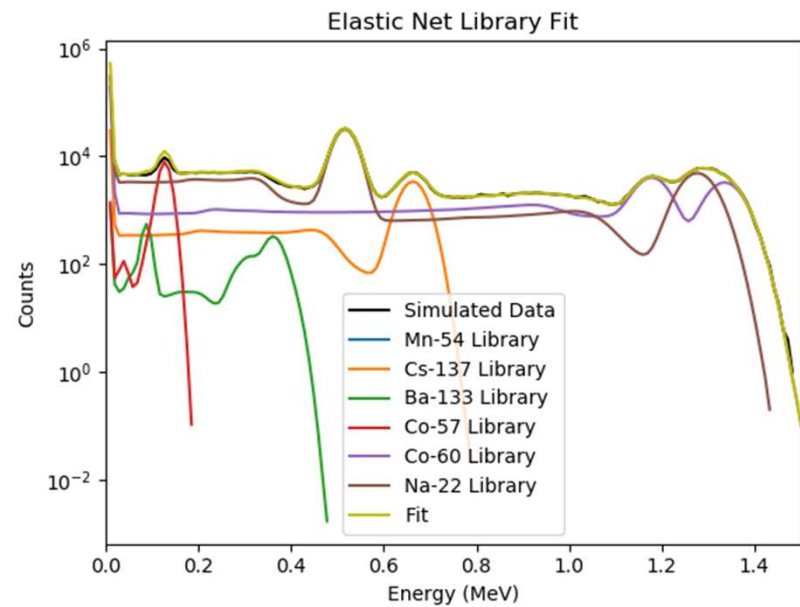
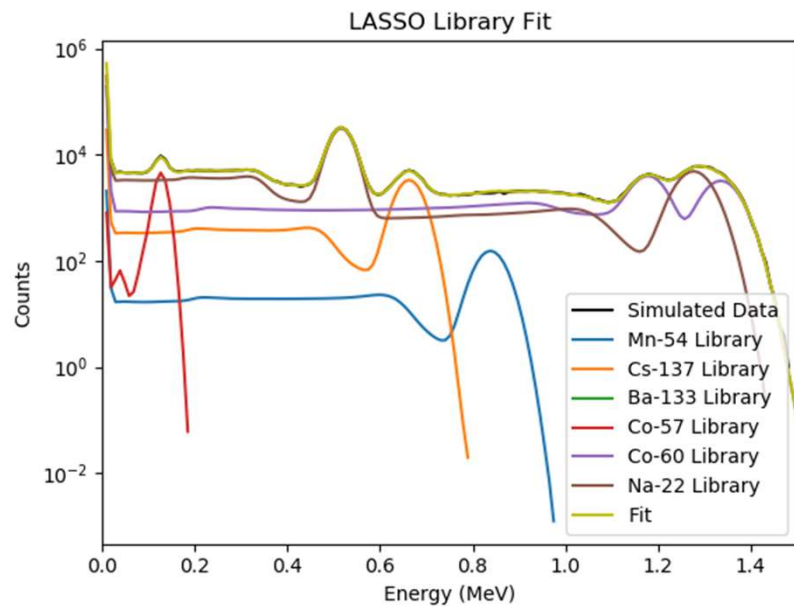
Convolution with Shielding – Low Counts



Convolution with Shielding – Medium Counts



Convolution with Shielding – High Counts



Convolution with Shielding – Summary

- Each method performed similarly in this case
- At each counting rate, LASSO and Elastic Net correctly identified both Na-22 and Co-60 100% of the time
- False positive rates increased with higher count rates for this trial
- Co-57 false negative rates improved over the non-shielded situation

Convolution with Shielding Prediction Accuracy						
	Lasso-Low	EN-Low	Lasso-Med	EN-Med	LASSO-High	Elastic Net-High
Ba-133	0.65	0.70	0.65	0.90	0.60	0.75
Na-22	1.00	1.00	1.00	1.00	1.00	1.00
Mn-54	0.70	0.60	0.50	0.45	0.50	0.50
Cs-137	0.70	0.80	1.00	0.95	0.95	1.00
Co-60	1.00	1.00	1.00	1.00	1.00	1.00
Co-57	0.40	0.50	0.70	0.65	0.60	0.80

Discussion/Conclusions

- LASSO performs better in each application, and shows promise for any radiation detection application with linear solutions
- Elastic Net is effective at times, and should still be considered in situations where the data is highly correlated
- Kansas State benchmarking tool experimental analysis will be improved by new techniques introduced by Aaron Feinberg
- Experiments with professional equipment should be conducted to better evaluate the full potential of LASSO and Elastic Net
 - LaBr or CeBr detectors may improve effectiveness
 - Use of experimental results to test against field data vs simulated libraries
 - Validation data sets may improve output from LASSO and Elastic Net

References

- A.Sood, R.P.Gardner / Nucl. Instr.and Meth.in Phys. Res.B 213 (2004) 100–104.
- Blackadar, J. et al. “Evaluation of commercial detectors.” INMM 44th Annual Meeting, Phoenix, Az, 2003. LA-UR-03-4020. Los Alamos National Laboratory.
- Bob Burkhardt, “Neutron Generator and Well Logging”, Sandia National Laboratories, SAND2006-3291C, www.osti.gov/servlets/purl/1264595
- Burr, T and Hamada, M. “Radio-Isotope Identification Algorithms for NaI Gamma Spectra.” Algorithms 2009, 2, 339-360.
- Committee on Radiation Source and Replacement, 2008, Radiation Source Use and Replacement, National Research Council, ISBN 0-309-110115-7, National Academies Press, Washington, DC (NAS-2008)
- E. Bai, K. Chan, W. Eichinger, P. Kump, “Detection of radionuclides from weak and poorly resolved spectra using Lasso and subsampling techniques.” Radiation Measurements, 46 (2011), pp. 1138-1146.
- Evans, R.D., *The Atomic Nucleus*. McGraw-Hill, 1955.
- Friedman, J. et al., “Pathwise coordinate optimization.” The Annals of Applied Statistics (2007), Vol. 1, No. 2, pp. 302-332.
- Friedman, J. et al., “Regularization paths for generalized linear models via coordinate descent.” Journal of Statistical Software (2010), Vol. 3, Issue 1.
- Gardner, et al., 2013, ANS Panel on “Recent Developments in Radiation Source Use and Replacement after the NAS Report of 2008”, Transactions of the American Nuclear Society, Vol. 109, 47.
- R.P. Gardner and A. Sood. “A Monte Carlo simulation approach for generating NaI detector response functions (DRFs) that accounts for non-linearity and variable flat continua”. *Nuclear Instruments and Methods in Physics Research, Section B: Beam Interactions with Materials and Atoms* (Jan. 2004), pp. 87-99.

References

- R.P. Gardner and C.W. Mayo. “Nai detector nonlinearity for PGNAA applications”. *Applied Radiation and Isotopes* 51.2 (Aug. 1999), pp. 189-195.
- R.P. Gardner and L. Xu. “Status of the monte carlo library least-squares (MCLLS) approach for non-linear radiation analyzer problems.” *Radiation Physics and Chemistry* 78 (2009), pp. 843-851.
- R.P. Gardner, et al. “Nal detector neutron activation spectra for PGNAA application.” *Applied Radiation Isotopes* (2000), 53, pp. 483-97.
- Gauraha, N. “Introduction to the Lasso: a convex optimization approach for high-dimensional problems.” *Resonance*, April 2018.
- Guo, W. et al. “Using the Monte Carlo – Library Least Squares (MCLLS) approach for the in vivo XRF measurement of lead in bone.” *Nuclear Instruments and Methods in Physics Research A*, 516 (2004), pp. 586-593.
- Han, Xiaogang, Ph.D thesis. North Carolina State University. 2005.
- Hastie, Trevor. *The Elements of Statistical Learning: Data Mining, Inference, and Prediction*. 2nd Edition. Springer Series in Statistics. 2009.
- Hou, Guojing, Ph.D thesis. North Carolina State University. 2017.
- Kim, K. et al. “Theoretical fluxes of gamma rays from the Martian surface.” *Journal of Geophysical Research*, Vol. 111, 2006.
- Knoll, G. F., *Radiation Detection and Measurement*. 4th Edition. John Wiley and Sons, Inc, 2011.
- Kump, P. et at., “Variable selection via RIVAL (removing irrelevant variables amidst Lasso iterations) and its application to nuclear material detection.” *Automatica*, 48 (2012), pp. 2107-2115.

References

- Liberman, A.D et. al., “A method to determine the absolute neutron output of small D-T generator”, *Nuclear Instruments and Methods in Physics Research Section B*, Volume 79, Issue 1-4, p. 574-578, June 1993
- M. Geretschlager, Nucl. Instr. and Meth. B 28 (1987) 289.
- MCNP Training Manual
- Pedregosa *et al.*, “[Scikit-learn: Machine Learning in Python](#).” JMLR 12, pp. 2825-2830, 2011.
- Pibida, L. et al. “Evaluation of handheld radionuclide identifiers.” Journal of Research of the National Institute of Standards and Technology. Vol 109, No 4, 2004.
- Preston R.M. et al, “Neutron generator burst timing measured using a pulse shape discrimination plastic scintillator with silicon photomultiplier readout”, *Journal of Instrumentation*, December 8, 2013.
- R.P. Gardner, A.M. Yacout, J. Zhang, K. Verghese, Nucl. Instr. and Meth. A 242 (1986) 399.
- R.L. Heath, Scintillation Spectrometry, Gamma-Ray Spectrum Catalogue, 2nd Ed., USAEC Report IDO-16880, 1964.
- T. Papp, J.L. Campbell, D. Varga, G. Kalinka, Nucl. Instr. and Meth. A 412 (1998) 109.
- Serra, Oberto. *Well Logging Handbook*. Ed. Technip, Paris. 2008.
- Tibshirani, R. “Regression shrinkage and selection via the lasso.” *Journal of the Royal Statistical Society, Series B* 58: 267-288. 1996.
- Wu, T. and Lange, K. “Coordinate descent algorithms for Lasso penalized regression.” *The Annals of Applied Statistics*, 2008, Vol. 2, No. 1, pp. 224-244.
- Y. Jin, R.P. Gardner, K. Verghese, Nucl. Instr. and Meth. A 242 (1986) 416.
- Yang, Y. and Zou, H. “A coordinate majorization descent algorithm for l1 penalized learning.” *Journal of Statistical Computation and Simulation*. (2014) 84, pp. 84-95.
- Zou, H. and Hastie, T. “Regularization and variable selection via the elastic net”. *Journal of the Royal Statistical Society Series B*. 67: 301-320. 2005.

Thank you

- Questions?



North Carolina
Agricultural and Technical
State University™

NC STATE UNIVERSITY



PURDUE
UNIVERSITY

This work was sponsored in part by the NNSA
Office of Defense Nuclear Nonproliferation R&D
through the Consortium for Nonproliferation Enabling Capabilities

